ISTANBUL TECHNICAL UNIVERSITY ★ GRADUATE SCHOOL OF SCIENCE ENGINEERING AND TECHNOLOGY

DESIGN OF DYNAMIC BRAILLE DISPLAY FOR MOBILE PHONES

M.Sc. THESIS

Remzi Yalın SÖNMEZ

Department of Control and Automation Engineering

Control and Automation Engineering Programme

NOVEMBER 2019

ISTANBUL TECHNICAL UNIVERSITY ★ GRADUATE SCHOOL OF SCIENCE ENGINEERING AND TECHNOLOGY

DESIGN OF DYNAMIC BRAILLE DISPLAY FOR MOBILE PHONES

M.Sc. THESIS

Remzi Yalın SÖNMEZ
(504171120)

Department of Control and Automation Engineering

Control and Automation Engineering Programme

Thesis Advisor: Assoc. Prof. Dr. Serhat İKİZOĞLU

NOVEMBER 2019

ISTANBUL TEKNİK ÜNİVERSİTESİ ★ FEN BİLİMLERİ ENSTİTÜSÜ

CEP TELEFONLARI İÇİN DİNAMİK BRAİLLE GÖRÜNTÜLEYİCİSİ TASARIMI

YÜKSEK LİSANS TEZİ

Remzi Yalın SÖNMEZ
(504171120)

Kontrol ve Otomasyon Anabilim Dalı

Kontrol ve Otomasyon Programı

Tez Danışmanı: Doç. Dr. Serhat İKİZOĞLU

KASIM 2019

Remzi Yalın SONMEZ, a M.Sc. student of ITU Graduate School of Science Engineering and Technology student ID 50171120, successfully defended the thesis entitled "DESIGN OF DYNAMIC BRAILLE DISPLAY FOR MOBILE PHONES", which he prepared after fulfilling the requirements specified in the associated legislations, before the jury whose signatures are below.

Thesis Advisor :	**Assoc. Prof. Dr. Serhat İKİZOĞLU** Istanbul Technical University	.....
Jury Members :	**Dr. Serkan TÜRKELİ** Istanbul Technical University	.....
	Asist. Prof. Dr. Hakan SOLMAZ Bahçeşehir University	.....

Date of Submission : 6 September 2019
Date of Defense : 20 November 2019

To never dying ideologies,

FOREWORD

I want to thank my family for their financial and emotional support throughout my education years. My friend and my mentor, Serkan Türkeli, for his guidance and advice he gave me during my graduate years. And my thesis advisor, Assoc. Prof. Serhat İkizoğlu for patience and understanding. Also, I would like to acknowledge people who put their efforts designing Braille displayers around the world.

November 2019

Remzi Yalın SÖNMEZ
(Electrical Engineer)

TABLE OF CONTENTS

Page

FOREWORD ..... **ix**
TABLE OF CONTENTS ..... **xi**
ABBREVIATIONS ..... **xiii**
SYMBOLS ..... **xv**
LIST OF TABLES ..... **xvii**
LIST OF FIGURES ..... **xix**
SUMMARY ..... **xxi**
ÖZET ..... **xxiii**
1. INTRODUCTION **1**
1.1 Research Topic and Purpose 1
1.2 Literature Review 4
1.3 Hypothesis 7
2. DESIGN **9**
2.1 Braille Cell Technologies 10
2.1.1 Piezoelectric braille cell 10
2.1.2 Electromagnetic braille cell 11
2.1.3 Motor based braille cell 11
2.2 Implementation 11
2.2.1 Actuator 11
2.2.2 Actuator driving 12
2.2.3 Mobile phone support 12
2.2.4 Battery system 13
2.3 Actuator Design 13
2.3.1. Solenoid equations and circuit 14
2.3.2. Mechanical equation 16
2.3.3. Modeling 16
2.3.2. Design constraints 17
2.3.3. Simulations 18
2.3.4. Material selection 18
2.4 Alternative Design 26
2.5 Mechanical Design 28
2.5.1 Paddle 28
2.5.2 Case 30
2.5.3 Step motor with screw rod 32
2.5.4 Braille display carrier 32
2.5.5 Pin headers 33
2.6 Electronic 35
2.6.1 Topology 35
2.6.2 Components 37
2.7 Software 53
3. RESULTS **57**
3.1 Components 57

3.2 Displays and Failures 63
3.3 Braille Cell Costs 66
3.3.1 Cost of electronic components 67
3.3.2 Cost of 3D printer Components 67
3.1.3 Cost comparison of Braille cells 68
3.4 Power Consumption 69
3.4.1 Standby power consumption 69
3.4.2 Power consumption in use 69
4. DISCUSSION 73
5. CONCLUSION 77
REFERENCES 79
APPENDICES 83
APPENDIX A 84
APPENDIX B 85
CURRICULUM VITAE 95

ABBREVIATIONS

FEM	: Finite Element Method
I/O	: Input /Output
NIST	**:** National Institute of Standards
NLSBPH	**:** National Library of Service for Braille People Health
PCB	: Printer Circuit Board
RAM	: Random Access Memory
USB	: Universal Serial Bus
UART	: Universal Asynchronous Receiver Transmitter
SD	: Storage Device
WHO	**:** World Health Organization
ASCII	: American Standard Code for Information Interchange
3D	: 3 Dimension
CAD	: Computer Aided Drawing

SYMBOLS

$\boldsymbol{V}$	**:** Voltage
L	**:** Inductance
R	**:** Resistance
I	: Current
F	**:** Force
$\boldsymbol{\mu_0}$	: Permeability
$\mathbf{I_{trim}}$	: Current in windings
$\mathbf{R_O}$	: Outer diameter of the ring magnet
$\mathbf{R_I}$	: Inner diameter of the ring magnet
$\mathbf{R_C}$	: Diameter of the copper wire
$\mathbf{h_R}$	: Height of the ring magnet
$\mathbf{h_C}$	: Height of the coil
$\mathbf{h_I}$	: Height of the core
$\mathbf{h_B}$	: Height of the block magnet
$\mathbf{d_R}$	: Distance between the ring magnet and coil
$\mathbf{d_B}$	: Distance between the block magnet and coil
N	: Number of turns

LIST OF TABLES

Page

Table 1. 1: WHO Statistics of blindness in the world population grouped in age [1]. **1**
Table 1. 2: WHO statistics of blindness in the world population regionally grouped .. [1]. **2**
Table 1.3: Size and spacing for a Braille cell..... **5**
Table 1.4: Comparison of the different types of Braille displays **7**
Table 2.1: Types of the materials planned for the actuator..... **17**
Table 2.2: Optimized values of the parameters..... **24**
Table 2.3: Truth Table for Braille Converting **31**
Table 3.1: Cost of Single Electromagnet Design. **66**
Table 3.2: Cost of Single Cell with step motor Design..... **67**
Table 3.3: Cost of Electronic Equipment of Step Motor Design **67**
Table 3.4: The Cost of 3D Components of Step Motor Design..... **68**
Table 3.5: Total Cost of Step Motor Design **68**
Table 3.6: Cost comparison of Braille Cells **68**
Table 3.7: Current usages of electronic equipment during embossing cycle..... **70**

LIST OF FIGURES

Page

Figure 1. 1: Braille alphabet for the English language **4**
Figure 1. 2: Braille dot distance specifications according to EU Standards..... **5**
Figure 2. 1: Design of hardware components regarding the Braille display..... **9**
Figure 2. 2: Piezoelectric Braille module with eight dots..... **10**
Figure 2. 3: Design of the Braille cell using an electromagnetic concept. **11**
Figure 2. 4: Position of 2 magnets attracting each other..... **15**
Figure 2. 5: Initial 2D model of the magnetic actuator..... **17**
Figure 2. 6: 3D model created in ANSYS Maxwell for actuator design. **19**
Figure 2. 7: A simple representation of the optimization process of Maxwell Ansys **20**
Figure 2. 8: The Genetic Algorithm population settings in Maxwell **20**
Figure 2. 9: Selection of objective function and solution type. **21**
Figure 2. 10: Assignment of the variables and constraints for optimization. **22**
Figure 2. 11: 2D drawing of an electromagnet with parameter positions..... **23**
Figure 2. 12: Force-Time graph of the actuator simulation **24**
Figure 2. 13: Position-Time graph of the actuator simulation **25**
Figure 2. 14: Current-Time graph of the actuator simulation..... **25**
Figure 2. 15: Force-Time graph of the actuator simulation without ring magnet..... **26**
Figure 2. 16: Micro Step Motor with Screw Rod **27**
Figure 2. 17: Pin Combinations for each three dots group. **28**
Figure 2. 18: The paddle model from the top view..... **29**
Figure 2. 19: The paddle model from the side view. **29**
Figure 2. 20: The Phone carrier side of the case..... **30**
Figure 2. 21: The Braille device carrier side of the case..... **30**
Figure 2. 22: Carrier Board. **32**
Figure 2. 23: Step Motor Model..... **32**
Figure 2. 24: Braille Display Carrier **33**
Figure 2. 25: Pin Header Model..... **33**
Figure 2. 26: Assembled parts of Braille Displayers 34
Figure 2. 27: Exploded view of Braille Displayer. **34**
Figure 2. 28: Exploded view of the Mechanical Assembly **35**
Figure 2. 29: Isometric view of the design model..... **35**
Figure 2. 30: Operation flow of Braille Display with Micro Step Motor as an actuator. **36**
Figure 2. 31: Operation flow of Braille Display with Micro Step Motor as an actuator controlled without a motor driver..... **36**
Figure 2. 32: DRV8835 Step motor driver carrier..... **38**
Figure 2. 33: DRV8835 Step motor driver Schematic..... **38**
Figure 2. 34: Timing diagram of the motor driver..... **39**
Figure 2. 35: Winding current in a period..... **39**
Figure 2. 36: Stepper motor drive diagram in Simulink **42**

Figure 2. 37: Open-loop controller for the modeled stepper motor. **42**
Figure 2. 38: The stepper motor's Shaft Angle-Speed vs. Time graph..... **43**
Figure 2. 39: The stepper motor's winding current (Phase A-B), torque, shaft angle, back emf voltage (Phase A-B), angular speed graphs vs. time.. **43**
Figure 2. 40: The stepper motors phase current voltage and power dissipation values with respect to time. **44**
Figure 2. 41: STEP-DIR signals for the simulation **45**
Figure 2. 42: Simulation results of applied STEP DIR signals. **45**
Figure 2. 43: Angular position of stepper motor respect to the time **46**
Figure 2. 44: Angular speed of stepper motor respect to the time **46**
Figure 2. 45: Generated torque of stepper motor respect to the time..... **46**
Figure 2. 46: Phase currents of stepper motor respect to the time **47**
Figure 2. 47: Phase currents of stepper motor respect to the time **47**
Figure 2. 48: The current graph obtained from PROTEUS simulation. 49
Figure 2. 49: Motor Driver Carriers Schematic Layout..... **50**
Figure 2. 50: Microprocessor Schematic Layout **51**
Figure 2. 51: Printed Circuit Design of Braille Display in 3D..... **51**
Figure 2. 52: Printed Circuit Design of Braille Display..... **52**
Figure 2. 53: Communication Layout. **53**
Figure 2. 54: Communication layout and setting on STM32. ..... **54**
Figure 2. 55: Algorithm flow cycle of STM. **55**
Figure 2. 56: Layout of a paddle for each position. 56
Figure 3. 1: The Display Carrier and Pinheads. **57**
Figure 3. 2: The Braille Displayer..... **57**
Figure 3. 3: Paddles on the step motors **58**
Figure 3. 4: The damaged paddle on the left, rigid paddle on the right **58**
Figure 3. 5: The carrier board in the main case..... **59**
Figure 3. 6: Topside of the circuit. **59**
Figure 3. 7: Downside of the circuit. **59**
Figure 3. 8: The enlarged design for Braille display..... 60
Figure 3. 9: The implementation of Braille displayer. **61**
Figure 3. 10: Top view of prototype Braille module. **61**
Figure 3. 11: The Braille prototype module with electronic components. **62**
Figure 3. 12: Motor Driver Phase output for position 1. ..... **62**
Figure 3. 13: Motor Driver Phase output for position 4. ..... **63**
Figure 3. 14: Motor Driver Phase output for position 7. ..... **63**
Figure 3. 15: The Solenoid Operation Cycle. **64**
Figure 3. 16: The Braille-Pin Carrier bending on the mechanical loading. **65**
Figure 3. 17: Embossment of Position 2,4, and 6. 65
Figure 3. 18: Embossment of Position 1,3,5 and 7. ..... **66**

DESIGN OF DYNAMIC BRAILLE DISPLAY FOR MOBILE PHONES

SUMMARY

This thesis consists of mechanical, electronic methodologies to design a biomedical product. A mobile Braille display is designed for mobile phones where can be carried as a mobile phone cover. Commercially Braille displayers are available with different design and operation concepts. The Braille alphabet is an embossed dot combination that helps blind people to read. Since the 19th century Braille alphabet has been used as static displayers with embossed dots. However, in the last 30 years' industry has come up with the idea to refresh dot positions to allow blind people to read fluently without using paper or books covered with dots. Although not all blind populations can use these refreshable Braille displayers become, smaller and more compact Braille displayers are presented in the market. Since mobile phones become a general commodity along with the humankind. The Braille displayers have to be intertwined with mobile phones.

The suggested Braille display is designed to take part in mobile phones on a small scale. Therefore, an electromagnet is designed to operate the dots individually controlled with an input-output expender integrated circuits. However, the size of the electromagnets has made it impossible to obtain electrical efficiency. Also, the size of these electromagnets made it impossible to reproduce them in large quantities. Thus a new method has been suggested. Instead of controlling each dot individually, a group of dots will control by using mechanical constrains to press dots combinations. The text data was taken from the mobile phone via Bluetooth connections.

The mechanical constraints in the design created specific problems due to the Braille dot space standards, which made the production of the part not possible with contemporary used three-dimensional printers. The parts or the paddles moved with step motors, which are controlled by a microprocessor to display combinations of dots. By decreasing the number of actuators, the lifespan of the Braille device can increase.

CEP TELEFONLARI İÇİN DİNAMİK BRAİLLE EKRANI TASARIMI

ÖZET

Bu tez, mekanik, elektronik metodolojileri içeren bir biyomedikal ürün tasarımını gerçekleştirmek üzere hazırlanmıştır. Ürün olarak cep telefonu kullanan körler için bir mobil Braille ekranı tasarlanmaya çalışılmıştır. Braille alfabesi, kör insanların okumasını sağlayan kabartmalı nokta dizileridir. 19. yüzyıldan beri Braille alfabesi, kabartma noktalar kullanarak olarak kullanılmıştır. Dünya nüfusunun yüzde 0.5 görme kusurlu olması bu alfabenin kullanımı yıllar geçtikçe arttırmıştır. Ancak son 30 yılda görme kusurlu insanların noktalarla veya kabartmalarla kaplı kitapları kullanmaktan ziyade noktaların veya kabartmaların harflere göre değişbileceği sistemler geliştirilmeye başlanmıştır. Görme kusurlu insanlar bu yenilenebilir Braille görüntüleyicileri günlük hayatta kullanmalarına rağmen, daha küçük ve hafif Braille görüntüleyicileri piyasada sunulmaktadır.

Braille görüntüleyiciler lineer, yuvarlak ve elektrik uyarımı olmak üzere üçe ayrılmıştır. Elektrik uyarımlı Braille görüntüleyicileri Panda sistemleri olarak tanımlanmış olup piyasada ürün halinde bir örneği bulunmamaktadır. Yuvarlak Braille görüntüleyicileri sınırlı sayıda karakteri göstermek için tasarlanmıştır. Bir silinidirin yüzeyine konulan kabartmaları döndürerek istenilen karakterleri göstermeye çalışmaktadır. Yuvarlak Braille görüntüleyicileri piyasda sadece Amerika'da kullanılmaktadır. Ürün halinde örneği sayılıdır.

Lineer Braille görüntüleyicileri piyasada en çok kullanılan cihazlardır. Lineer denmesinin sebebi kabartma görevi gören pin veya noktaların dikey şekilye hareket etmelerini sağlayacak eyleyicilerin görev almasındandır. Noktalar yerçekimine karşı yer çekimi yönüne doğrusal eylemlerini gerçekleştirirler. Lineer Braille görüntüleyicileri elektromıknatıs, piezo elektrik veya akıllı hafızalı alaşım gibi eyleyicilerden oluşmaktadır. Elektromıknatıslı lineer Braille görünteliyicileri çok ucuz olmasına rağmen her nokta için elektromıknatıs koymak sistemi hem mekanik olarak karmaşık hale getirmekte hem de enerji tüketimi için dezavantajlı. Birden fazla hücreli Braille görüntüleyicilerde verimli olması mümkün değildir. Akıllı hafızalı alaşımlar ise üretimlerinin seri üretim halinde olmaması ve tekrarlanabilirliği düşük olmasından dolayı endüstiride örneği bulunmamaktadır. Piezo elektrik eyleyicileri hem boyut olarak hem de tekrarlanabilirlik olarak Braille uygulamalarına ideal bir araç olmuştur. Braille görüntüleyicileri çoğunlukla piezo sistemlerden oluşmasına rağmen genel kullanım için çok pahalı bulunmaktadır.

Tasarlanmak istenen Braille modülü cep telefonların arkasına yer alacak ve koruyucu kap görevi görmesi planlanmıştır. Diğer Braille cihazlarından farklı olarak, bu Braille cihazı telefonun yere göre olan pozisyonu değişeceğinden dolayı lineer hareketi çift yönlü yapması gerektiği düşünülmüştür. Elektromıknatısların düzgün bir şekilde çalıştırılması için gerekli olan giriş çıkış terminal sayısının fazlalığı sistemin elektronik tasarımını karmaşıklarştırmıştır. Elektromıknatıs sisteminin içersinde bulunan solenoid ve ferromanyetik mıknatısların kuvvet ve yer değiştirme hesapları sonlu eleman methodu ile ANSYS'de yapılmıştır. Sonlu eleman analizinde kullanılan

materyallerin özellikleri, boyutları, birbirlerine olan uzaklıkları göz önünde alınarak elde edilebilecek en az akım değeri ile sistemin yeterli gördüğü kuvveti sağlamak hedeflenmiştir. Elde edilen sonuçlarda 600 miliamper ile 75 milinewton elde edilmiş olup 1 milimetrelik yerdeğiştirde sağlanmıştır. Kullanılması planlanan bakır kabloların 600 miliamper değerinde sargılarda zarar vermesinde sebep olabilir. Ayrıca elektro-mıknatısların boyut olarak üretiminin zor olması, sonlu eleman sonuçlarındaki akım değerlerinin çok yüksek olması ve sistemin işlevi için çok fazla eyleyiciye gerek duyulması bu modülün elektromıknatıs eyleyicilerle tasarlanılmasını imkansız kılmıştır.

Braille modülü için hem kolay kullanımı sağlamak amacıyla kalınlığını ince tutmak hem de enerji tüketimini azaltmak için yeni bir yöntem önerilmiştir. Tüm Lineer Braille cihazlarında olduğu gibi her noktayı ayrı ayrı kontrol etmek yerine, nokta kombinasyonlarını mekanik kısıtlamalarla sağlayan pedallar kullanılması planlanmıştır. Bu pedalların pozisyonlarını kontrol etmek içinse rotorlarında vida mili olan stepper motorlar yer almıştır. Braille alfabesinde bir harfi tanımlamaya hazır altı nokta yer alması sağlanmıştır. Harf veya karaktere göre ikili grup halinde bulunan altı noktanın en fazla dört noktası kullanılmakdır. Tasarlanan yeni sistemte üçlü nokta gruplarının düşey halde alabileceği sekiz kombinasyonu sağlayan pedal sistemi yer almaktadır. Vida milinde hareket edecek olan pedal üzerindeki boşluklar sayesinde bir grup üçlü noktanın sağladığı 8 kombinasyonu sağlaması düşünülmüştür. Bu sayede eyleyeci sayısı üçte birine düşmesi amaçlanmıştır. Pinler içinse gerektiğinde mekanik olarak sıkışmaya hazır "pogo pin" kullanılmıştır. Bu pinler taşıyıcı bir platforma konulmuş olup pedallar pozisyonlarını aldığında elektromıknatıs yardımı ile yer değiştirilmesi ön görülmüştür. Sıkışması planlanan pinler yüzeye çıkmayacak ve bu sayede geri kalan pogo pinler kabartma görevi görmektedir.

Braille modülünün çalışması için okunması istenilen karakterlin Braille diline aktarlması gerekmektedir. Bunun için üçlü noktalardan elde edilen posizyonların vida milindeki karşılıkları ölçülmüştür. Bu sayede normal alfabeden Braille alfabesine dönüştürme esnasında hangi harf için hangi ikili grubun ait oldukları vida milinde hangi pozisyona geleceği hesaplanmıştır. Bu sayede bir dönüştürme tablosu oluşturulmuştur. Bu tablo üzerinden bir harfi tanımlamak için 6 eyleyici kullanmak yerine 2 eyleyici kullanılması sağlanmıştır. Ancak Braille sistemlerinin mekanik kısıtlamaları,kullanılan step motorların ufak ve hassas olmasını gerektirmiştir. Mekanik kıstaslar ve step motorların boylarının ufak olması pedalların boyutlarının da ufak olmasını gerektirmiştir. Bu yüzden geometrik töleranslar sistemi etkileyen bir etken olmasına sebep olmuştur. Sistemde ön görülen pozisyonlar sistemin kurulumu esnasında veya motorlarda yaşanabilecek sıkıntılardan kalibrasyon yapma ihtiyacı hissedilmesi ön görülmüştür.

Metin verileri, cep telefonunun üzerinden Bluetooth bağlantı uygulaması kullanılarak Bluetooth aracılığı ile mikroişlemciye aktarılmaktadır. Alınan veriler string formatında tutulup gerektiğinde karaktere dönüştürülmüştür. Dönüştürülen karakter sayısı modülde bulunan hücre sayısı ile aynıdır. Yayınlanan karakterler okunduktan sonra bir dokunmatik sensörle pinleri geri çekmesi ve ardından pedalları vida milinin başına çekmesi planlamıştır. Yeni karakterler kaydedilen string verisinden çekilir ve Brallie hüclerinde yayınlanmaya devam ettirilmiştir.

İstenilen hacimde çalışması ön görülen Braille modülü, o hacim içersinde yer alacakabilecek ve kuvvet standartlarını sağlayan elektromıknatıs sağlanamadığından dolayı modülün kalınlaştırılması gerekmiştir. Pinleri gerektiğinde itiş sağlayacak olan

elektromıknatısların boyutlarının büyük olması hacimsel olarak Braille modülünü ufaltmanın önünü kapamıştır.Yeni tasarlanan sistemde kullanılan elektromıknatıslar pinleri taşıyan sistemi itebilme kabiliyetini göstermiştir.

Kullanılacak olan admı motorlarının her biri adım(step) motor sürücü ile sürülmesi ön görülmüştür. Bu sürücülerin bir tanesi mikroişlemciden iki adet genel giriş çıkış sinyaline gerek duymaktaktadır. Bir tanesi adım motorunun kaç adım atması gerektği diğeri is hangi yöne dönmesi gerektiğini tayin etmektedir. Motorların hareket kabilyetlerini MATLAB üzerinden, seçilen entegrenin çalışma düzeniğini modelleyen bir sistem oluşturularak test edilmiştir. İstenilen hedefe veya pozisyona ulaşmak için yön ve adım sinyalleri tayin edilmiştir. Simulasyonlardan alınna sonuçlar sisteminin ön görülen yük değerlerinde düzgün çalıştığı görülmüştür.

Pedallar, Braille görüntüleyicisi, pin taşıyıcı gibi parçların SLA denilen deneysel bir üç boyutlu basım tekniği ile üretilmesi istenilen geometrik töleransları sağlamıştır. Ancak montaj esnasında yaşanan problemler sistemin çalışmasına engel olmuştur. Bu parçaların mekanik dayanımları ve esneme özellikleri içersinde konan reçine değerine göre değişmektedir. Mukavvemetleri kalınlıklarına bağlı olarak artmakta olup beklenmedik şekilde kırılmalara sebep olabilmektedir.

Modülün mekanik motajları yapıldıktan sonra, pedallar nokta kombinasyonlarını göstermek için bir mikroişlemci tarafından kontrol edilen adım (step) motorlarıyla hareket ettirildi. Ancak pedalların Braille görüntüleyicisinin üzreinde hizada gitmesi için açılan yollarda oluşan sürtünmeler ufak adım (step) motorları zorlanmasına ve yanmalarına sebep olmuştur. Pedal kullanılarak elde edilmek istenen mekanik çıktılar elde edilmiştir. Ancak sistemin dayanıklılığı ve tekrarlanabilirliği kullanılan ürünlerin ve malzemelerin özelliklerinden dolayı istenilen seviyeye getirelememiştir.

Önerilen yeni Braille sistemi enerji tüketimi ve finansal olarak elektromıknatıs sistemlerinden daha pahalı olmasına rağmen piezo sistemlerine göre daha ucuz kalmaktadır. Sistemin üretimi yaklaşık 150 dolara yaklaşmakta olup, batarya tüketimi sürekli kullanımda 5 saate kadar çıkmaktadır. Aralıksız olarak 17000 defa yeni harf dizisi oluşturabilmektedir. Bu sayıların arttırabilmesi için enerji kaynağının veya pilin enerji kapasitesi arttırılmalıdır. Güç tüketiminin sebep olan parçaların step motor ve elektromıknatısların olduğu düşünüldüğünde bu ürünlerin çalışması güç tüketimlerine değil boyutlarına bağlıdır. Bu yüzden bu parçların değişme koulu sadece dayanımlarının gerçekleştirmediği zaman düşünülebilir.

Ayrıca önerilen bu sistemin diğer sistemlerden farkı sistemin taşınabilir olmasıdır. Sistemin üretimi ve testleri esnasında yaşanan problemler kullanılan veya üretilen ürünlerin dayanımlarının fazla olmamasından dolayı kaynaklanmaktadır. Montaj esnasında oluşabilecek en ufak bir geometrik kayma sistemin çalışmamasına sebep olabilmektedir. Bunun için dayanımı ve tork değerleri daha yüksek vida mili bulunduran adım (step) motorları seçilmelidir.

1. INTRODUCTION

1.1 Research Topic and Purpose

The Braille reading system is based on touching individual pins. Visually impaired people use the Braille alphabet to accomplish tasks such as reading and writing in daily life by sensing individual pins. Nowadays, blind people reach out to knowledge through audio and haptic (touchable) feedbacks to communicate. However, it is not always possible to provide audio platforms continuously for all daily activities. According to WHO, there are over a quarter billion people in the world who have visual disabilities, 14% of them are blind, and the rest have a significant level of impairment [1]. These numbers might increase in the future as a result of population growth. Most of the visual impairments, approximately 80%, can be avoided or healed [2]. According to table 1.1 and table 1.2, up to 300 million people have visually impaired; meanwhile, 40 million are blind, and 250 million people have low vision. Also, %90 of people who have visual impairments live in low income. More than %80 of people who have blindness are aged 50 and above. Braille alphabet is one of the ways to increase the quality of life for people with visual disabilities. Louis Braille, who was also blind, invented the system over two centuries ago, and it is named after him [3].

Table 1. 1: WHO Statistics of blindness in the world population grouped in age [1].

Age Group [Years]	Total Population [Millions]	Blindness [Millions]	Low Vision [Millions]	Visual Impairment [Millions]
0-14	1848.500	1.421	17.518	18.939
15-49	3548.200	5.784	74.463	80.248
50 and older	1340.800	32.160	154.043	186.203
All ages	6737.500	32.160	246.024	285.389

Table 1. 2: WHO statistics of blindness in the world population regionally grouped [1].

WHO REGION	Total Population [Millions]	Blindness [Millions]	Low Vision [Millions]	Visual Impairment [Millions]
Africa	804.900	5.880	20.407	26.295
America	915.400	3.211	23.401	26.612
Eastern Mediterranean	580.200	4.918	18.581	23.499
Europe	889.200	2.713	25.502	28.215
South-East Asia(India excluded)	579.100	3.974	23.938	27.913
Western Pacific (China excluded)	442.300	2.338	12.386	14.724
India	1181.400	8.075	54.554	62.619
China	1344.900	8.248	67.264	75.512
World	**6737.500**	**39.365**	**246.024**	**285.389**

The Braille alphabet system is a profound solution to provide a simple tool to communicate without using eyes. Most of the Braille applications are static glyphs that provide small vital information in common areas for visually impaired people. Braille alphabets can vary depending on the language symbols and abbreviations. With recent developments such as 3D printing, open-source Braille applications started to appear. These applications can refresh the Braille text and formats. Most of these Braille display devices use electromechanical systems that can transfer texts such as articles news, messages from a computer, or even cell phones to Braille display. Each character can be transformed into the Braille alphabet. The combination of pins provides a span of pin layouts. Thus, it makes these electromechanical systems sufficient enough to represent all characters. The electromechanical system in Braille displayers always operates or moves one direction against gravity. The device usually used in the same position where the pins always move upwards. However, in order to use these devices more in daily life, blind people should be able to carry the display device without causing any hindrance.

A Braille display cell contains six or eight dots arranged in three rows, two columns. Alternatively, four rows two columns of cells and raised with different combinations to represent letters, numbers, and symbols. The cell must be fit a specific mechanical size. The dots are embossed as glyphs and can be read by passing the index finger over glyphs. Braille alphabet first started to be implemented in textbooks as static glyphs. Lately, refreshable Braille devices have become popular. Braille is an alphabet, not a language a way to express words. Therefore, every language may have a way of expressing letters or expressions. [4-7].

Refreshable Braille devices may offer many benefits for visually impaired people. Importantly, they require much less space than a Braille book. Hence the user can use the device anytime without trouble. Such a device can be programmed to display any desired data; it reduces the amount of space needed to compare to printed Braille books. Today, these devices can interact with smartphones and computers and increase the user's experience with the technology. A survey conducted among students shows that students use static Braille less than the dynamic Braille displayers [8].

There are two types of grades of Braille. Grade 1 Braille provides a large number of pins to present multiple letters, signs, or special Braille characters individually. It does these tasks simultaneously, which is considered for significant texts or documentation. Grade 2 Braille was designed for minimizing space considerations. Instead of showing each character in grade 2 Braille, regularly used words can be represented within a single cell. A Braille device has to include additional formatting marks, which have to correspond with other written languages, such as the number and letter sign.

There are potential users of Braille displays are worldwide 266.450, which results in a percentage of 4% of the overall population and 93% of all blind and severe visually impaired people [1]. Another survey was done by the British Royal National Institute of Blind People that participated partially blind and blind people, most of them adult aged. %80 of visually impaired people have their computers or smartphones. These people spend their time on computers or smartphones to do tasks such as communicating (e-mail, messaging), reading or writing documents, and surfing the internet [9]. Also, the survey asked people who do not use Braille devices, and most of them found it too expensive and costly also too complicated to use. These people mostly in a groupage above 65.

The main goal is to design a Braille display device which is capable of having simple use features. There is a various amount of Braille displayers; however, there is a lack of movable (easily deployable) refreshable Braille displayers in industry. One of the solutions is to create a smartphone case where it will provide Braille display behind the phone case. To create such a device, this thesis will rely on:

Evaluation of Braille cell technologies

Design and development of 3D printable components

Implementation of open source available resources for the software application

Design and implementation of required electronics

1.2 Literature Review

1.2.1. Braille alphabet definition

Braille is a tactile writing system that is used by visually impaired people. The Alphabet consists of combinations of six or eight different dots raised, representing the different letters and abbreviations in a language, as shown in Fig. 1.1. Combinations may differ for languages, and may or may not contain abbreviations.

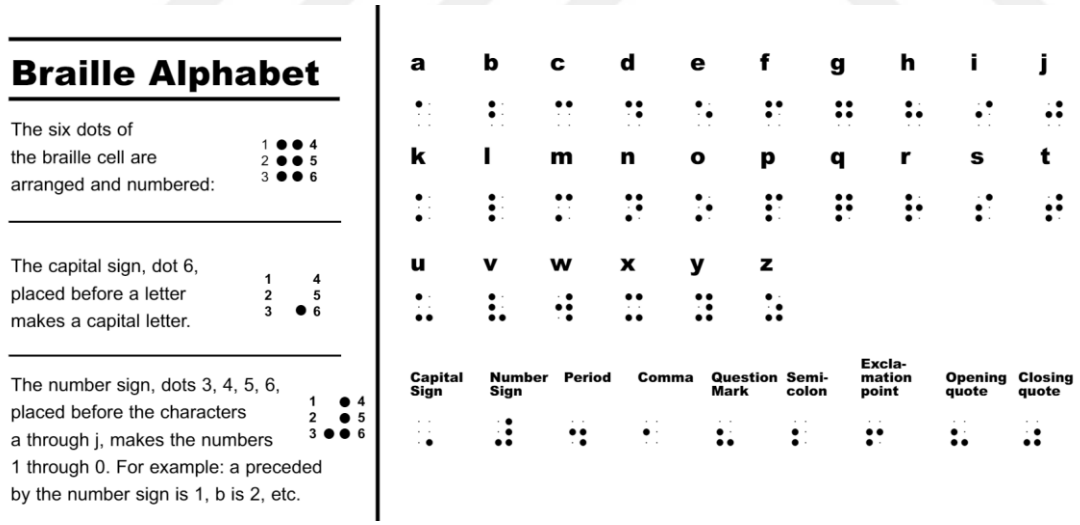

Figure 1. 1: Braille alphabet for the English language [10].

1.2.2 Standards for writing braille

A Braille letter occupies the same amount of space regardless of the number of dots. Therefore, some conventions are followed by Braille producing countries. Table 1.3 shows the size and spacing for Braille dots.

Table 1.3: Size and spacing for a Braille cell.

Measurement Range	Minimum in Inches Maximum in Inches
Dot Base Diameter	0.059 (1.5mm) to 0.063 (1.6mm)
Distance between two dots in the same cell	0.090 (2.3mm) to 0.100 (2.5mm)
Distance between corresponding dots in adjacent cells	0.241 (6.1mm) to 0.300 (7.6mm)
Dot height	0.025 (0.6mm) to 0.037 (0.9mm)
Distance between corresponding dots from one cell directly below	0.395 (10.0mm) to 0.400 (10.2mm)

One convention that is commonly used and published by the National Library Service for the Blind and Physically Handicapped of the Library of Congress [10]. Also, in Fig. 1.2, Braille dot distances specifications are given.

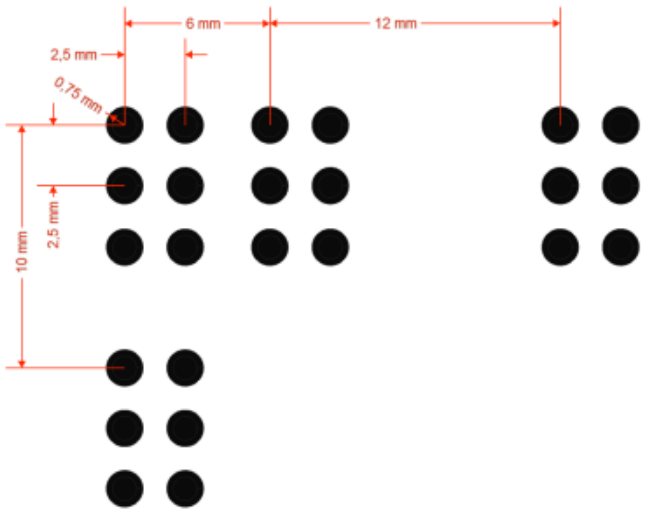

Figure 1. 2: Braille dot distance specifications according to EU Standards [11].

1.2.3 Braille display

Braille displays focus on converting texts from a given input into Braille characters by creating displacements on Braille dots; by doing so, it creates a touch sense for the reader. Many types of methods proposed to complete this task, such as linear Braille, rotating Braille, and panda Braille [12].

Linear Braille displays use actuators like magnetic, piezoelectric, and pneumatic. Each dot in a cell requires to have an actuator. This type of Braille displayer has been more popular amongst the other type of Braille displayers because of their more straightforward structure. Users can read the characters by sliding their fingers through the cells. The size variations of the display can reach up to 100 characters simultaneously. Thus, most of the linear Braille displayers are made on large scales. An example of large scale linear Braille displayers is a device developed by Bristol Braille company [5]. The company focused on providing large scale Braille cells such that the reader would not bother with switching to the next readout frequently. It has 672 actuators. Thus, the device requires a continuous power source.

Rotating Braille first developed in the USA by the National Institute of Standards and Technology (NIST). This device requires a relatively less amount of actuators and can create a longer length of characters [13]. The system includes two rotating wheels with different combinations of pins set in groups of three. Readers can place their fingers on the part of the wheel exposed, and the device creates a static line for the text. These devices are sophisticated compared to linear displays. Also, it has fewer cells compared to linear Braille displays. The combinations of cell groups used for describing certain words or time and dates.

Panda Braille methodology creates an electrical impulse that is sufficient enough to give a sense of Braille dot and not harm the reader. This type of device requires serious calibration and safety standards. Electrode layers represent Braille dots, and when these electrodes layers came in contact with the finger, the pulse is sent. This method reduces the cost due to less amount of mechanical parts are used. However, there are no records of testing the device on subjects [14]. A comparison has been made amongst the types of Braille, and the following table is created [12]. Table 1.4 shows the comparison of Braille display types.

Table 1.4: Comparison of the different types of Braille displays

Braille	Mechanism	Design Complexity	Reliability	Cost
Linear Braille Display	Braille cells along the length of the device	*	***	***
Rotating Braille Display	A rotating wheel with Braille cells along the surface	***	**	**
Panda Braille Display	Electro cutaneous stimulation	***	*	*

The review on Braille displayers shows the most efficient also, the cheapest method is to move pins with linear translation. One of the new generation Braille display device was designed by a company called Perkins. The Perkins Mini is capable of connecting smartphones and computers via both USB and Bluetooth. Also, it has its SD card in which users can put their text documents. The device has 16 cells, each cell with eight refreshable dots. The capability of this device shows the integration capability of Braille devices. However, the cost of Perkins Mini is around 1500$. [15].

1.3 Hypothesis

The Braille display is designed to operate behind the mobile phones on a small scale. Therefore, an electromagnet is designed to operate the dots individually controlled with an input-output expander integrated circuits. However, the size of the electromagnets has made it impossible to provide electrical efficiency. Thus a new method has been suggested. Instead of controlling each dot individually, a group of dots will be controlled with mechanical constrains to press dots combinations. The text data are taken from the mobile phone via Bluetooth connections.

2. DESIGN

Most of the Braille display applications designed to have a Braille displayer, a keyboard, and interfaces modules. That does not mean all functions have to be provided in a Braille display product. However, specific tasks must be considered. For example, to be able to provide data to a Braille display, the display needs a USB or a Bluetooth connection. Unlike stationary Braille displayers, mobile displayers require rechargeable battery via battery charger or USB. The prototype design and development lies in high interoperability between the most widely used devices using open standards. Additionally, it has to use the technologies that will reduce the manufacturing costs compared to available devices significantly. Fig. 2.1 shows Braille display components.

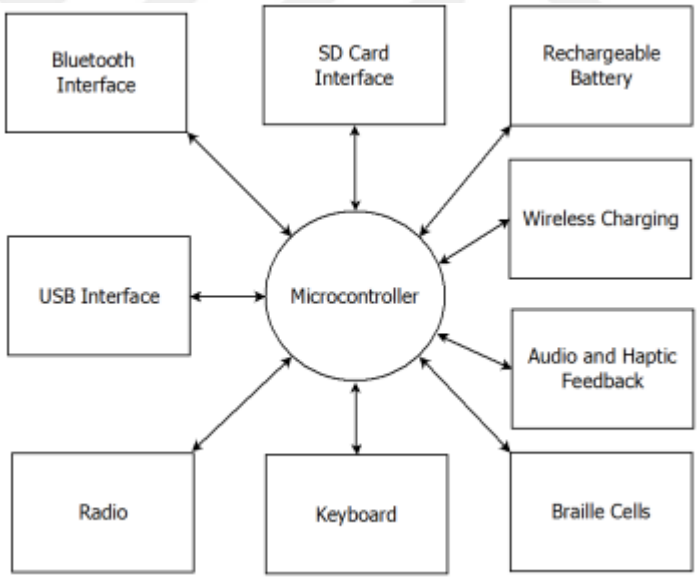

Figure 2. 1: Design of hardware components regarding the Braille display

The basic requirements are deducted from Braille market research as well as state of the art devices [16]:

- Refreshable display of minimum of eight cells each holding six-dots
- Reading the content of files on an SD card for stand-alone operation
- Computers and portable devices can be connected via USB and Bluetooth
- Eight Braille input keys and space bar

- Four-way arrow and selection control keys
- Two panning control bars
- Date, time and calculator function
- Rechargeable battery with additional wireless charging
- Audio and haptic feedback

However, the main goal of this project is to design a phone case that will provide Braille displays. Therefore, it is not necessarily providing all essential requirements. The smartphone case provides Braille pins when the user wants to read characters from the mobile phone. By neglecting some of the requirements, it will be possible to increase the battery usage time.

2.1 Braille Cell Technologies

One Braille cell must have at least six dots, which each dot has to individually controlled. Thus, cell dots can be embossed in a combination referring to the desired character. To be able to emboss each dot, there are certain actuator technologies. The most three used topologies are the piezoelectric, electromagnetic, and micro motor based mechanisms. However, there are unique topologies, such as shape memory alloy and electroactive polymers [16].

2.1.1. Piezoelectric braille cell

The most common mechanism used for operating Braille cells is the piezoelectric actuators. The Braille cell consists out of piezoelectric bimorphs. The system has PCB and mechanical construction to drive pins. However, a high voltage of 200V has to be applied, which will bend the bimorphs through electric excitation with the desired elongation. Those bimorphs are connected to a lever that embosses a dot of the Braille cell. [17,18]. In Fig. 2.2 a piezoelectric Braille module can be seen.

Figure 2. 2: Piezoelectric Braille module with eight dots [18].

2.1.2 Electromagnetic braille cell

This type of Braille cell, each dot is moved by electromagnetic actuators. Small magnets can move up and down that are placed in a cylindrical component between the coil. Two ferromagnetic materials magnetic force attraction hold the dot in the desired position. A project covering this technology is the so-called Modular Low-cost Braille Electronic Display (MOLBED). This project is constructed and designed in a way to produce the module as cheap as possible. [19] However, each coil will be driven with H Bridge topology to move bidirectionally. Also, all electromagnetic actuators in Braille displayers operate in one direction. The design can be seen in Fig. 2.3.

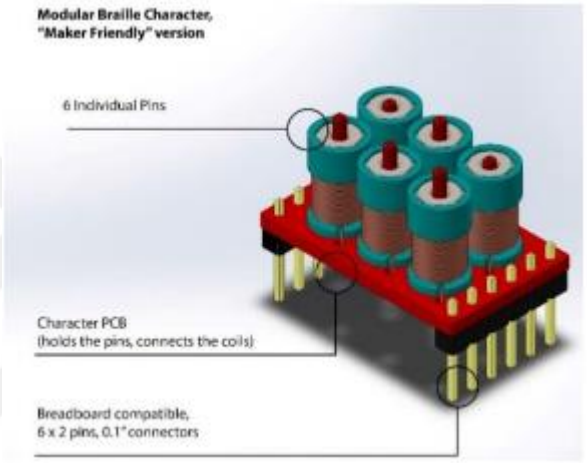

Figure 2. 3: Design of the Braille cell using an electromagnetic concept. [19]

2.1.3 Motor based braille cell

The small-sized motors are used in a variety of applications, such as positioning lenses in image applications. Fortunately, these motors can be used as positioning dots as well. There are various motor types such as step, dc vibration motors that are capable of moving an object in millimeter dimensions. Vibration motors are used to move each dot individually. Thus, one motor requires to move a single dot. By tapering the metallic mass on the driveshaft of the vibration motor, it is possible to lift a pin vertically up and down if it turns to a certain degree [20].

2.2 Implementation

2.2.1 Actuator

An actuator considered to operate bidirectionally in the Braille displayer. The design considerations and constraints have taken into account, such as Braille display

standards. A solenoid is the best selection for the considered actuator. The solenoid will contain a coil winding a plunger and neodymium magnets each side of the solenoid. Solenoids are used for multiple applications such as locking, translation move, switching. The design of solenid is vital to provide enough force to be able to move an object to a certain distance. The commercially available electromagnets either consumes much power, or they do not fit in the physical dimensions to be able to operate Braille display standards.

2.2.2 Actuator driving

Bidirectional solenoids are used in valve operations and linear movement applications. Solenoids consist of windings rounded a ferromagnetic material, plunger, relays, and springs. Due to its inductive characteristics, the movement of the plunger changes the dynamics of magnetic circuits. Thus to obtain a precision movement, physical modeling is required. In order to drive solenoids bidirectional, the winding has to take current from two directions. H- bridge topology is capable of providing positive and negative voltage by using switch-mode components such as bipolar junction transistor.

2.2.3. Mobile phone support

A Bluetooth connection allows pairing a Braille display with smartphones. Thus, it is possible to extract messages shown on the smartphone display and transfer them to the Braille cells. A smartphone operating system called Android has an application service called Braille Back. The settings of the operating system and can be activated when required. As soon as a supported Braille device is connected, the touchscreen behavior changes. Swiping and tapping on the screen will highlight elements on it and display the information on the Braille device. It is required to tap twice or use the buttons on the Braille keyboard to perform a click event if there is one. Similar to Android and Apple includes support for Braille displays and readers. These assistive technologies are implemented for the most widely available and known Braille displays products. For Bluetooth communication, the BLE5 module will be used [21]. The communication between the module and the central processing unit is achieved through Universal Asynchronous Receiver Transmitter (UART).

2.2.4. Battery system

The battery has to be charged in a proper way to use its lifespan as much as possible. Thus, a battery control unit is needed, which can track current and voltage values also inform the microprocessor when the battery is at a critical level. The battery will be selected as Lithium-ion or polymer houses a capacity of 380mAh at 3.7V output voltage [22]. Depending on the solenoids operation voltage, a boost converter will be applied as well. For the battery controller unit, TP4056 module is selected. The integrated circuit has set limitations for voltage limitation at 4.2V and maximum current drainage at 1 ampere [23].

2.3 Actuator Design

The design concept of electromagnets consists of two parts. One is the plunger or moving part; the second part is the static parts, such as the coil and magnet parts. The plunger can be a softcore metal or a ferromagnetic metal. The coil must be wrapped around the plunger's move traction. In order to provide enough electromagnetic force, the turn ratio must be high to lower the current value. Choosing a cross-section of copper will allow putting more turns on the design; however, it will limit the amount of current flowing through the copper, which is 4 Ampere per mm^2. The permanent magnets can be used to provide constant electromagnetic force to keep the plunger in specific positions to maintain it without activating the coils. As mentioned before, most of the Braille displayers had one direction of actuation. However, since the cell phones can be held multiple directions, including towards and against the direction of gravity. The electromagnet has to operate bi-directionally along the plunger's path. Also, it must be able to carry both finger pressure force and gravity force as well. The equation of plunger force can be estimated as in equation 2.1.

$$\boldsymbol{F = \frac{(NI)^2 * \mu_0 * A}{2 * g^2}} \qquad \textbf{(2.1)}$$

where N is the coil turn, *I* is coil current, and A is the area length units squared $\boldsymbol{\mu_0}$ is the permittivity constant and g is the distance between the coil and the solenoid. The plunger must be able to carry 50mN force, including its weight. The plunger has been selected as a softcore metal that has 2g weight. Thus the total force must be higher than 60mN including the dynamic load of the plunger during the startup.

2.3.1. Solenoid equations and circuit

The solenoid can be considered as an inductance-resistance circuit because of having winding copper components. However, inductance value changes depending on the location of the plunger. The voltage equation can be taken as equation 2.2.

$$V = R * i + \frac{\partial Li}{\partial t} = Ri + L\frac{\partial i}{\partial t} + i\frac{\partial L}{\partial t} \quad \textbf{(2.2)}$$

The levitation force that has been produced in the core of the coil. This force is a combination of block and ring magnet's interactions with the magnetic field created by the coil. The magnetic field strength of a coil is defined as

$$H = \frac{NI}{l} \quad \textbf{(2.3)}$$

where N is the number of turns, l is the length of solenoid and I is the current going through the coil. Then, the magnetic field intensity is

$$B = H\mu_m \quad \textbf{(2.4)}$$

where μ_m is the magnetic permeability of the area.

A solenoid essentially acts as a cylindrical magnet; therefore, it can be modeled as one for the force calculation. For simplicity, the bottom block magnet will be modeled as a cylindrical magnet as well with similar dimensions. In the case of the top ring magnet, ring magnets' magnetic properties are obtained with radius R_1, extracted from another cylindrical magnet with radius R_2. Suppose the system is positioned at cylindrical symmetry axis z. Superposition theorem applies for magnetic calculations, so total force acting on the core can be written as in equation 2.5.

$$\vec{F}_{total} = \vec{F}_1 + \vec{F}_2 \quad \textbf{(2.5)}$$

where $\vec{F}_1$ is the force between the bottom magnet and the coil. $\vec{F}_2$ is the force between the top magnet and the coil. The force between two magnets can be expressed as the derivation of the total system energy, E

$$\vec{F}_z = -\nabla E \quad \textbf{(2.6)}$$

then the interaction of two magnets can be expressed as in equation (2.6).

$$F_z = -\frac{\partial E}{\partial Z} = 2\pi\mu_0 M^2 R^3 \frac{\partial J_d}{\partial Z} \quad \textbf{(2.7)}$$

where μ_0 is the permeability of the gap, J_d is the dipolar coupling integral, M is the saturation magnetization of the magnet and R is the outer radius [24].Dipolar coupling integral is defined by Beleggia and De Graef,

$$J_d(\tau_1, \tau_1, \delta) = 2\int_0^{+\infty} \frac{J_1^2(q)}{q^2} \sinh(q\tau_1) \sinh(q\tau_2)\, e^{-q\delta} dq \qquad \textbf{(2.8)}$$

where $\delta = Z/R$ is the reduced distance between the centers of magnets Fig. 2.4, $J_1(q)$ is a modified Bessel function, $\tau_{1,2} = L/2R$ is the aspect ratios of the cylinders [25].

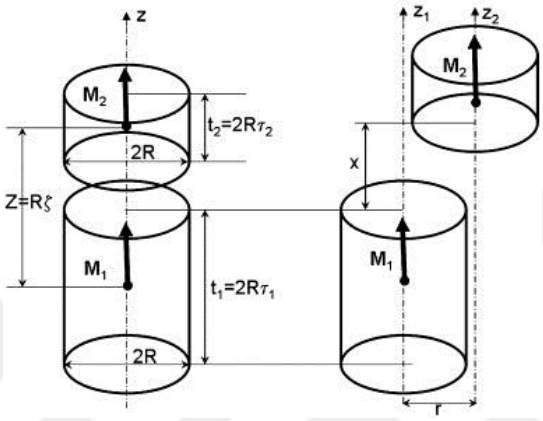

Figure 2. 4: Position of 2 magnets attracting each other[25].

If the integral converges uniformly, expression in equation 2.9 can be rewritten [24].

$$F_Z = -8\pi K_d R^2 \int_0^{+\infty} \frac{J_1^2(q)}{q^2} \sinh(q\tau_1) \sinh(q\tau_2)\, e^{-q\delta} dq \qquad \textbf{(2.9)}$$

$K_d = \mu_0 M^2/2$ is the magnetostatic energy constant. Here, it is suggested in [28] to convert the integral into a more suitable form for numerical evaluation, then integral becomes,

$$A_{\mu\nu}^{\propto}(a, b, c) = \int_0^{+\infty} x^{\propto -1} e^{-ax} J_\mu(bx) J_\nu(cx) dx \qquad \textbf{(2.10)}$$

Equations 2.11 is a representation of hyperbolic integral in terms of exponentials, and the integral in Eq. (2.9) transforms into,

$$F_Z = -2\pi K_d R^2 \sum_{i,j=-1}^{1} i \cdot j \cdot A_{11}^0(\delta + i\tau_1 + i\tau_2, 1,1) \qquad \textbf{(2.11)}$$

According to an article published in 1955 about integrals involving Bessel functions, A_{11}^0 is defined,

$$A_{11}^0(\omega, 1,1) = \frac{\omega}{\pi k_1} E(k_1^2) - \frac{(2+0.5\omega^2)k_1\omega}{2\pi} K(k_1^2) + \frac{1}{2} \qquad \textbf{(2.12)}$$

where $k_1^2 = 4/(4+\omega^2)$, and K and E are complete elliptic integrals of the first and second kind [27]. Complete elliptic integrals of the first and second kind are defined respectively [28].

$$K(k) = \int_0^1 \frac{dt}{\sqrt{(1-t^2)(1-k^2t^2)}}$$

$$E(k) = \int_0^1 \frac{\sqrt{1-k^2t^2}}{\sqrt{1-t^2}}\,dt \qquad \textbf{(2.13)}$$

By using equations above, the force between two magnets of the same type can be calculated. An example code is written in MATLAB. The code is given in Appendix A. However, this solution assumes magnets are the same type and similar in dimensions; therefore, it will not be accurate for the solution of this project. When it comes to forcing analysis between two magnetic objects with different stats, it is quite a challenge to come up with an analytical solution [28]. Therefore, the FEM solution is used for calculations.

2.3.2. Mechanical equation

The mechanical model gives information on the plunger's position, velocity, and acceleration, which is affected by the different forces such as actuators, load, and the movement induced force. By deriving the acceleration from Newton's second law of motion states that the acceleration is equal to the sum of all forces divided by the accelerating mass. The accelerating mass is considered as the plunger.

- Actuator force: The force generated by the coil in the closing direction.
- Movement induced force: The force exerted by the finger touching the dots.

It has been said that magnetic actuators in Braille displays require every dot to be controlled individually. This increases the amount of space that actuators will occupy significantly. Therefore, the design of the actuator is a significant and challenging step.

2.3.3. Modeling

A 2D model of the desired actuator was created before actually analyzing and optimizing at first. The model was made arbitrarily to get an idea of the system. The design is quite similar to magnetic actuators currently in the market. Additionally, a permanent ring magnet was added to the system. The two-dimensional model of the actuator is shown in Fig. 2.5.

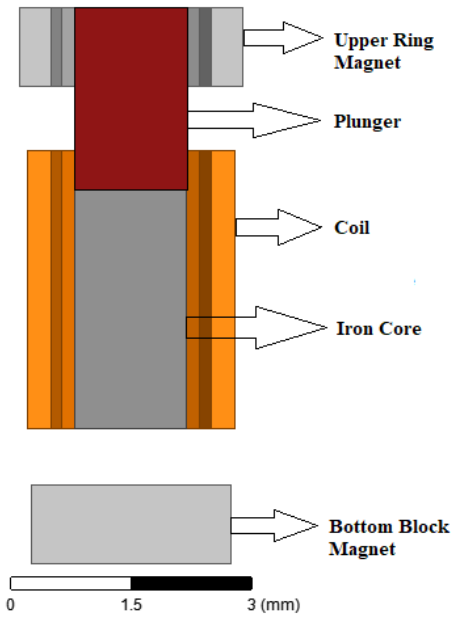

Figure 2. 5: Initial 2D model of the magnetic actuator.

Types of the materials that are selected are shown in Table 2.1. Neodymium magnets are known with their high magnetic flux density; therefore, they are commonly used for electromagnets. The plunger has been chosen iron core because the magnetic field effect may not be able to move lighter materials due to being less ferromagnetic. Soft iron core increases magnetic field strength moderately, due to its high relative permeability. The coil material is selected as copper, which has high electrical conductivity and pretty standard for electromagnetic actuators. The gauge size of copper is taken 0.4mm to have enough current limit value as well as enough turn in a confined area.

Table 2.1: Types of the materials planned for the actuator

Material	Type
Magnets	Neodymium type permanent magnets
Plunger	Soft Core
Coil	Copper Wire

2.3.2. Design constraints

The final form of the Braille display is desired to be relatively small and easy to assemble. To achieve that designed actuator must satisfy the requirements. These requirements highly depend on the spacing standard of a Braille cell, and they are quite strict. Parameters that have been used in design can be listed as:

- The maximum distance between two dots in the same cell is 2.5 mm. Therefore, ring magnet and coil diameters should not exceed that value.
- The height of the actuator does not affect the cell spacing. However, it has been limited to a maximum of one cm long so that the design size would be as thin as phone cases.
- Keeping power consumption at a minimum level. The maximum current value should not exceed 100 milliamperes.
- The plunger must not move larger than 0.5 +- 0.25 mm

2.3.3 Simulations

A Braille dot has to generate a minimum of 50 millinewtons holding force. This value is an essential requirement for the actuator. Therefore, the main goal of the simulations is optimizing the actuator around that requirement. Simulations were made using ANSYS Maxwell, which is a finite element analysis software designed for magnetic studies [29]. A transient type of study has been created, and a 3D model of the desired actuator has been made in Fig. 2.6. The transient study is a great way to perform force analysis. It allows the user to define each parameter freely and obtains accurate results.

2.3.4. Material selection

Maxwell provides a large list of materials to be used, previously decided material types have been added to the solution. Specifications of the materials are given below. In Fig. 2.6, the 3D Model of the electromagnet is shown.

N35 (NdFe35) Type Neodymium Magnet

Relative permeability: 1.099

Magnetic Coercivity: 890 kA/m

Magnetic Flux Density: 1.23 Tesla

Bulk Conductivity: 625000 siemens/m

Iron

Relative permeability: 400

Bulk Conductivity: 10300000 siemens/m

Copper

Relative permeability: 0.99

Bulk Conductivity: 58000000 siemens/m

Figure 2. 6: 3D model created in ANSYS Maxwell for actuator design.

2.3.5. Optimization

Optimization has a vital role in physical model designs. Due to precise dimensions, sizes and working in a small range. Force analysis between two magnetic objects is quite a challenge to come up with a finite element solution [30]. Therefore, optimization is made by manually manipulating parameters and comparing the results of the finite element analysis. The optimization of finite element analysis uses the genetic algorithm, as is shown in Fig. 2.7. The program steps up or down changeable parameters depending on the outcome. The outcomes must be identified with modeling, thus having a mathematical equation. Using the energy or power equations will enough to get the desired result. The magnets' dimensions or material characteristics will not be included. The optimization will be carried out on Ansys Maxwell [29]. Then, the Genetic Algorithm population properties have been set in Fig. 2.7. 1000 iterations and 2 hours elapsed time have been chosen from the program as stopping conditions. 4 parents have been chosen among the best fitness value and a new generation of 30 individuals is created from randomly chosen parents' offsprings. In Fig. 2.8 the set of properties of genetic algorithm has shown.

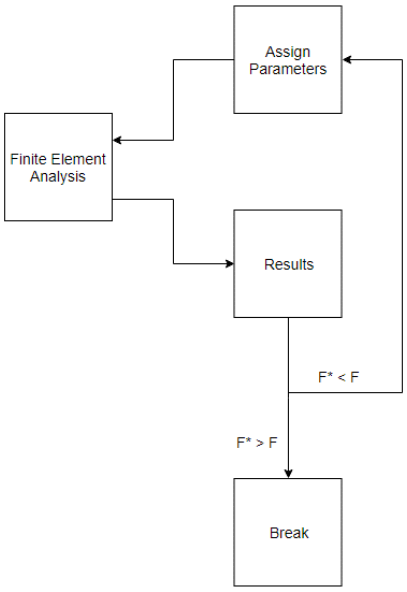

Figure 2. 7: A simple representation of the optimization process of Maxwell Ansys

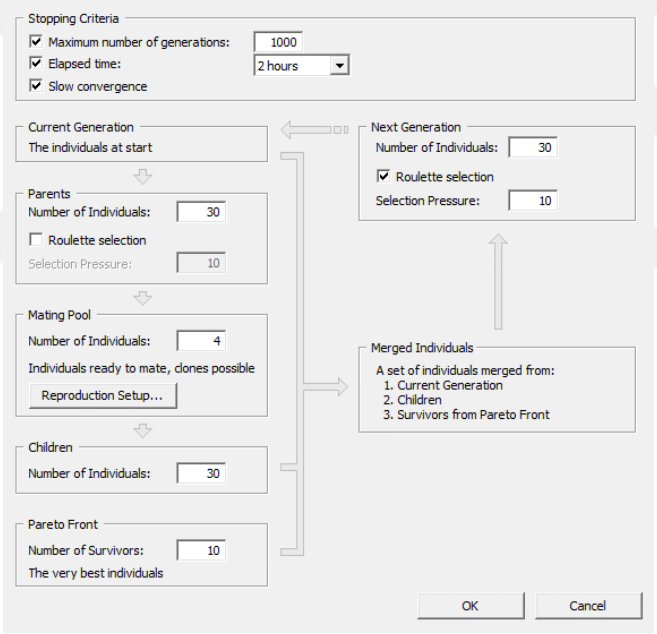

Figure 2. 8: The Genetic Algorithm population settings in Maxwell

The force on the z-axis has chosen as an objective function, and the maximizing property has been, which can be seen in Fig. 2.9.

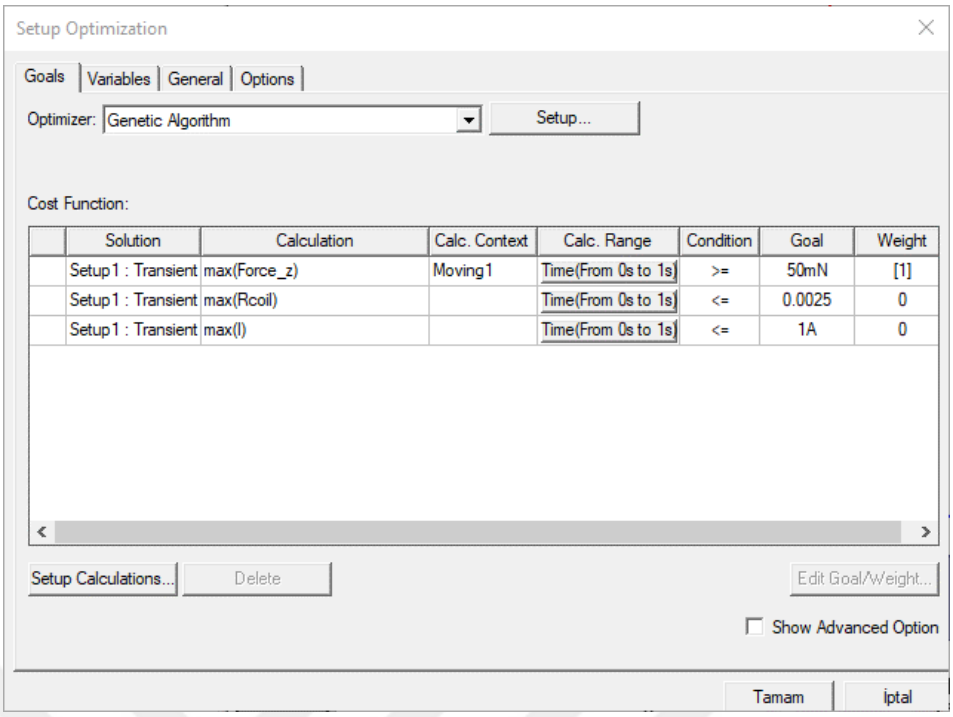

Figure 2. 9: Selection of objective function and solution type.

The optimization problem consists of two main elements:

Objective Function: Primary concern of an optimization problem, which is wanted to be maximized or minimized.

Constraints: Criteria that define the limits of the objective function.

After that optimization problem for magnetic actuator design can be defined as follows:

Objective Function

- Maximizing holding force (min 50mN).

Constraints

- The outer diameter of the coil and ring magnet should not exceed 2.5mm.
- The inner diameter of the ring magnet should not be less than 1.5mm.
- Current flows through the coil should not be more than the current capacity of copper wire.

	Name	Include	Nominal Value	Min	Unit	Max	Unit
	I	☐	V/Res				
	Ro	☐	2.4mm	2.4	mm	2.4	mm
	Ri	☐	1.6mm	1.6	mm	1.6	mm
	hr	☑	1mm	0.5	mm	2	mm
	Rc	☑	0.05mm	0.05	mm	0.2	mm
	hc	☑	4mm	4	mm	6	mm
	hi	☑	3mm	2	mm	4.5	mm
	hb	☑	1mm	0.5	mm	2	mm
	dr	☑	0.5mm	0.25	mm	1	mm
	db	☑	0.5mm	0.25	mm	1	mm
	N	☑	1000	400		1200	
	Res	☐	1.724*(10^(-8))*lc...	14		42	
	Ind	☐	4000*(N^2)*(pi*(R...	2.5		7.5	
	lc	☐	2*3.14*(hc/Rc)*(...				
	V	☐	12V	6	V	18	V

Figure 2. 10: Assignment of the variables and constraints for optimization.

The constraint values of the parameters can be seen in Fig. 2.10. Also in Fig 2.11, The two-dimensional drawing of the electromagnet is shown. Parameters that are manipulated for optimization are:

r_O : Outer diameter of the ring magnet

r_I : Inner diameter of the ring magnet

r_C : Diameter of the copper wire

h_R : Height of the ring magnet

h_C : Height of the coil

h_I : Height of the core

h_B : Height of the block magnet

d_R : Distance between the ring magnet and coil

d_B : Distance between the block magnet and coil

N : Number of turns

I : Current

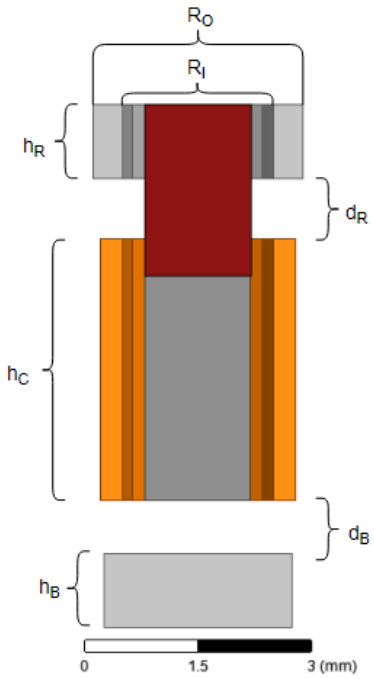

Figure 2. 11: 2D drawing of an electromagnet with parameter positions.

As mentioned earlier outer diameter of the ring magnet should not exceed 2.5mm and inner diameter should not be less than 1.5mm to provide a passage for the plunger. Therefore, ring magnet dimensions cannot be changed. Same as ring magnet, the inner diameter of the coil is bound to the core; therefore, it has kept the same. The outer diameter of the coil depends on the length of the coil and the diameter of the copper wire. It is not included in parameters, because it cannot be directly controlled. Since windings need to go over, equation 2.15 has been used to calculate outer diameter (dimensions are in millimeter).

$$r_o = \frac{2NR_C^2}{h_C} + 1.5 \qquad \textbf{(2.15)}$$

Distances between magnets and coil are important because longer distances might not be sufficient enough to provide enough force. Meanwhile, shorter distances might lock the plunger in the middle due to the static magnetic field of permanent magnets. The current must be controlled to prevent wire damage.

The outer diameter has been found as 2.5 mm using equation 2.16, to be able to find coil resistance and inductance coil length must be known. Coil length can be found with equation 2.16 below.

$$l_C = 2\pi K_C \sum_1^{\frac{N}{K_C}} \frac{R_C}{2} \qquad \textbf{(2.16)}$$

After that resistance and inductance can be calculated as in equation 2.17 and equation 2.18 below.

$$R \cong \frac{\rho l_C}{A} \quad \textbf{(2.17)}$$

$$L \cong \frac{\mu N^2 A}{l_C} \quad \textbf{(2.18)}$$

where ρ is the resistivity of the wire and defined as 1.724×10^{-8}, A is the cross-sectional area of the wire, N is the number of turns and μ is magnetic permeability. Then resistance and inductance are obtained as 120Ω and 90 mH, respectively.

After running several simulations, optimized values of the parameters have been found that are shown in Table 2.2.

Table 2.2: Optimized values of the parameters

Parameter	Optimized Value
$\mathbf{R_O}$	2.4 mm
$\mathbf{R_I}$	1.6 mm
$\mathbf{R_C}$	0.05 mm
$\mathbf{h_R}$	1 mm
$\mathbf{h_C}$	4 mm
$\mathbf{h_I}$	3.5 mm
$\mathbf{h_B}$	1 mm
$\mathbf{d_R}$	0.5 mm
$\mathbf{d_B}$	0.5 mm
N	750
I	0.1 A

After running simulations with optimized values, it is seen that optimization came up with satisfied the objective function previously defined. The optimized finite element results are shown below. Approximately 65 mN of holding force has been obtained, as shown in Fig. 2.12.

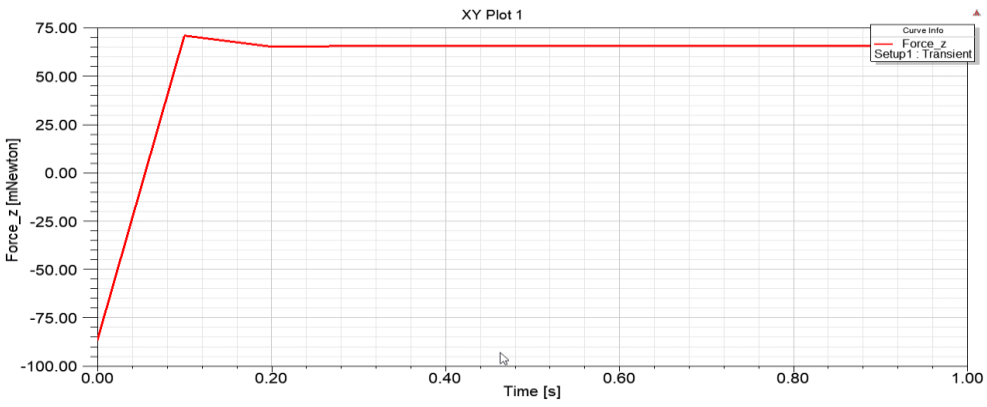

Figure 2. 12: Force-Time graph of the actuator simulation

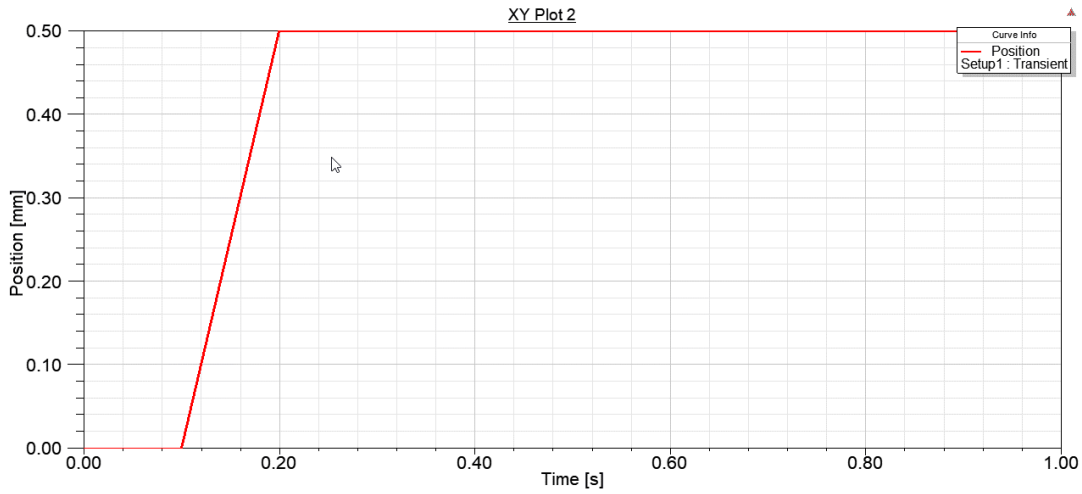

Figure 2. 13: Position-Time graph of the actuator simulation

Fig. 2.13 shows the desired 0.5 mm displacement. It can be seen that the core does not start moving until a certain amount of time. The current value needs to be at a certain value to generate enough force to move the core. Also, a certain amount of time is required to overcome the magnetic force that is holding the core. In Fig. 2.14 the current of the coil is shown. At first ten milliseconds, the slope of the current graph changes because the core started to move, which changed the magnetic response of the system.

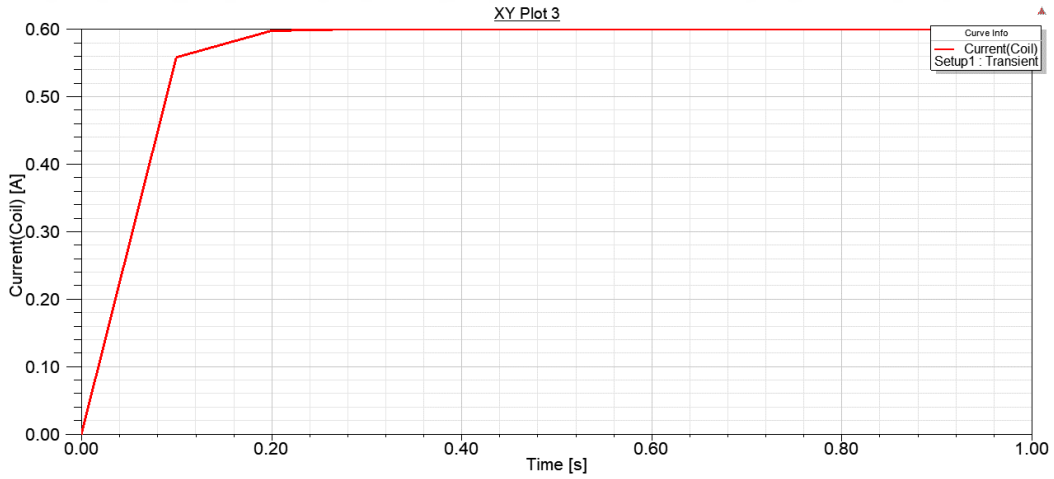

Figure 2. 14: Current-Time graph of the actuator simulation

Coil properties have not been graphed. Instead, they are calculated as follows.

Outer diameter: 2.437 mm

Coil inductance: 138 mH

Coil resistance: 92 ohm

Furthermore, the effect of the ring magnet is examined. The ring magnet was removed from the solution, and simulation is repeated. Fig. 2.15 shows the holding force decreased drastically without the top ring magnet.

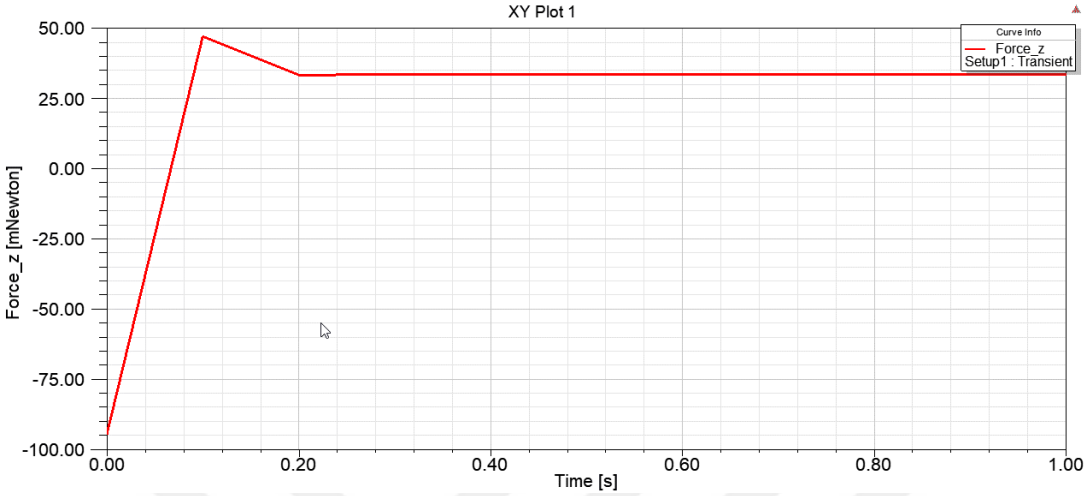

Figure 2. 15: Force-Time graph of the actuator simulation without ring magnet

2.4 Alternative Design

Although the electromagnet operates with satisfactory ranges, it consumes much power. Fig 2.14 shows the current value to hold the plunger is 600 milliamperes. To be able to drive each dot, the system requires 144 I/O to operate all electromagnets. Assuming each electromagnet will be driven with H-Bridge, which will use four transistors. Even with I/O integrated circuit packages, the system becomes too complicated. Therefore power consuming. The designed system requires 100 milliamps to be able to operate at a satisfactory level. The selected I/O expander can provide current up to 160 milliamps. However, the amount of actuators is making the system non-operational in the long run. Also, considering the cost, the production, and operation method of these electromagnets, a practical method is required by lowering the number of actuators.

The portability concept of design on a mobile phone size creates many constraints during the designing process. The selection of the new actuator will have to provide multiple operating dots. However, none of the actuators in the commercial can do that task alone. Actuators require specific physical-mechanical constrain to able to perform numerous dots.

2 phase step motors are widely used in cameras to position lenses and other objects. These motors provide high speed and low torque ratings. Although they provide low torque values, these motors are precise when it comes to positioning. The size and power rates of these motors are suitable for small-sized electromechanical applications. To be able to move objects linearly, these motors attached with a linear ball screw, which propagates along the screw as the motor rotates.

Considering the size and operation constraints, one commercially available step motor has been found. A Chinese vendor called AIYIMA has a step motor with a 3mm diameter and an 8mm screw shaft that operates between 3.3V and 5V in Fig 2.16 [31]. The windings resistances are 15 ohms.

Figure 2. 16: Micro Step Motor with Screw Rod [31].

Along with the motor, a paddle is required to move along the screw rail. Due to low torque ratings of the motor, the paddle must be light-weighted. The stepper motor can divide a full revolution into several steps. The motor can be moved or held at a specific position as long as rated sized in terms of torque and speed are applied. There is a transfer function to how much current is needed for the torque value or how much voltage is required for the speed. Since voltage and current values depend on the impedance of windings, both values affect the mechanical output of the step motor. The value K_i defines as torque constant shows the linear relation of torque and current. K_i can be changed depending on the construction style of the motor. The torque current relation can be seen in equation 2.19.

$$T = K_i * I \tag{2.19}$$

T is torque I is current and K_i is the torque constant. Unfortunately, there are not available datasheets regarding the characteristics of the step motor that will be used.

The size and mechanical shaft specifications made there were no other options to use alternative step motors at this rating with given proper documentation.

The mechanical tolerances and the positioning of the step motor become crucial due to the alignment of dot positions. There are six dots for each cell. Each step motor will be responsible for displaying three dots. Thus, two step motors will be showing one character.

The paddle must be long enough in order to provide all combinations of three dots. Also, the height of the paddle is critical due to the platform that will be the position under the paddles. The platform details will be discussed later on. The paddle designed performing certain pin positions, as shown in Fig. 2.17.

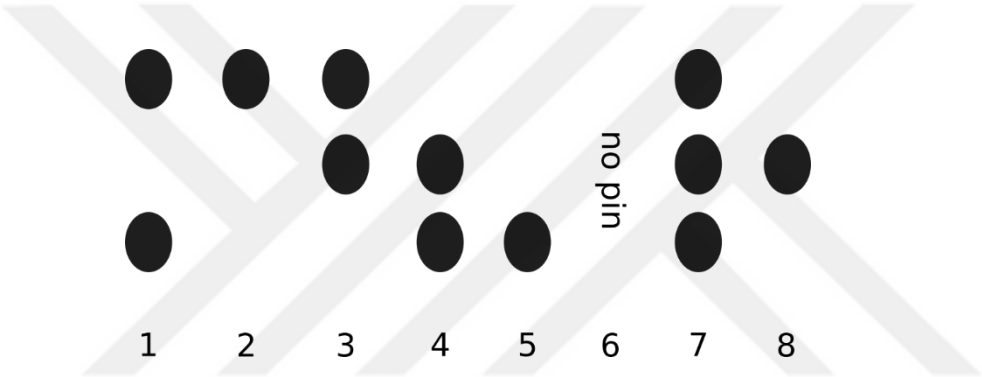

Figure 2. 17: Pin Combinations for each three dots group.

2.5 Mechanical Design

2.5.1. Paddle

The paddle will translate over the screw rod to display pin positions showed in Fig. 2.17. Due to the size and having small geometric tolerances, the paddle can be produced with laser or heat sintering 3D printer method. The top view of the paddle is shown in Fig. 2.18. The paddle is 15mm long, and its height is 8mm. The height of the paddle also determines the height of the Braille display. The height should be enough to create space for pin movements. The higher height values may make the part more brittle in terms of the strength of materials.

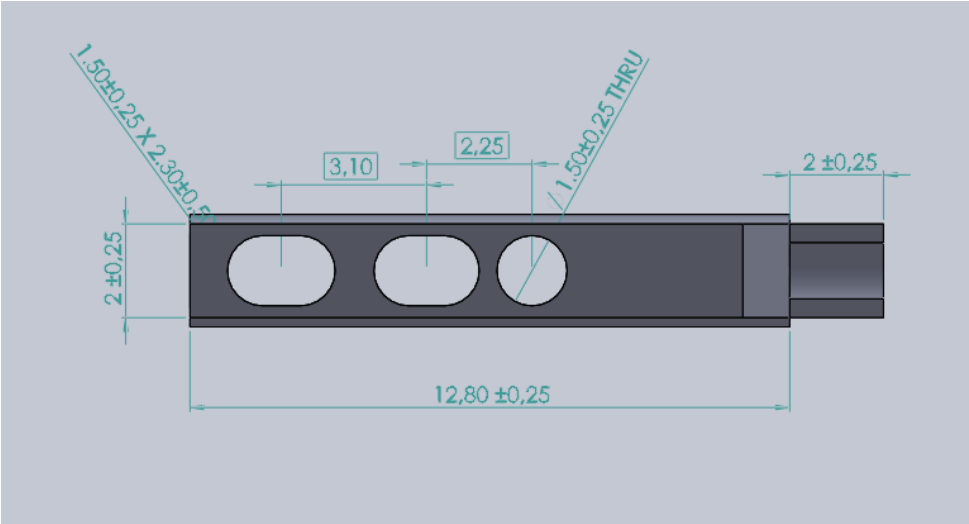

Figure 2. 18: The paddle model from the top view.

As can be seen above, the paddle has two different hole sizes in order to provide pin positions mentioned in the previous section. The size of the paddle can be seen in Fig 2.19. The height of the moving part will be 8mm. However, the height of the whole design may vary due to mechanical structures. By using Fig 2.17, the truth table is created.

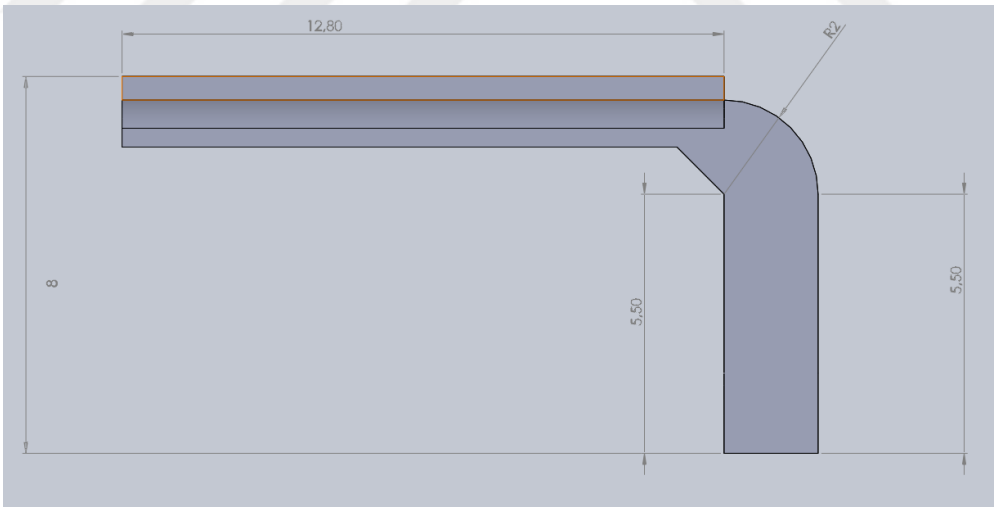

Figure 2. 19: The paddle model from the side view.

The truth table configured from the pin position sets is shown in Table 2.3 below. All characters that are used in the computer keyboard are shown with respect to pin positions. Step motors take positions opposite sides of the Braille display. The pin positions will be taken as distance reference to figure out how many steps that are required to operate the step motors depending on the screw pitch. The number of steps

can only be found after the location of the installation of step motors is established during the mechanical design.

2.5.2. Case

The device will be designed for the mobile phone model called OnePlus 6. There will be two parts of the device. One part is the case to hold the device next to the mobile phone. The other part will contain mechanical, electronic components. In Fig 2.20 shows the component holder side of the device. There are small pinouts in order to position the step motors to position respect to the Braille display. Fig 2.21 shows the Braille device carrier side of the case.

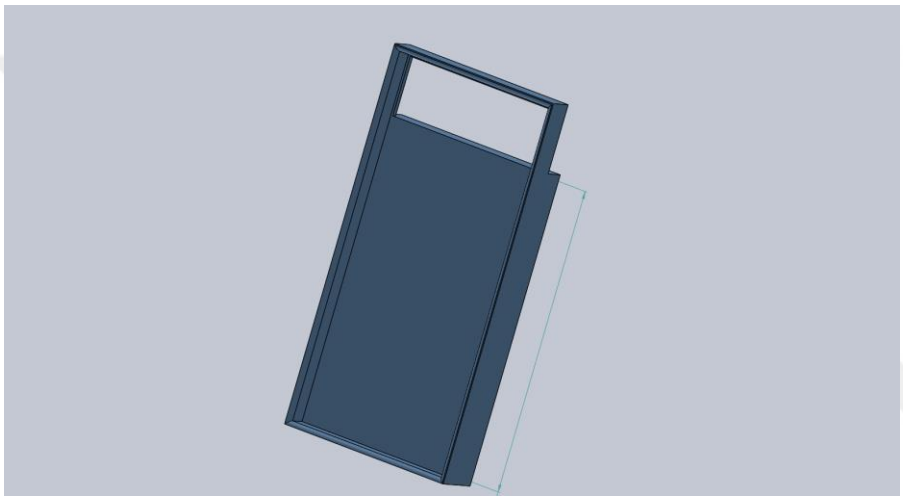

Figure 2. 20: The Phone carrier side of the case.

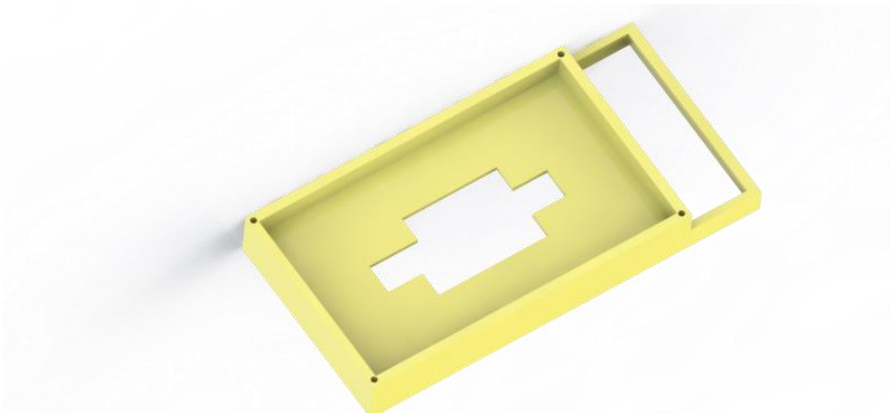

Figure 2. 21: The Braille device carrier side of the case.

Table 2.3: Truth Table for Braille Converting

Character	Pin Position	Character	Pin Position
A	2,6	6	3,5
B	3,6	7	2,6
C	2,5	8	8,4
D	2,4	9	1,6
E	2,8	0	7,6
F	3,5	.	8,3
G	3,4	,	8,6
H	3,8	;	4,6
I	8,5	:	8,8
J	8,4	/	2,5
K	1,6	?	4,2
L	7,6	!	4,8
M	1,5	@	2,4
N	1,4	#	2,7
O	1,8	+	4,8
P	7,5	-	8,8
R	7,4	*	2,8
Q	7,8	“	4,2
S	4,5	”	5,3
T	4,4	‘	5,6
U	1,2	<	3,2
V	7,2	>	5,4
W	8,7	(	4,3
Y	1,7	)	4,3
Z	1,3	Capital letter	6,2
1	2,6	_	5,2
2	3,6	And	7,1
3	2,5	Letter	6,3
4	2,4	number	5,7
5	2,8		

The carrier board is design to align or position crucial equipment in order to move the paddles in a desired direction and magnitudes. The carrier board is a mechanical referencing tool to montage step motors, solenoids, pin holders. Fig. 2.22 shows the carrier board.

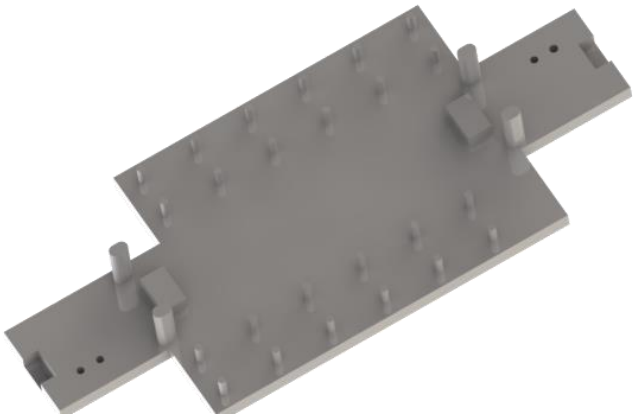

Figure 2. 22: Carrier Board.

2.5.3. Step motor with screw rod

The motor model has modeled respect to given sizes by the commercially available website. The holes on the bottom of the motor will allow the motor to stabilize itself to the mainframe during the operation. The model of the stepper motor model is shown in Fig. 2.23.

Figure 2. 23: Step Motor Model

2.5.4. Braille display carrier

The Braille display carrier will allow paddles to move along the path. The lines next to the Braille holes are designed for paddles to move along. The pins will go along holes that are dispersed by taking account of Braille display standards [10]. The dimensions are 57mm x 10mm x 2mm. There are two holes to attach the display piece to the mainframe with M5 screws. The braille display part can be seen in Fig. 2.24.

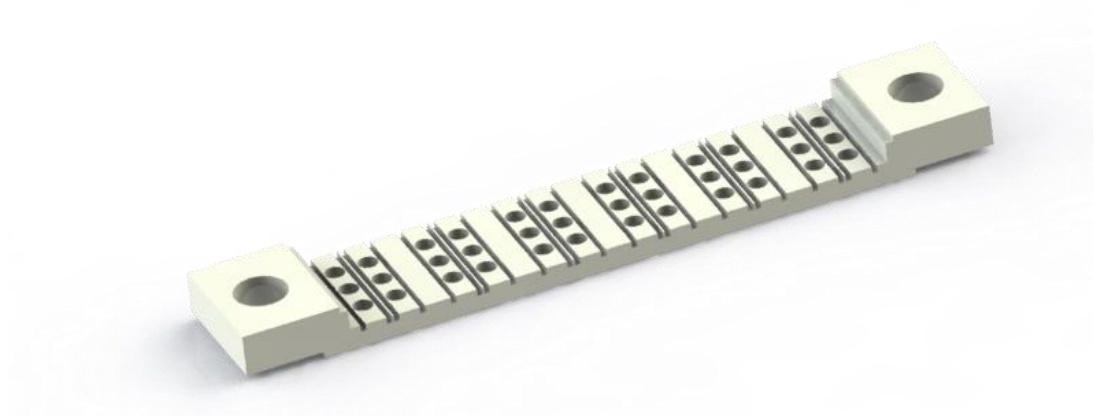

Figure 2. 24: Braille Display Carrier

2.5.5 Pin headers

In order to display dots specific pins, pins have to go through the holes of Braille display. Thus pin arrays are required to move along the path. Pins have to have a spring attachment system when a force is applied; they have to squeeze. After the force is removed, the pin must be retraced back to its original points. Thus a pogo pin system has been selected with two columns 3-row pin alignment, which is precisely the same dot amount in Braille display. The mode of the pin header is shown in Fig. 2.25.

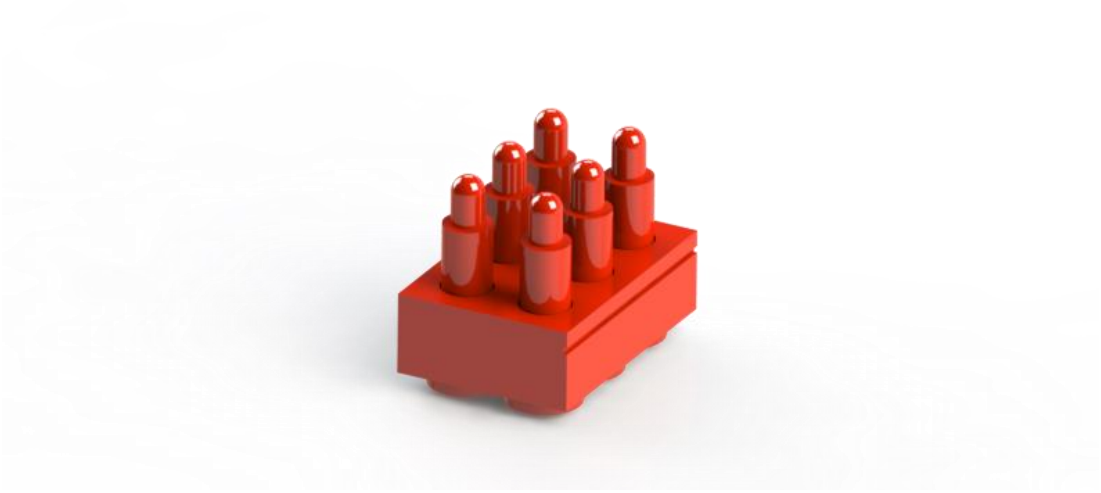

Figure 2. 25: Pin Header Model

The whole mechanical design based on physical constraining. Items that are required to move are squeezed certain parts in order to make sure they move only one-

directional path. The assembly piece of motors paddles and Braille display can be observed in Fig 2.26.

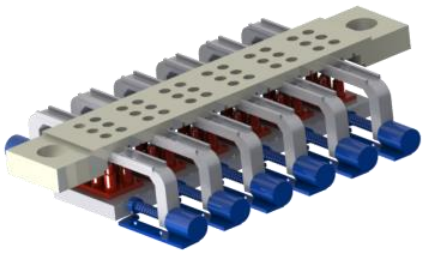

Figure 2. 26: Assembled parts of Braille Displayers

The whole Braille mechanical system's exploded view has shown in Fig 2.27. The pogo pins will be carried out towards the Braille display part by a generic electromagnet.

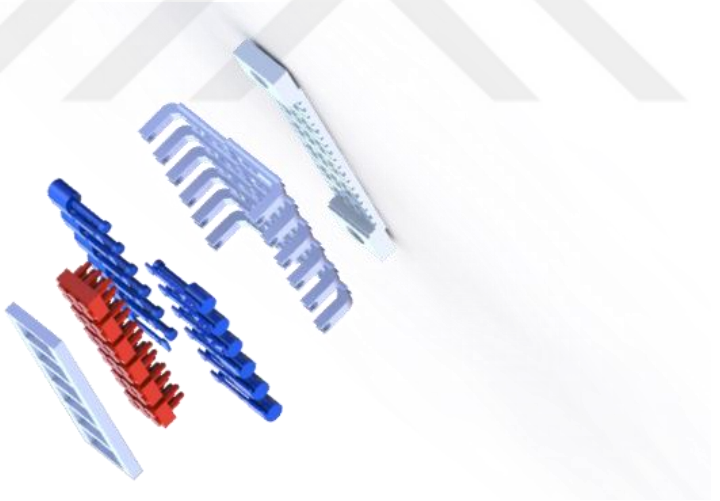

Figure 2. 27: Exploded view of Braille Displayer.

The exploded view of mechanical systems has shown in Fig 2.28.

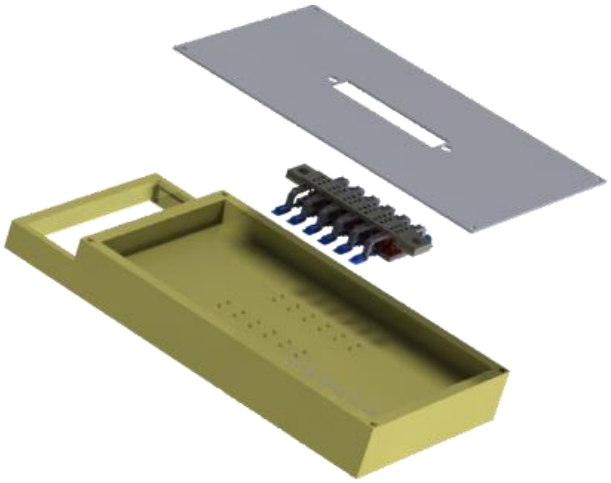

Figure 2. 28: Exploded view of the Mechanical Assembly

The whole mechanical model, including the electronic components, can be seen in Fig 2.29.

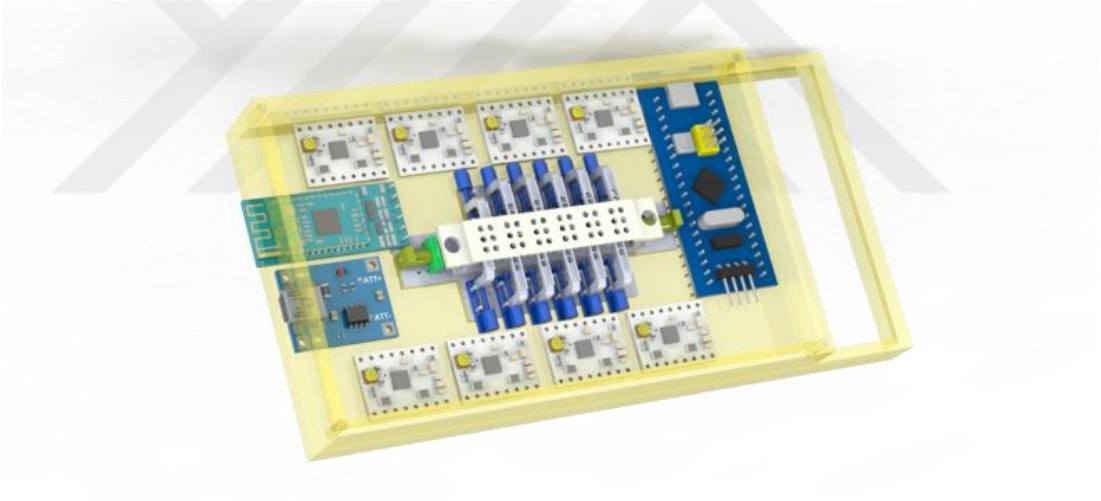

Figure 2. 29: Isometric view of the design model

2.6 Electronic

2.6.1. Topology

Step motor is used in precision applications in the industry due to its basic winding structure, size, and driving topology. Solenoid requires four outputs to push the plunger bidirectionally, and two phases step motor also requires four outputs for each phase in and out. A step motor driver integrated circuits available commercially which operate step motors. The step motor driver can be controlled from microprocessors

Depending on the rotation amount, the operation cycle must be determined to track the position of the paddle on the rod. To minimize the generally proposed input-output pins are used to command step motor drivers. The other option will be using the input-output expenders as considered for solenoids. Although, input-output expander integrated circuits are cheaper than step motor drivers, for the sake of easy, direct and efficient driving step motors are driven with step motor driver integrated circuits. Fig. 2.30 shows the operation flow of the device with a step motor driver.

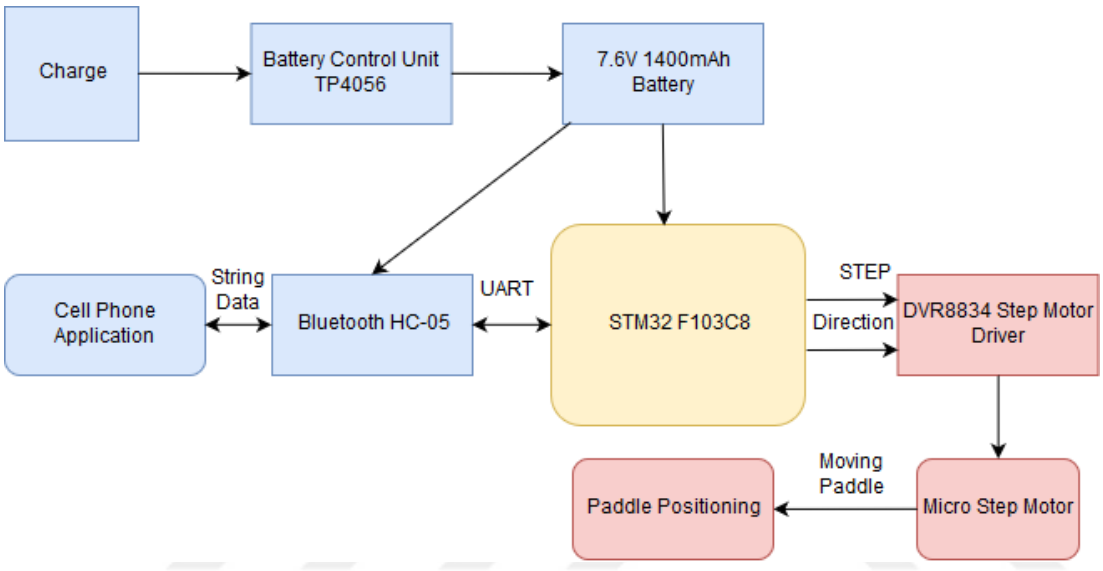

Figure 2. 30: Operation flow of Braille Display with Micro Step Motor as an actuator.

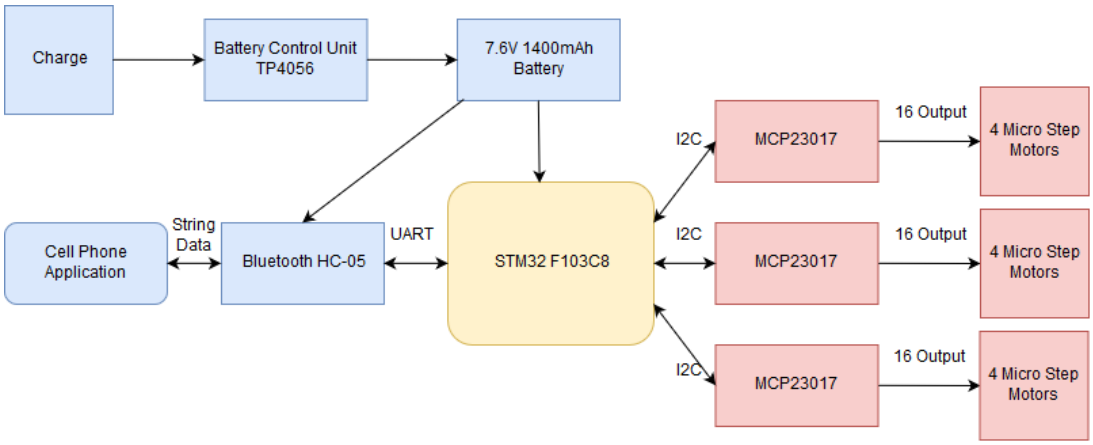

Figure 2. 31: Operation flow of Braille Display with Micro Step Motor as an actuator controlled without a motor driver.

The Fig 2.31 also shows another workflow except micro-step motors is driven with generic input-output expenders. The output current of I/O expander integrated circuit is a maximum of 50 milliamps. The selected step motor can operate at 50 milliamps;

however, under the slightest load, the rod does not move. The resistive and the inductive values of windings vary. The gauge size or the turn size is not available to consumers. For the resistor, each phase value between 15-20 ohm value. The inductive value was measured around one and five micro Henry. The measure was done with a generic LCR meter. Considering a load of the paddle, although it is less than 2gr, the maximum value of operation current for step motors taken as 160 milliamps. Therefore, the I2C input-output expenders cannot be used for this application. However, the integrated circuit can be considered for large module control systems where no current output is used for actuator source.

2.6.2 Components

The Braille display will be controlled with a microcontroller board set with a 32-bit ARM Cortex- M0 chip. The set has a microprocessor speed up to 72 MHz. It provides 32Kbyte Flash along with 8Kbyte RAM, 12 analog input and output ports, hardware Serial, Serial Peripheral Interface, I2C connections a total of 27 input-output pins [32].STM32 F103C8 Bluepill is a development board housing the ARM Cortex M0 processor chip with all required communications port and a power supply. The headers of the board can be attached to the main circuit board. In order to drive the motors, a step motor controller integrated circuit DRV8834 by Texas Instruments will be used [33]. The driver requires direction and the amount of step that the motor needs to take, which can be provided through the microprocessor with generic input-output pins. The motors rated current value is 120 mA. The usage of the step motor driver provides logging for positions of paddles on the screw rod. Thus it will be easy to locate the position of paddle compared to driving motors with an input-output expender integrated circuit. A step driver carrier is given Fig. 2.32.

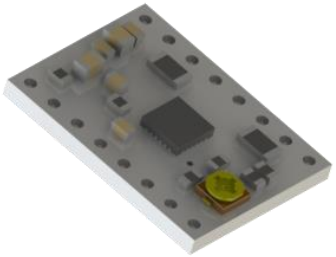

Figure 2. 32: DRV8835 Step motor driver carrier.

The carrier has required resistors to set fault voltage and limit current values for step motor drivers. The current limit value can be set by regulating the potentiometer. The maximum operation current of the driver is 1.5A. In order to operate the micro-step motors, the current limit has been set to 160 milliamps. Fig. 2.33 shows the schematic of the motor driver carrier.

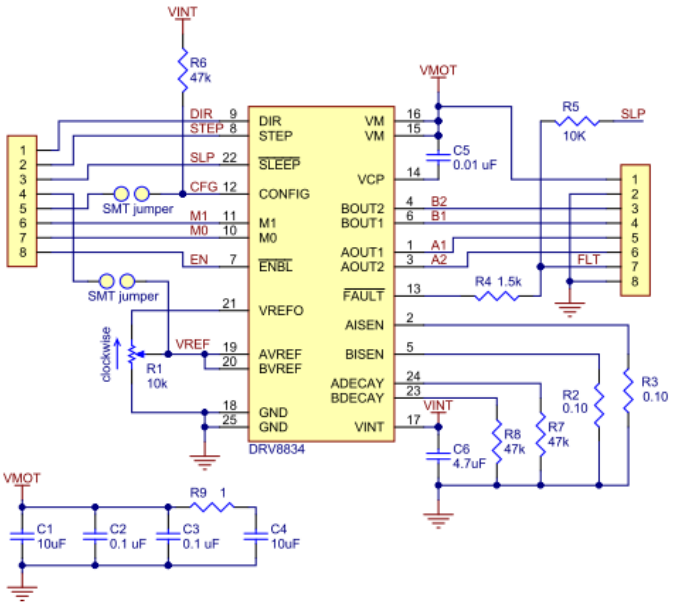

Figure 2. 33: DRV8835 Step motor driver Schematic [33].

The distance of the screw mill is small, as well as the screw pitch. One full step means one rotation of motor which means the mill carrier will move along the size of a screw pitch. Thus the step will always be set to full cycle. The period of movement or occurrence of step can be given in general pull up signal according to datasheet [33].

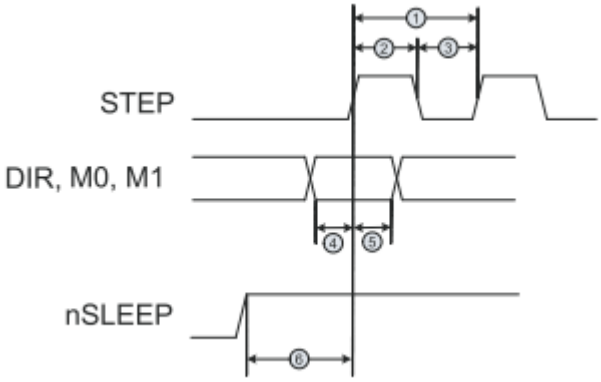

Figure 2. 34: Timing diagram of the motor driver [33].

The frequency of the step signal is 1kHz. In order to activate the driver for the first time, the integrated circuit must be enabled to "nSleep" pin with a high step signal. Afterward, direction and step size will be provided. As seen in Fig. 2.34 step signal must have a high and a low signal in a single period [33]. The amount of square will define the amount step that will be taken by the step motor. The electrical behavior of step motors creates specific problems. The current flowing in the windings does not discharge instantaneously. Thus there is a decay time every time a step winding has been excited. However, the decay can be dampened faster with a decay resistor, but this will create a voltage drop. The speed of the rotor has to operate, considering the decay time, which is small. Also, considering the rated current value is 160mA shortens the decay time as well.

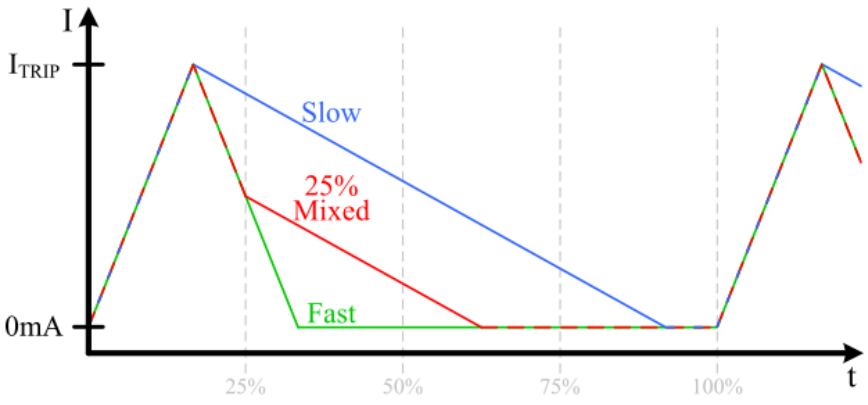

Figure 2. 35: Winding current in a period [33].

The operation voltage of the step motor is recommended at 5 volts. Tempering with the dampening effect may drop the voltage value. Although the step motors can operate

under the rated value, it is not efficient as to do so as well as ending up having lesser torque value as well.

The motor was selected depending on its mechanical features, such as being small and having a screw rod. However, mathematical modeling is needed to understand the capabilities of the step motor. Step motors are brushless direct current motors that require no encoders since they can accurately move between their many poles. These poles are designed with magnet teeth. Due to that, one rotation of a stepper motor requires current exchanges through the windings. Another feature of the stepper motor is to be able to operate in the open-loop constant current mode. Thus no encoder is needed since there is no space for encoders on a 3 millimeter-sized diameter motor. Unless step motors are operated out of their rated values, step motors usually don't lose steps. Also, steppers are capable of stabilizing and holding at their positions without fluctuation, especially under dynamic loads. The Braille paddle does not need to move instantaneously, where stepper motors are the optimal choice for low-speed applications.

Traditional step motors can operate in a constant current mode. The continuous current flow can heat the windings. Therefore, stepper motors may require a resting period or a limitation on current value. The winding impedance and supply voltage determine the current flow; however, the current can be limited by a stepper motor driver or a power electronic circuit pretending the total impedance or load is much higher, which will result in lowering the current value.

By using the datasheet of the selected stepper motor, a control simulation will be prepared. The controller method will be the same one DRV8834 analog circuit control. In order to move the rotor, the windings are excited with supply voltage; thus, creating a current, an electromagnetic field is generated. The collision of electromagnetic fields from both windings and magnets forces the rotor to find its superposition, which is the balance where two magnetic forces cancel out each other. Equation 3.1 and 3.2 show the current change for each phase A and phase B.

$$\frac{di_i}{dt} = \frac{(v_A - Ri_A - e_A)}{L} \quad \textbf{(3.1)}$$

$$\frac{di_i}{dt} = \frac{(v_B - Ri_B - e_B)}{L} \quad \textbf{(3.2)}$$

Where R is the winding resistance, L is the winding inductance, i_A and i_B are the A and B phase winding currents, v_A and v_B are the A and B phase winding voltages. The rotor movement will be depending on the speed, amount of magnet teeth, and the angle. The rotor generated an induced voltage on the windings, which cause voltage drop depending on the angular speed and teeth amount for each phase A and B as shown in equation 3.3 and 3.4.

$$e_A = -K_m \omega \sin(N_r \theta) \quad \textbf{(3.3)}$$

$$e_B = K_m \omega \cos(N_r \theta) \quad \textbf{(3.4)}$$

Where e_A and e_B are the back electromotive forces (EMFs) induced in the A and B phase windings, respectively. N_r is the number of teeth on each of the two rotor poles. The full step-size parameter is $(\pi/2)/N_r$, ω is the angular rotor speed. and Θ is the rotor angle. The mechanical load can be calculated in equation 3.5.

$$J \frac{d\omega}{dt} + B\omega = T_e \quad \textbf{(3.5)}$$

Where T_e is the electrical torque, J is the inertia of the rotor and B is the rotational dampening of the rotor. The generated torque formula is shown in equation 3.6.

$$T_e = -K_m i_a - e_a R_m \sin(N_r \theta) + K_m i_B - e_B R_m \cos(N_r \theta) - T_d \sin(4N_r \theta) \quad \textbf{(3.6)}$$

Where K_m is the motor torque constant, R_m is the magnetizing resistance, T_d is the detent torque amplitude, which can be given 0 for steady-state applications. By using the equations above the plant, the model is prepared. Matlab has a stepper motor tool that provides a parameter input interface to design a controller. The modeling is used in Matlab Simulink where a model of the stepper motor is generated. Fig. 2.36 shows the simulation model of the selected stepper motor.

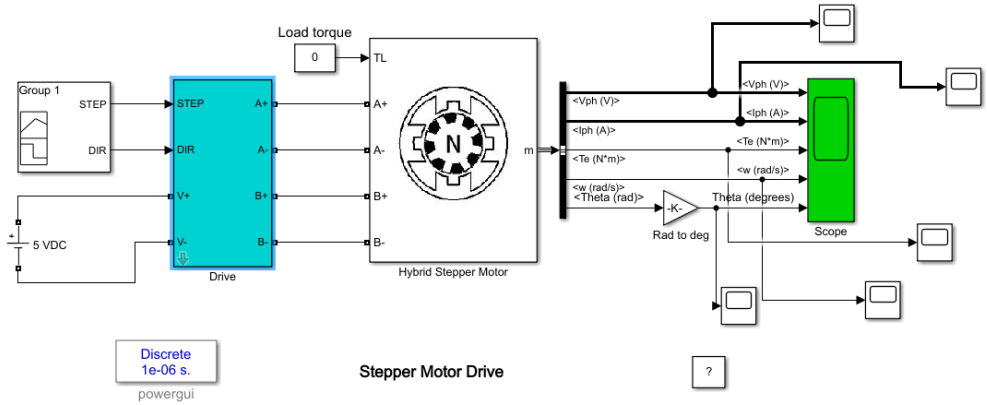

Figure 2. 36: Stepper motor drive diagram in Simulink

The driver has a discrete comparator. The values that are given from STEP and DIR can be taken as high or low conditions. DIR value determines the direction of rotation of the stepper motor. The direction value activates the line of activation of windings. STEP value determines the number of steps that will be taken. The signals must be synchronized as in Fig. 2.32. The driver STEP value triggers the I_{ref} reference value. Depending on the activation, the I_{ref} value is given to the gate driver. Each gate trigger comes from a high value of the STEP driver. However, before current approaching windings, the driver has a shunt current measurement system as there are 2 for each phase for DRV8834. The block diagram of the driver can be seen in Fig. 2.37.

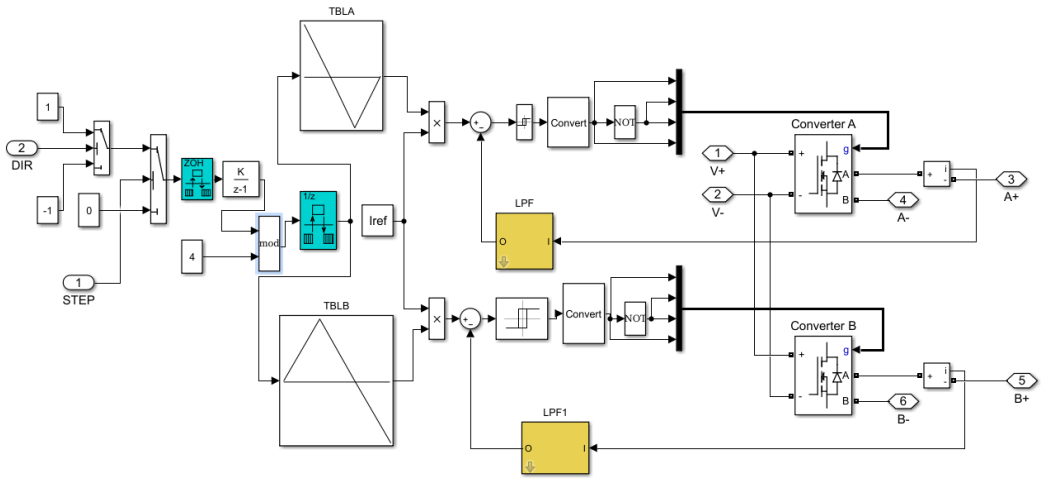

Figure 2. 37: Open-loop controller for the modeled stepper motor.

The register of values will be discretely taken into account. Thus zero-order holders are used in order to operate the system in a desirable period. Also, the comparison of

signals may take time; therefore, the signal must be delayed on purpose. DRV8834 has a current measurement system where checks out whether the current value is at I_{ref} value or not. The movement of full revolution movement, also electrical and mechanical outputs be seen in Fig. 2.38, and Fig. 2.39.

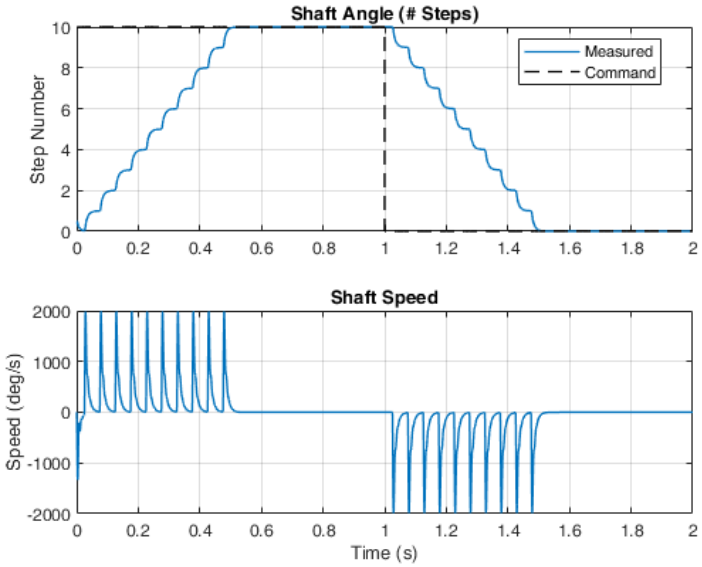

Figure 2. 38: The stepper motor's Shaft Angle-Speed vs. Time graph

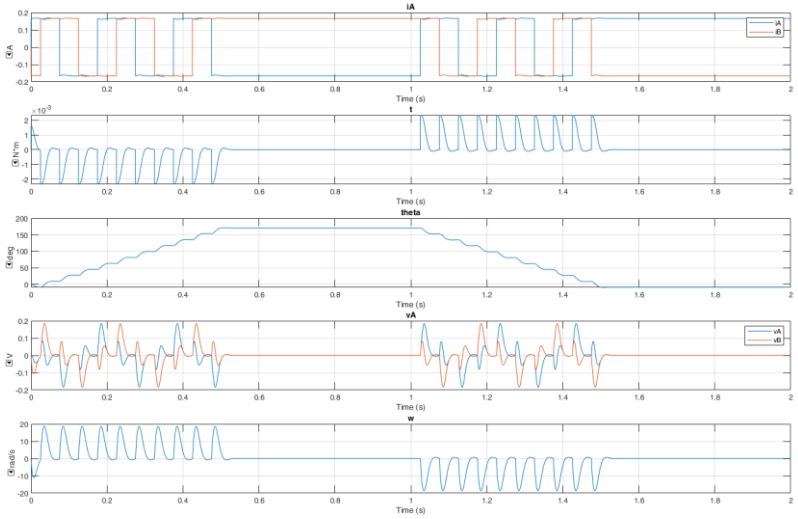

Figure 2. 39: The stepper motor's winding current (Phase A-B), torque, shaft angle, back emf voltage (Phase A-B), angular speed graphs vs. time

Fig. 2.40 shows the phase current and voltage values of one phase of the stepper motor. The maximum current value is 160mA, and the maximum power dissipation

is 0.8 watt. However, the average power dissipation can be considered as 1.6 watts since there are two windings on the motor.

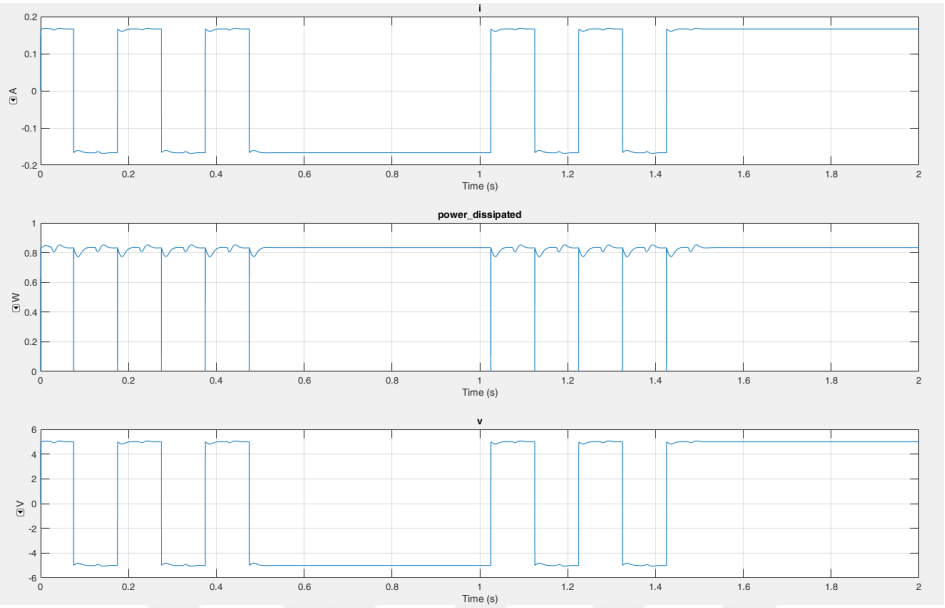

Figure 2. 40: The stepper motors phase current voltage and power dissipation values with respect to time.

The time to take full revolution depends on the stepper motor design. The amount of poles affects the rated speed of the motor due to the back electromagnetic force, which generates a voltage drop on the windings. The simulation is done with the motor characteristics. The values of the motor characteristics are given below.

- R: Winding Resistance 15 ohm
- L: Winding Inductance 7 µH
- Step Angle: 18 Degrees
- Torque Constant: 0.0009 Nm/A
- Maximum Detent Torque: 9e-6 which be taken as zero (kg.m/s)
- Total inertia of rotor: 1.2e-7 ($kg.m^2$)

STEP and DIR signals are generated in order to initiate the simulation or the movement. The motor will do a full step movement clockwise then a half step movement counterclockwise. In order to achieve the desired movement, a pulse signal is generated, both STEP and DIR for 0.1 seconds. Then only a square wave of the signal is generated for STEP signal and DIR kept 0. The signal of both STEP and DIR are shown in Fig. 2.41.

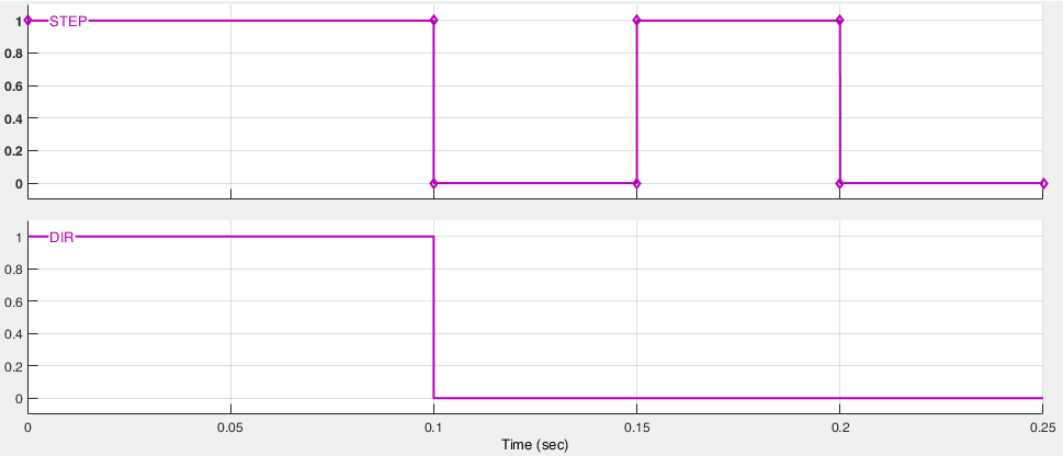

Figure 2. 41: STEP-DIR signals for the simulation

The phase voltage and current values have to correlate with torque and angular velocity movements. Fig. 2.41 shows the simulation results of applying STEP-DIR signals in Fig. 2.31. The motor draws 0.15 amperes maximum. Also, the cogging torque is so low that it does not affect the angular positioning.

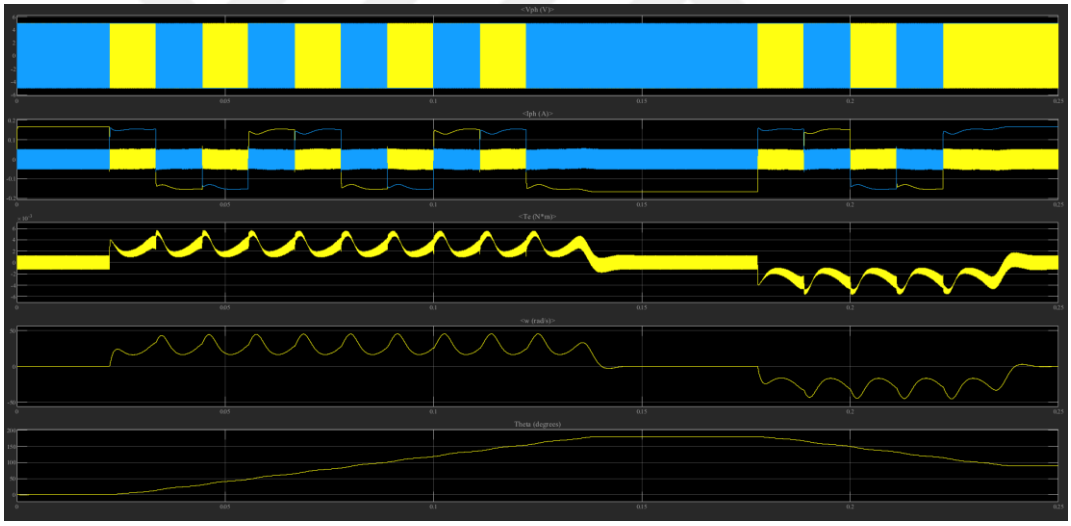

Figure 2. 42: Simulation results of applied STEP DIR signals.

Each graph in Fig. 2.42, the angular position, the angular speed, the torque, phase currents, and voltages respect to time will be shown in Fig. 2.43, Fig. 2.44, Fig. 2.45, Fig. 2.46 and Fig 2.47 accordingly. The most relevant results are the angular positioning when the step signal goes to 0 at 0.1 seconds. The motor continues to move clockwise 0.5 seconds more. The cut of step signal is crucial due to the dampening of current, as mentioned in Fig. 2.23. 0.1 second step gives the driver to go 180 degrees' rotation in 1000 steps. The STEP signal determines how fast the step motor needs to go to the desired position. Thus the angular speed can be adjusting accordingly.

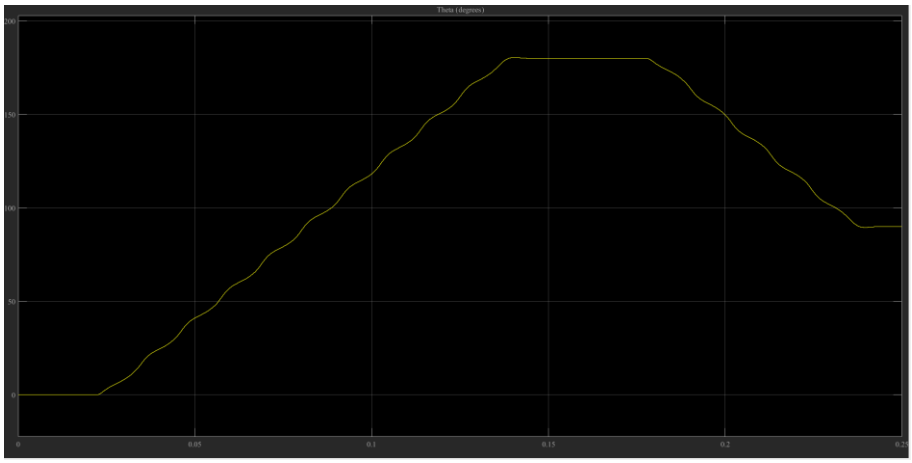

Figure 2. 43: Angular position of stepper motor respect to the time

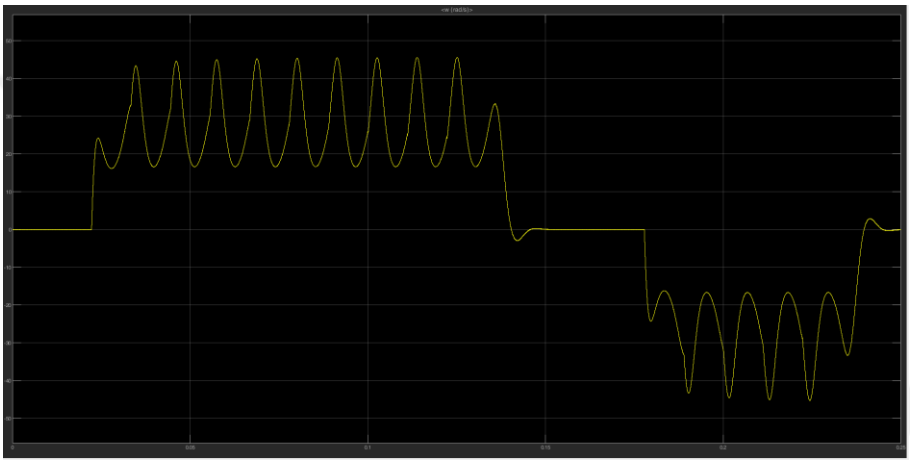

Figure 2. 44: Angular speed of stepper motor respect to the time

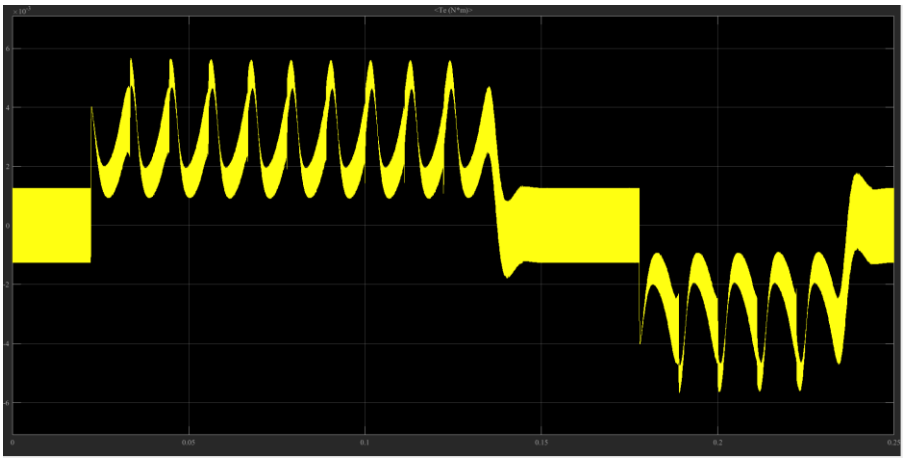

Figure 2. 45: Generated torque of stepper motor respect to the time

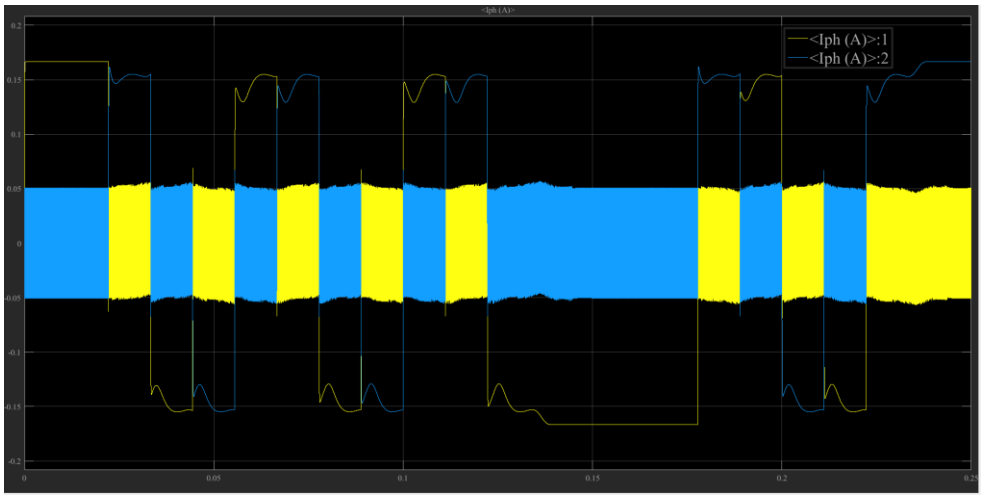

Figure 2. 46: Phase currents of stepper motor respect to the time

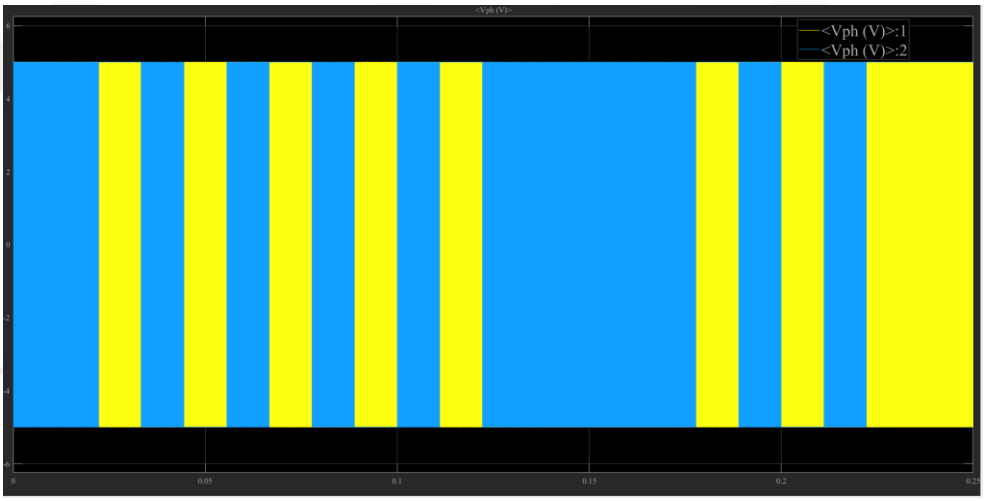

Figure 2. 47: Phase currents of stepper motor respect to the time

In order to operate the stepper motors, a library file has been used as an open-source that can be used for microprocessors such as Arduino, STM, and Teensy. The library has stepper motor driving classes as well as moving multiple stepper units at once for 3D printer applications. The code is given in appendix B.

For communication HC-05 Bluetooth module is used in order to connect every mobile phone in the market. The microprocessor communicates with the HC-05 Bluetooth asynchronous UART protocol. However, the receiver pin of the HC-05 Bluetooth module works with 3.3 volts while the microprocessor works at 5-volt maximum. Therefore, between the microprocessors transmitter pin and receiver pin of the Bluetooth module, there must be a voltage divider to protect the receiver pin. The power consumption of HC-05 during transmission is stated by 40 milliamps [36]. The

circuit is supplied with a lithium-polymer battery, which has the highest power weigh ratio in the commercial market due to the lack of space. The circuit is located in the back frame part where the motors are located. The area of the circuit covers the full size of the inner part of the back frame. A 3.7 volt 380 milliamp per hour lithium polymer has been selected for powering the circuit. However, a future implementation can be done on the mechanical design to create more space for larger power capacity. This will likely increase the thickness of the module. Instead of having a lithium polymer battery, a lithium-ion battery can be installed. Such as The Sony Li-Ion houses a capacity of 2600mAh at 3.7V output voltage. The motor drivers and microprocessors need 5V to operate. The microprocessor carrier has its voltage regulator to operate the microprocessor at 3.3V.

However, the step motor driver needs 5V in order to operate with enough torque lower current values. It is possible to supply 3.3V to the motor, but the motor may not be able to move the paddle with all the friction and side forces applying to the Braille displayer. This action may result in a stall or may miss micro-steps along the way. A stall can harm the windings. Each motor driver was set to draw 150 milliamps per windings. For moving the rotor, two windings must be supplied with 150 milliamps. The traveling of the paddle along the rod occurs less than 2 seconds. During the rotation steps for each half rotation, only two windings are active. Thus means one carrier will consume 120 milliamps per hour. There are 8 of the carriers which make total battery usage of motors will be 960 milliamps per hour. For every paddle to travel on the whole rod, the motors will consume 0.88 milliamps per second.

The step motors provide positioning of paddles. The pins need to be pulled and pushed up and down after and before getting the paddles into their position. The electromagnets are used for moving the Braille pins by moving a carrier. Fortunately, there are commercially available solenoids which look like the designed electromagnet in chapter 2. The solenoids have 5miliHenry inductance and 30 ohms. Electromagnets datasheets are not given; therefore, the turn and copper gauge values are not known. The electromagnet is modeled as an inductor and resistor circuit. The inductor and the resistor values are five mHenry and 25 ohms, respectively. The circuit has been driven with 5 volts supply voltage, and it is shown in Fig. 2.48 that single actuator draws 0.42 amperes, which is satisfactory enough for the desired response.

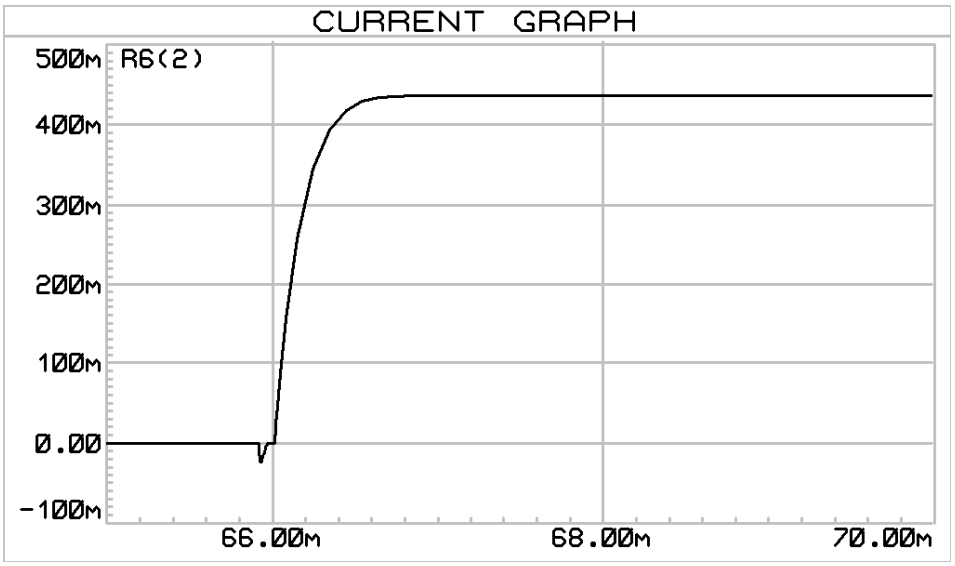

Figure 2. 48: The current graph obtained from PROTEUS simulation.

The pin carrier is made of 3D printing material around 2 grams adding the six pinouts, which each weights 2 grams whole carrier is 14grams. The solenoids are capable of carrying out this weight. In order to drive these solenoids in bidirectional, a H-Bridge module will be used. In order to provide enough current, a Darlington circuit will be used. The transistor is connected with flyback diode from the ground to remove the remaining inductive current flowing in the windings.

The motor driver schematic can be seen in Fig. 2.49. Due to lack of space, only 8 step motor drivers are installed. The microprocessor circuit schematic can be seen in Fig. 2.50. The printed circuit design of Braille display in three dimensions can be seen in Fig. 2.51. The printed circuit board of the circuit can be seen in Fig. 2.52. The traces were too small due to lack of space even though the two-sided copper layer has been used.

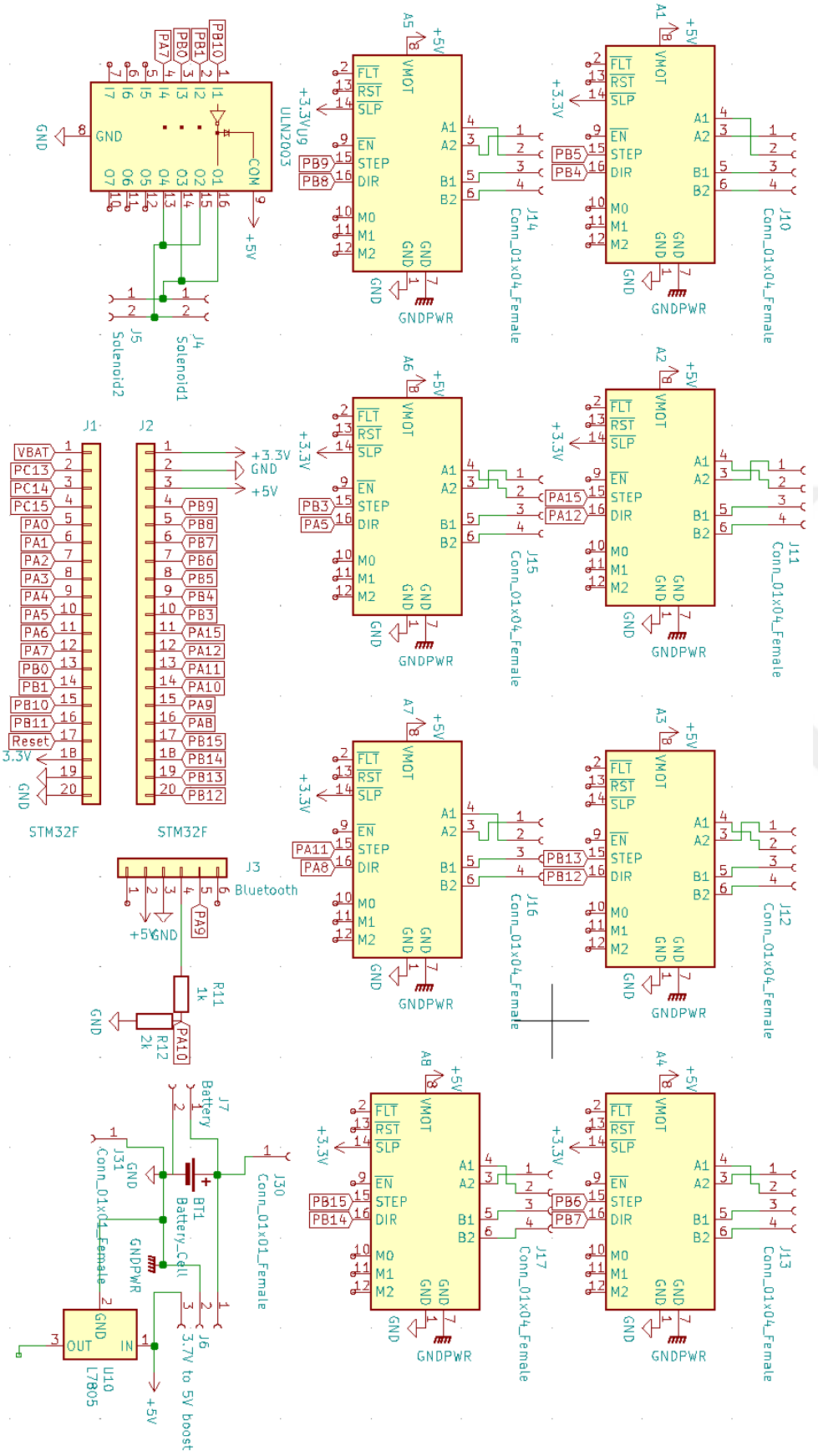

Figure 2. 49: Motor Driver Carriers Schematic Layout

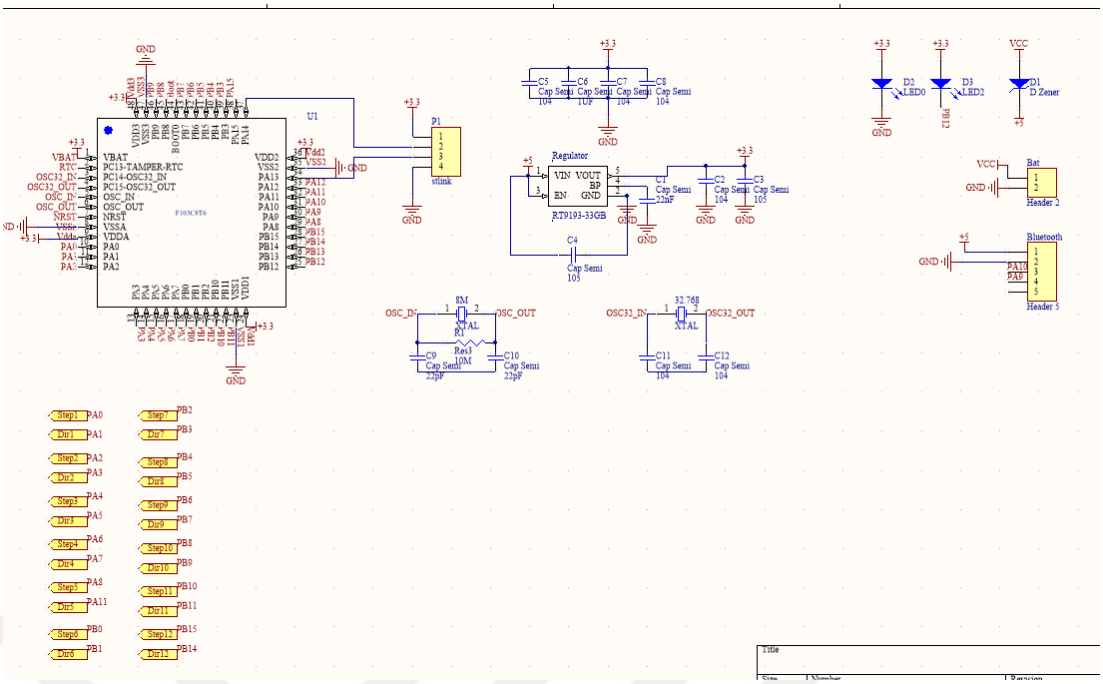

Figure 2. 50: Microprocessor Schematic Layout

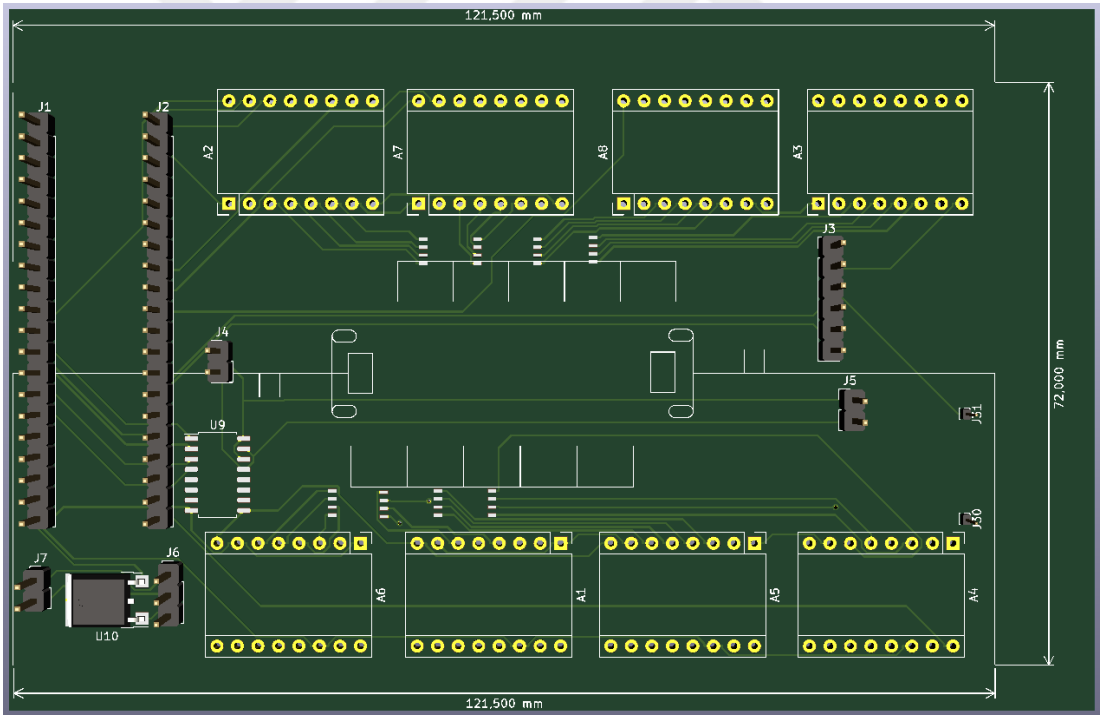

Figure 2. 51: Printed Circuit Design of Braille Display in 3D

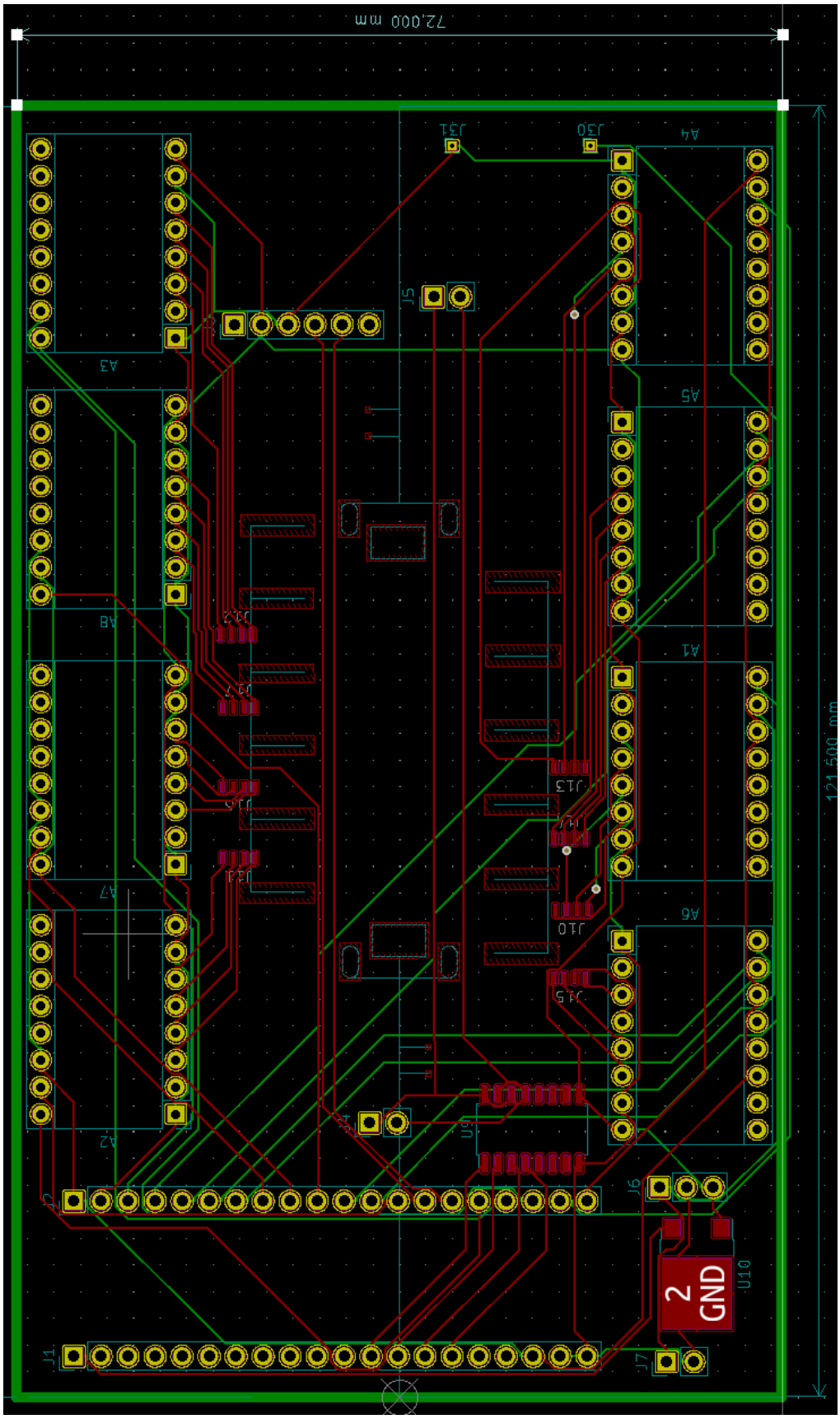

Figure 2. 52: Printed Circuit Design of Braille Display

2.7 Software

In order to gather text data from the phone, an android application has been selected for data gathering. The mobile application mates with the HC-05 Bluetooth module. The module is left at enable position as soon as the device is powered up. The android application transfers each character in ASCII code. ASCII provides a decimal indication of each letter and symbols used in daily language. The English language has been selected for the application. Fig. 2.53 shows the communication layout of the Braille module.

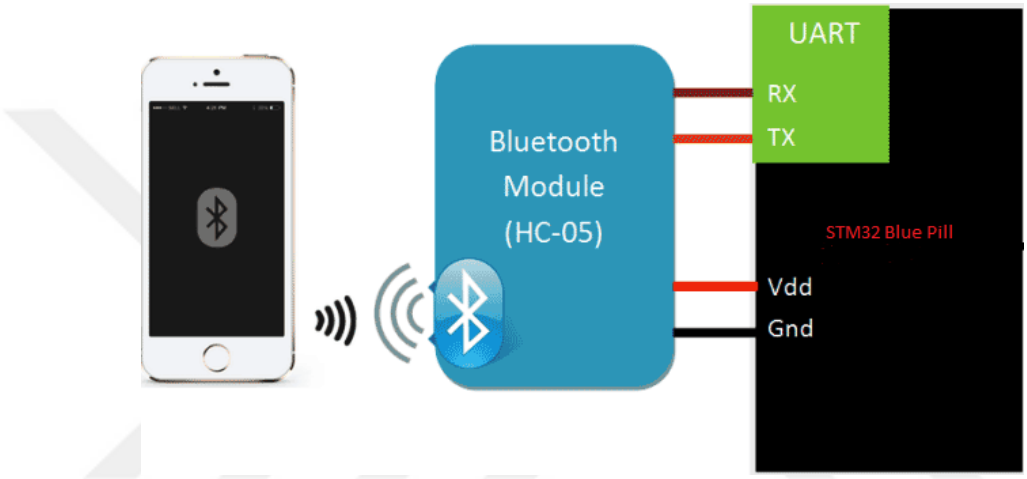

Figure 2. 53: Communication Layout.

The HC-05 module communicates with a mobile device at 115200 baud rate due to Bluetooth standards of mobile phones. However, for the UART protocol, the baud rate can be changed. Since each character takes 8 bits each, the baud rate does not have to be as fast as Bluetooth connection. Thus the baud rate of UART communication between HC-05 and STM32 modules is taken 9600 baud rate for decimal readout. In order to read it hexadecimal, the baud rate will be taken 0x2580 bits/s to minimize the parity errors. Each character will be sent three times to check the parity errors. Since only four characters will be able to display on the board. The algorithm is based on predefined arrays of characters and their binary counterparts. Binary representation is obtained by setting raised pins to 1 and the others to 0, starting from top left to right. For example, the binary equivalent of the letter “A” is 100000, and “G” is 111100. After taking user input, the corresponding indexes of the characters are found in letters array. Then, using those indexes binary expressions obtained from binary values array. Afterwards corresponding pins are set to high and low.

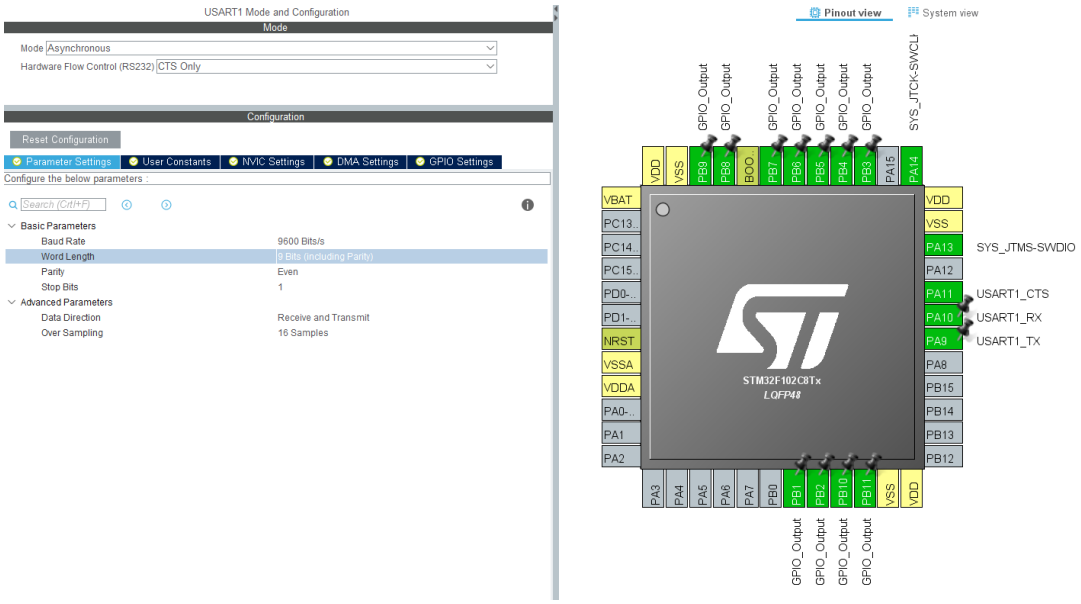

Figure 2. 54: Communication layout and setting on STM32.

STM32CubeMX provides pinout and communication setting arrangements on a java supported platform. During the setting, the program gives warnings related to the capability of selected microprocessors, depending on the usage of functionalized pinouts. Fig 2.54 shows the UART settings of the microprocessor. The word length indicates the number of bits that will send for one character. A character is defined with 8 bits; thus each transmits will identify a character. However, the read access memory value of the microprocessor cannot keep an infinite amount of characters, although it has 8 Kbytes. Since 1 byte is 8 bits, the microprocessor can hold up 8000 characters. There is a significant amount of characters that can be kept in RAM for single usage. However, for simplicity, the storing character amount has been held at 96 characters. The microprocessor will shift the logged characters stored in the RAM as it displays on the Braille display. The shifting command will come from a force sensor there. The user may able to pressure the sensor with the index finger while finishing the readout of Braille display. The sensor will generate a high pulse where it will be a command to shift the next character group to the display. The workflow of the algorithm is shown in Fig. 2.55.

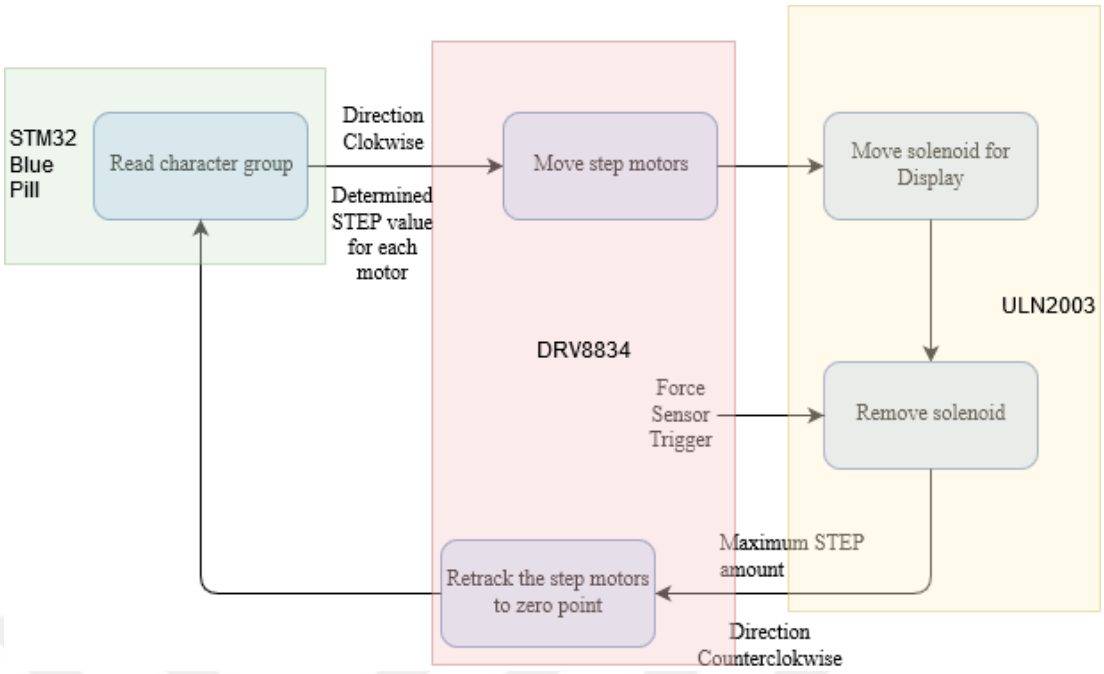

Figure 2. 55: Algorithm flow cycle of STM.

The lack of robustness of step motors and screw rods may not work well on an open-loop controlled system. Due to the limited area and lack of amount of input-output pins, there is no alternative way to measure the position of paddles except keeping the last movement of the paddle. However, the mechanical failures of screw rods or even paddle itself may disable the system. The distances that are required to take are measured in computer-aided drawing program SOLIDWORKS. The paddle length, the position of holes on the paddle, and the screw pitch can affect the number of steps that will be taken into consideration in order to move the paddle to the required position. The screw pitch is 0.5 millimeters which means in one revolution of the rod will move itself 0.5 millimeters along the screw. By programing the motor driver to take a half step the rod can be move half revolution which moves the rod by 0.25 millimeter for each step time command has been delivered. Eight positions were needed for Braille display for a single paddle. To be able to get these eight positions, the paddle needs to move the exact location. Due to working with small-sized items with a lack of robustness, it is hard to get low geometrical tolerances. By using a computer-generated drawing program, an assembly has been made to measure the distances required to get the step amounts, which is shown in Fig. 2.56.

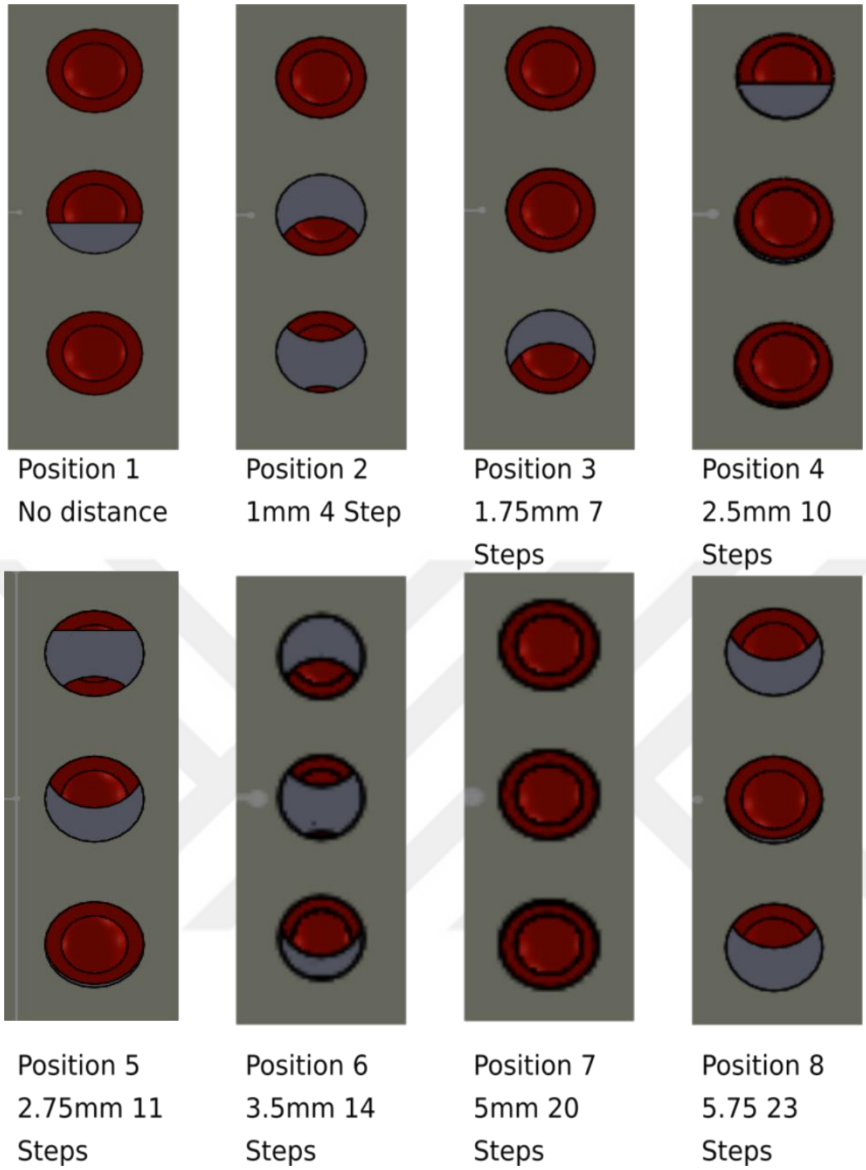

Figure 2. 56: Layout of a paddle for each position.

3. RESULTS

3.1 Components

The components that were designed for the alternative method produced by using SLA type 3D printer ordered via company and PCB printer by LPKF D104. Fig. 3.1 shows the display carrier and pinheads assembled from the top view. In Fig. 3.2 the Braille displayer can be seen.

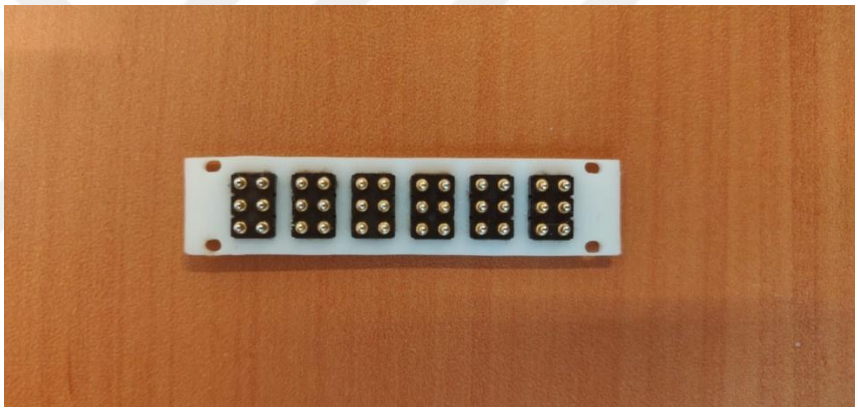

Figure 3. 1: The Display Carrier and Pinheads.

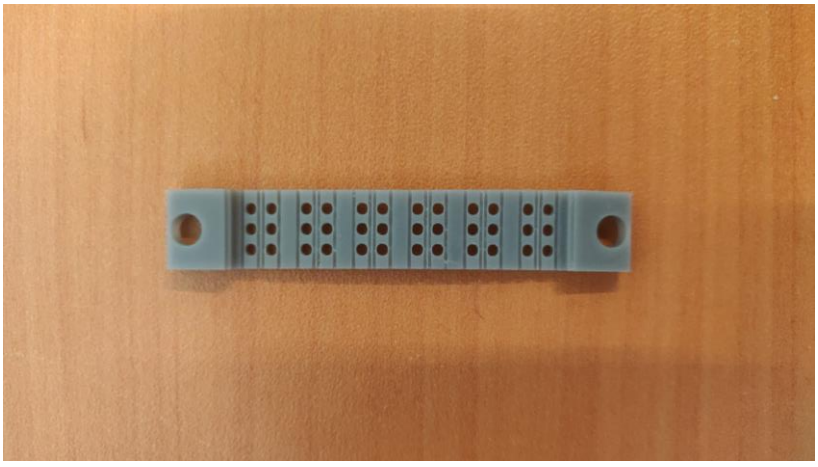

Figure 3. 2: The Braille Displayer.

However, the paddle and the Carrier Board geometry have some defects. The production of the paddle with 3D printer machines was not successful due to the small size dimensions of the paddle. The paddles on the motor is shown in Fig. 3.3. For the

size comparison, a ten kuruş Turkish lira has been put next to the paddles. Due to the paddles' small size, the strength of components has become fragile. Fig 3.4 shows the damaged paddle. The line extrusions are not strong enough, as well as the rod connector part. Moreover, the rigidness of the carrier board has created bending along the longitude of the carrier board. The carrier board in the case module can be seen in Fig. 3.5. Fig 3.6 and Fig 3.7 shows the printed circuit board.

Figure 3. 3: Paddles on the step motors

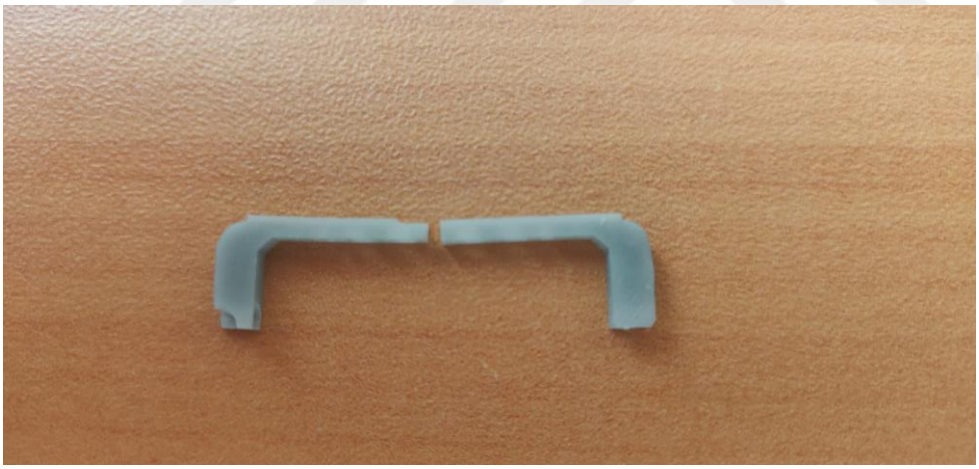

Figure 3. 4: The damaged paddle on the left, rigid paddle on the right

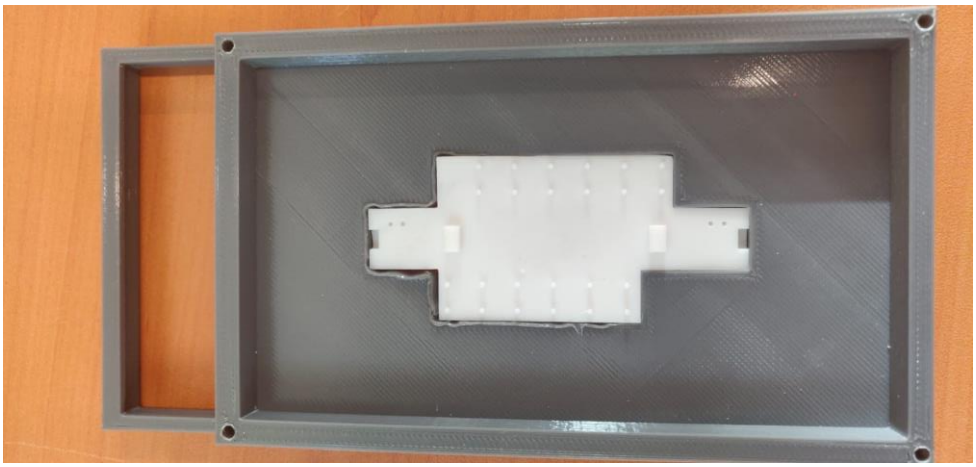

Figure 3. 5: The carrier board in the main case.

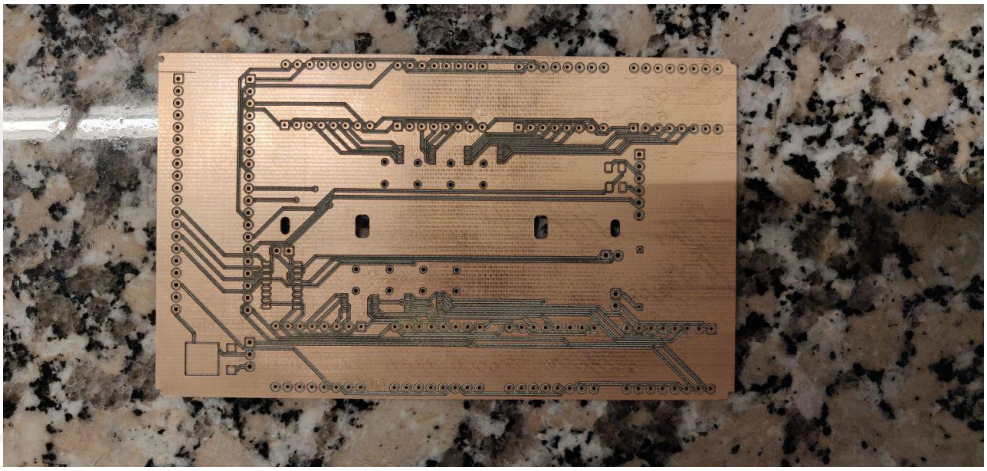

Figure 3. 6: Topside of the circuit.

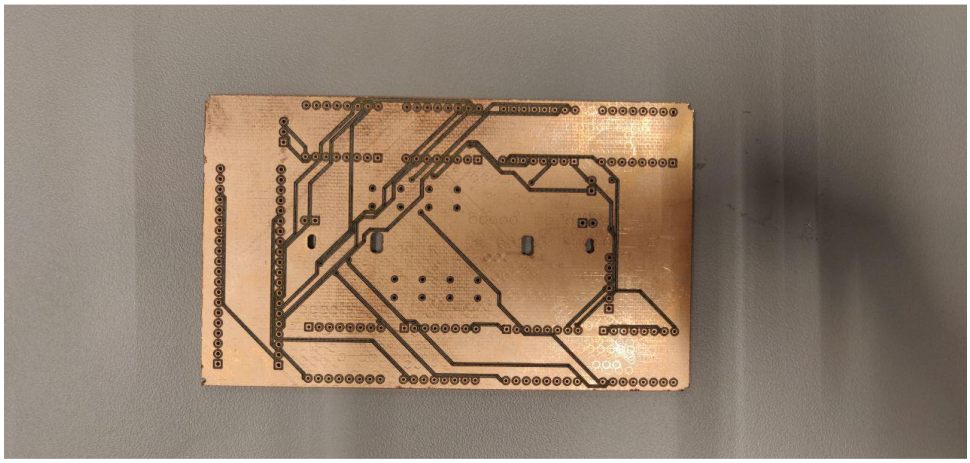

Figure 3. 7: Downside of the circuit.

However, due to lack of geometric tolerances, the module couldn't be assembled. Also, the small electromagnets were not sufficient enough to squeeze the pogo pins due to spring and friction forces. A portable device could not obtain due to a lack of marketing material and production capabilities. It is possible to prototype a mobile device with

better financial and logistical support. In order to prove the stepper motor technique, another design has been done and produced, which has larger space, and electronic parts are not confined in a case. Fig. 3.8 below shows the larger design. The size of the displayer is 80mmx30mmx40mm. The assembly of design can be seen in Fig. 3.9 and Fig. 3.10.

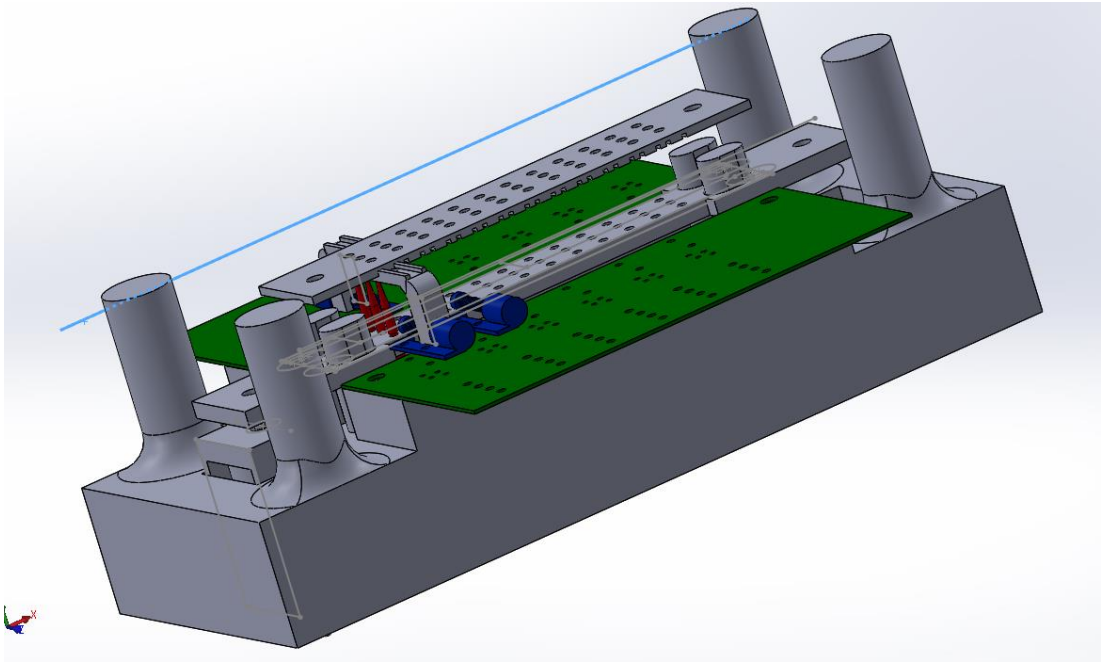

Figure 3. 8: The enlarged design for Braille display

The completed prototype module can be seen in Fig. 3.11. With stepper motor drivers and other electronic components included in Fig. 3.12.

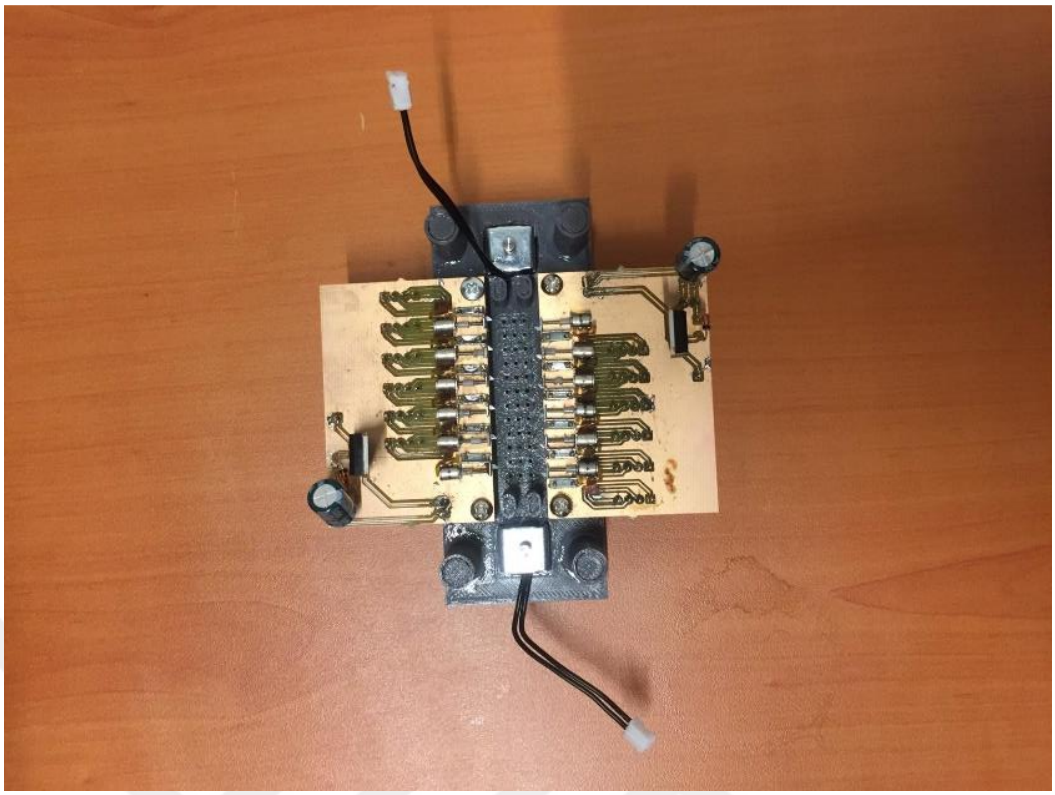

Figure 3. 9: The implementation of Braille displayer.

There are geometric defections on the board due to the printing process. However, the traces and holes do not have any problems. The circuit visuals are shown in Fig. 3.10 and Fig. 3.11.

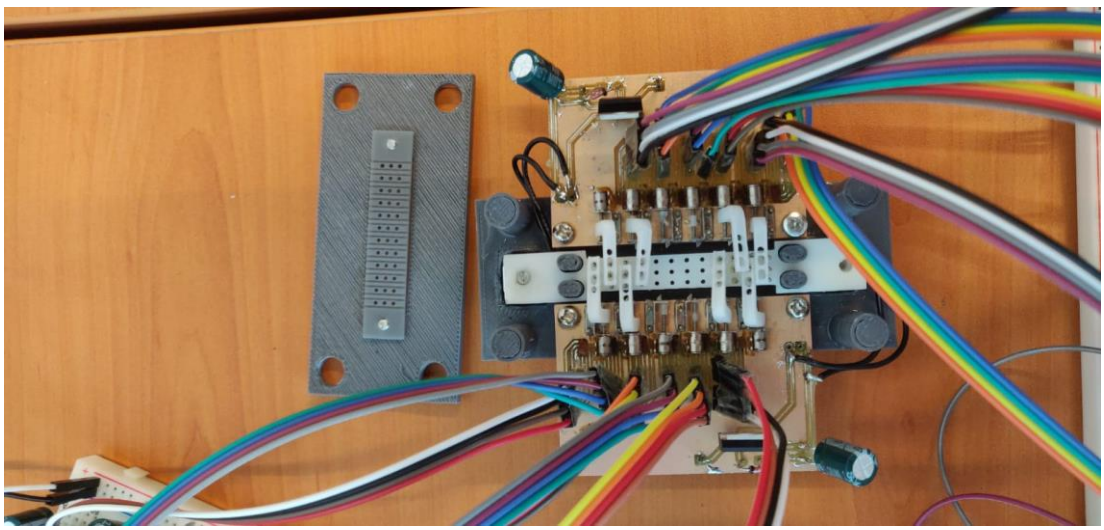

Figure 3. 10: Top view of prototype Braille module.

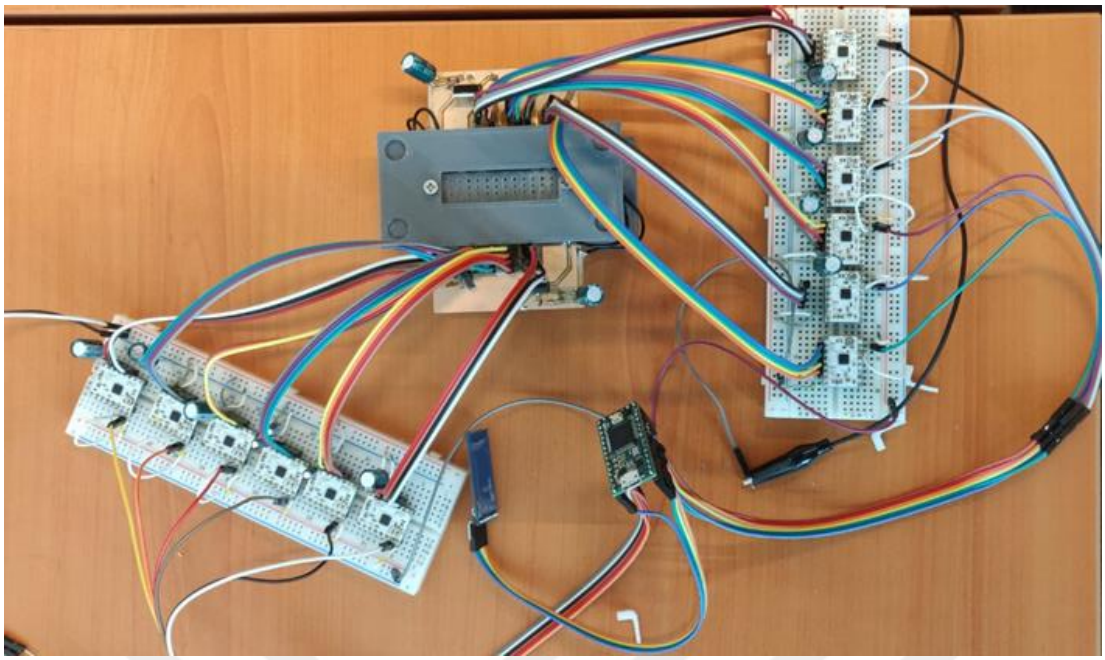

Figure 3. 11: The Braille prototype module with electronic components.

As mentioned in the electronic design, the step motor driver will generate phase steps depending on the desired location of paddles. The generated outputs from the desired cycles position 1,4 and 7 are given in Fig. 3.13, Fig.3.14 and 3.15.

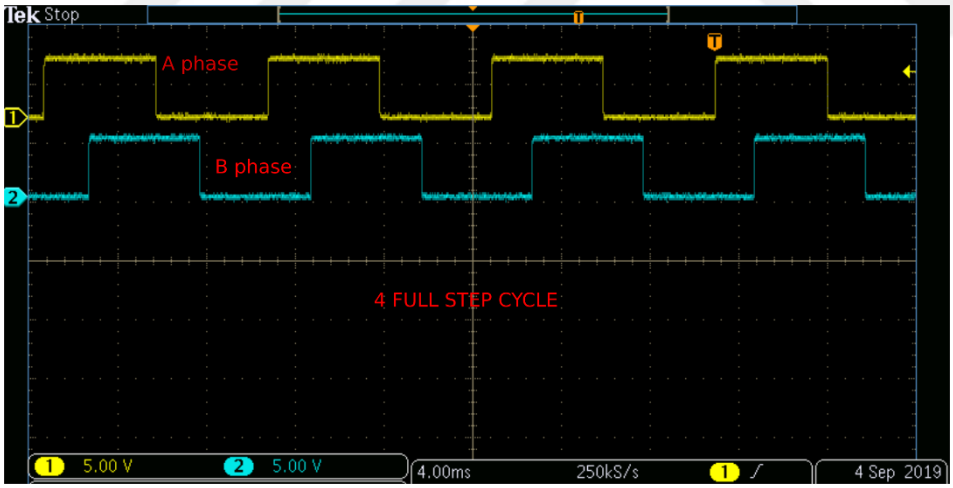

Figure 3. 12: Motor Driver Phase output for position 1.

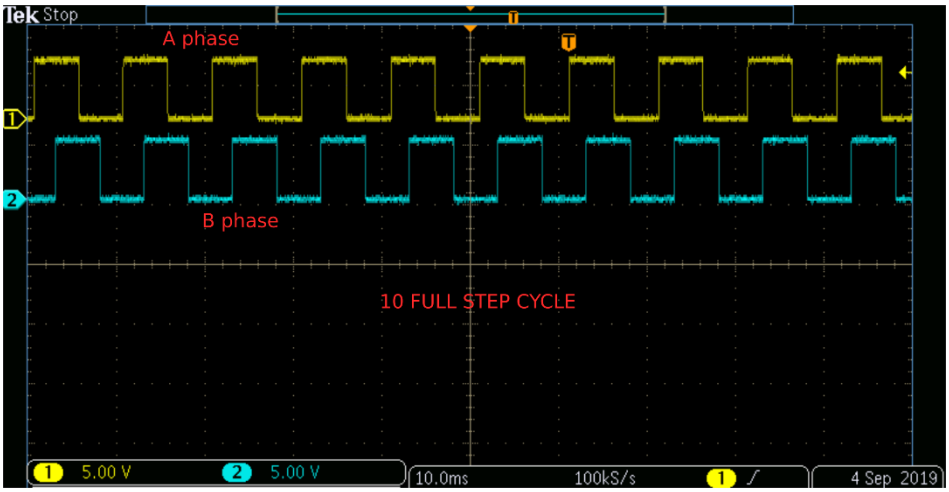

Figure 3. 13: Motor Driver Phase output for position 4.

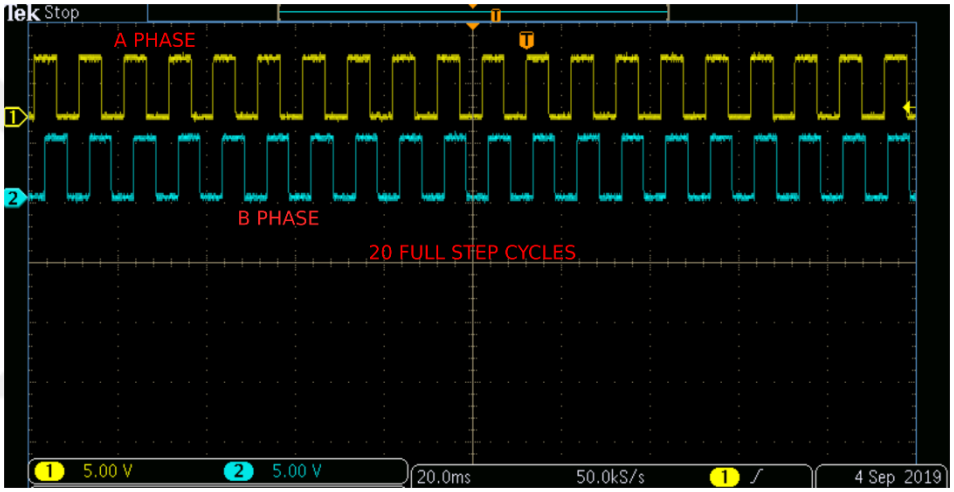

Figure 3. 14: Motor Driver Phase output for position 7.

3.2 Displays and Failures

The design of paddles and step motors did not work at a satisfactory level. The paddles could not move along the Braille displayer unit due to the rough surface of 3D components. Also, the step motors could not keep up the constant current applied on the winding. The motors require rest time to be able to operate again in healthy conditions. A proper surface mount device connector for the step motor terminals, could not be found due to sizing limitation. The connectors are connected to the circuit via surface mounted device pads. However, during the soldering applying heat to the connection may have damaged the stepper motors' insulators. Removal or damaging of insulators in windings may create shortcuts, which means less turn ratio, torque and step inaccuracies. However, a replacement of the current stepper motor could not be

found within the same size in terms of screw rod and motor casing diameter. Choosing a larger and more robust stepper motor would provide better accuracies and easier assembly. However, a larger stepper motor will increase the physical size of the Braille holes and distances, which will not be in Braille standard, as mentioned in chapter 1. The solenoids operated well continuously and managed to carry pogo pins and squeeze them under the pallets. Adding a capacitor parallel to the solenoid terminal provided faster excitations. As can be seen in Fig. 3.15 the solenoid can operate every 2 seconds. Considering the alignment of paddles and readout process. One Braille read cycle will take more than 5 seconds.

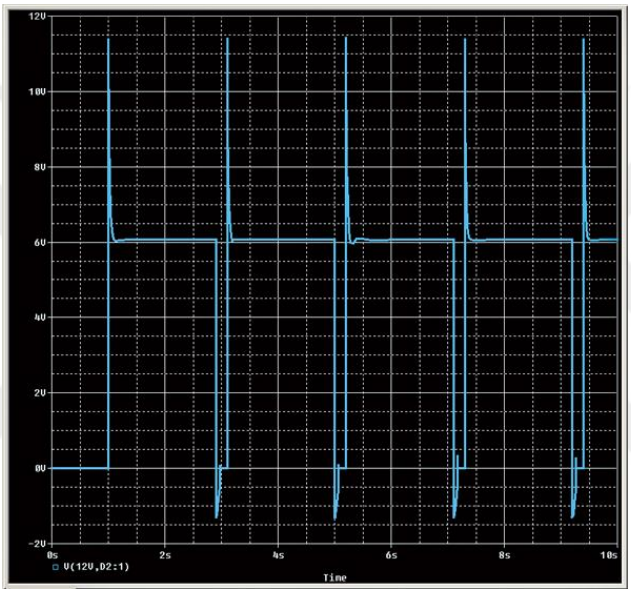

Figure 3. 15: The Solenoid Operation Cycle.

The small micro-step motors are tending to break down quickly. During this project, out of 60 micro-step motors are broken down during the tests and assemblies. The electromagnets were sufficient enough to enforce pins to move; however, the Braille carrier started bending rather than moving the pinhead. Fig. 3.16 shows the bending of the pin carrier.

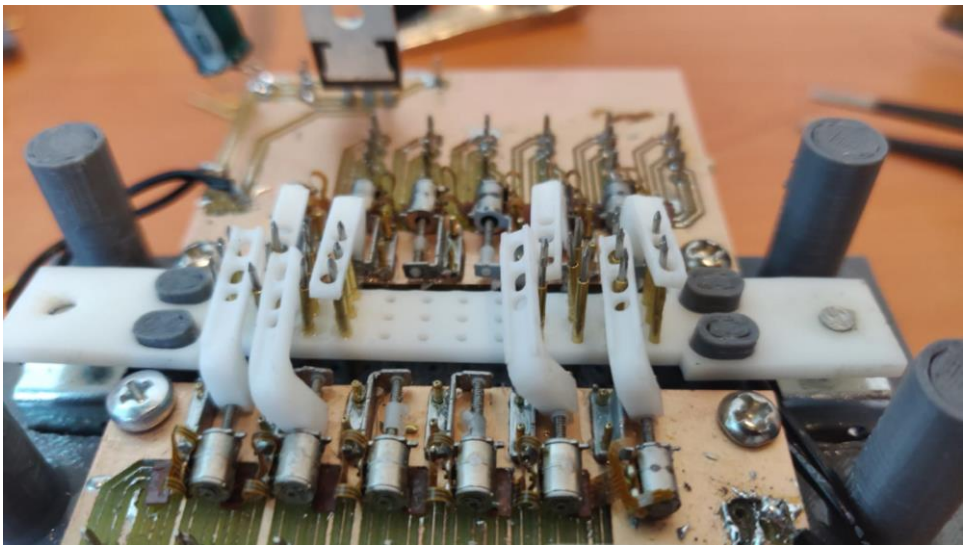

Figure 3. 16: The Braille-Pin Carrier bending on the mechanical loading.

The motor failed due to constant current applied on the windings. The positions of desired locations are gathered to prove the mechanical part of the system. Fig. 3.17 shows the positions 2-4-6 the figure Fig. 3.18 shows the position 1-3-5-7. Position 8 cannot be achieved without a longer screw rod. The location of the furthest point on the screw road does not emboss the single pin in the middle. A larger screw rod with the same diameter stepper motor is needed to operate the paddle system entirely.

Figure 3. 17: Embossment of Position 2,4, and 6.

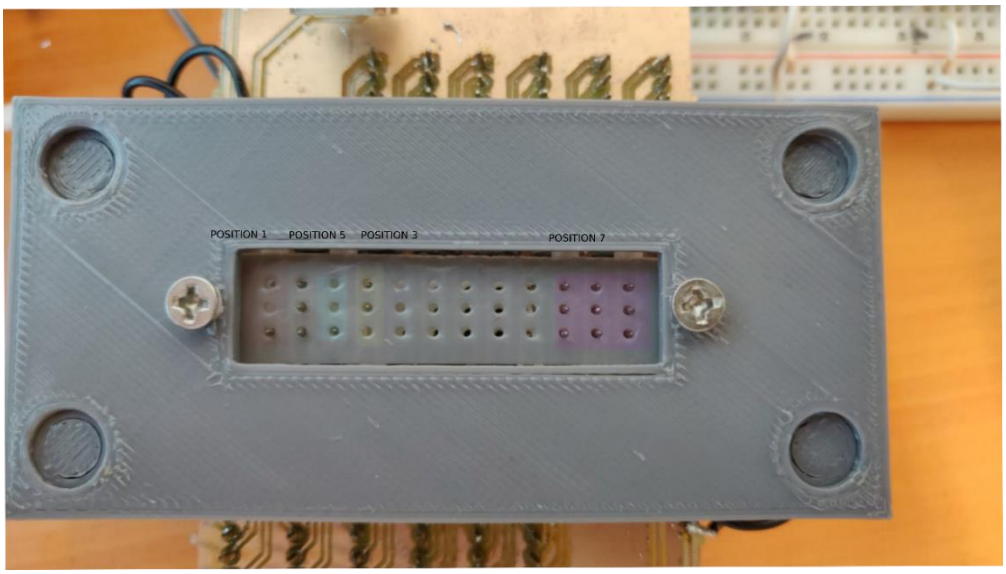

Figure 3. 18: Embossment of Position 1,3,5 and 7.

3.3 Braille Cell Costs

Braille cell technologies are evaluated in terms of their cost. As mention in the introduction, the comparison was made between piezoelectric, electro-mechanic and motor-based mechanisms.

The cost of a Braille cell with a piezoelectric mechanism with eight refreshable dots is estimated at 35 USD, which is equal to 4.38 USD per dot [17]. The cost of a single dot with an electromagnetic Braille cell technology is 0.85 Euros [20]. Assuming there are six dots, the total price is 5.1 Euros for a one-character display.

The design for the electromagnet method costs per 6 dots is shown in Table 3.1.

Table 3.1: Cost of Single Electromagnet Design.

Name of part	Price ($)
3D Printer Part	2
Copper Winding	0.5
Magnets	10
Plunger	0.1
Soft Iron	5

The total amount of the creation of six pins is 23.2 dollars. Since there are six groups of dots, the complete module costs 139.2 dollars. The design for the motor method costs are summed in Table 3.2.

Table 3.2: Cost of Single Cell with step motor Design

Name of part	Price ($)
3D Paddles	4 $
Step Motor	1.6 $
Step Motor Driver	2 $
Carrier Cost	1$
Braille Displayer	1$

The total value for the six dots group becomes 9.4 dollars. The total amount becomes 56.4 dollars.

3.3.1 Cost of electronic components

The costs for the required Printed Circuit Board with the equipment are shown in Table 3.3, including the components and board production.

Table 3.3: Cost of Electronic Equipment of Step Motor Design

Name of part	Type of Material
Copper Board	3 $
STM32 Blue Pill	2 $
Step Motor Drivers	24$
Battery Charger Unit	2.5$
Boost Converter	4$
HC-05 Bluetooth	3$
Lithium Polymer Battery 3.7V 380 mA	4$
Step Motors	10$
Solenoid	1$

3.3.2 Cost of 3D printer Components

The cost of Polylactic acid (PLA) is way cheaper than Stereolithography (SLA). The PLA components were used for coverage of the equipment inside the product, whereas SLA components were designed to be small in dimensions with having low geometric tolerances. Table 3.4 shows the cost of 3D Components of step motor design.

Table 3.4: The Cost of 3D Components of Step Motor Design

Name of part	Type of Material	Amount	Price($)
Case	PLA	1	10
Case Cover	PLA	1	4
Paddle	SLA	10	50
Pin Holder	SLA	1	15
Pogo Pin	Copper	8	8
Paddle Carrier	SLA	1	25

Without achieving low geometric tolerances, the paddle system may not work or has to be calibrated. Thus SLA products are much expansive than the PLA products. The total cost of mechanical products is 112 $. The total cost of the Braille displayer prototype can be seen in Table 3.5.

Table 3.5: Total Cost of Step Motor Design

Name of part	Type of Material
Mechanical Parts Cost	112 $
Electronic Parts Cost	53.5 $
Screws Inserts Pins	5$

3.1.3 Cost comparison of Braille cells

The total material cost of all required components for the Braille display are listed in Table 3.6.

Table 3.6: Cost comparison of Braille Cells

Name of part	Number of Cells	Cost Per Dot	Cost Per Cell
Piezo electric Cell[17]	8	4.375	35
Electromagnetic Cell[20]	6	0.85	5.1
Motor Based Cell[35]	6	0.338	2.03
Portable(Step)Motor Based Cell	6	1.56	9.56

The motor-based and the electromagnetic based cell displayers can be implemented on a portable scale for the mobile phone application. However, the design cost would be higher than the mentioned value in Table 3.6 above. Also, the thickness and weight of the material would be higher than the current suggested design.

3.4 Power Consumption

The power consumption of the Braille display depends on the usage. Thus there will be two types of battery life span calculated one for the standby mode, and the other one is for continuously reading.

3.4.1 Standby power consumption

By using a 5V voltage supply, the Braille display has an average current consumption on standby around 28mA where the microprocessor and the Bluetooth are on sleep mode. STM32 consumes 20mA where Bluetooth module consumes 8mA [32, 36]. The calculation is shown below in equation 3.1.

$$P = U\ x\ I = 5V\ x\ 28mA = 140mW \quad \textbf{(3.1)}$$

The battery used for the suggested design has 370 milliamps per hour, which leads to a battery life close to 13 hours. The amount of battery discharge can be calculated with the equation shown where C is the capacity of the battery, and I is the standby current consumption. The standby duration can be calculated by using equation 3.2.

$$t_{standby} = \frac{C}{I} = \frac{370mAh}{28mA} = 13.2h \quad \textbf{(3.2)}$$

3.4.2 Power consumption in use

Compared to the standby consumption, the usage of step motors will increase the energy required for the Braille cells. Assuming paddles will always move the furthest distance on the screw rod.

As the prototype of the Braille display houses six cells, it is assumed all paddles move long the whole screw rod. The time to complete the travel is less than 1 second. The ability of step motor drivers is set to operate a higher revolution per second up to 10000. However, the step motors are not reliable when operated at higher speeds. For this prototype, the paddles will travel rod in around 1 second. The rod needs to rotate 25 revolutions to reach to the end of the rod. Thus in the longest distance, the step motor will consume 200 mAh in 1 second. According to the DRV8834 datasheet, the power dissipation of the motor can be calculated as in equation 3.3.

$$Power = {I_{rmscoil}}^2 * (Highside\ R_{Ds(on)} + Lowside\ R_{Ds(off)}) \quad \textbf{(3.3)}$$

Assuming the maximum current is 200 milliamps, the root means the square value of the maximum current will be 120 milliamps. The resistance value of field emitted transistors value is given 1 ohm at 35 degrees Celsius [33]. Each solenoid consumes 400mA when the pins of solenoids push the Braille carrier to the display. The dots can be read within 2 seconds. Thus, the active operation of solenoids is taken as 2.5 seconds. The time to complete the embossed process for 6 characters takes 6 seconds. 2 seconds for aligning the paddles 2 seconds for the readout process than the last 2 seconds for retracting the embossed pins. The equation 3.4 shows the t_{line} calculation.

$$t_{line} = t_{clear} + t_{alingment} + t_{emboss} + t_{read} \quad \textbf{(3.4)}$$

$$= 2.2+2+0.2+2=6.4seconds$$

During the clearing, alignment and embossing time, eight motors will be driven which each of them will consume 115mA around 4 seconds in total for one cycle. The solenoid will stay excited during embossment and clear time also 4 seconds as well. Table 3.7 shows the current consumption for one embossing cycle.

Table 3.7: Current usages of electronic equipment during the embossing cycle

Name of part	Operation Current (A)	Operation time(s)	Battery Usage (Ampere per second)
Step Motors	960 mA	4	1.77 milliamps
Solenoids	400 mA	4	0.56 milliamps
Bluetooth	40mA	5	0.208 milliamps
STM32 Blue Pill	60mA	6	0.112 milliamps

The Bluetooth module will not consume 40mA continuously since it sends characters when it is needed. The total amount of battery usage of one cycle can be calculated as equation 3.5 bellow.

$$Battery\ Usage = I_{stm} * t_{line} + I_{stepmotor} * (t_{clear} + t_{alingment}) I_{solenoids*}(t_{clear} + t_{emboss}) \quad \textbf{(3.5)}$$

The total battery usage for the one-line cycle is 7.6 mA per second. The battery has 370mA per hour. The amount of cycle repeat can be found by the equation 3.6 below.

$$Amount\ of\ cycle = \frac{Total\ Charge\ (mAh)}{One\ cycle\ Batter\ Usage(mA\ per\ s)} \quad \textbf{(3.6)}$$

where

$$Amount\ of\ cycle = \frac{370mAh*3600(s/h)}{7.6m(A/s)} = 17526 \quad \textbf{(3.7)}$$

The emboss cycle can be done 17500 times if the operation times are divided as mentioned above. However, for continuous operation of whole items would drain the battery less than an hour.

4. DISCUSSION

Comparing the variety of concepts for Braille cells, this study focused on an intertwined product where the system can be used in any condition. The focus lies on prototyping and manufacturing the design in an affordable and easily reproducible manner while obtaining mobility usage. The piezoelectric effect has the advantage of easy access and high precision. However, the dots require high voltage to be embossed. In order to achieve high voltage, a boost converter is needed.

Moreover, the cost for the cells, even in a higher amount, is not efficient and economically viable for piezoelectric systems. The boost converter operation efficiency drops due to an increase in the voltage value. The promising concept using an electromagnetic mechanism shows a possibility to be manufactured as a prototype using commercially available materials such as neodymium magnets and soft iron cores. Although the cost of designing such systems is cheaper due to the size problem spacing problem occurs in order to comply with Braille display standards. Also, the number of dots can be implemented to the module as long as the thickness of the module can be increased. However, the downside of using electromechanical systems has too many individual parts. Also another problem that has not been investigated is the requirement to balance the electromagnetic effects such as mutual inductance in order to operate them without hindering each other. By using micro motors, either direct cuırrent or step can provide cost-efficiency among other types of Braille technologies. The number of actuators and the complexity of design can be decreased as well as power usage. Required mechanical components can be implemented or modified attached to the module by using three-dimensional printing. Producing 3D materials with low geometric tolerances are not cheap. Not all 3D printing methods provide rigid products in terms of small dimensions and strength. Any slightest dimension error can cause failure in the system. There are cases in mechanical design that requires low geometric tolerances regardless of the size of the pieces. General 3D

printing materials do not provide enough geometric tolerances such as PLA, ABS. In order to obtain robust and consistent production, such as the Selective Laser Sintering method, thus increases mechanical production price.

Operating step motors individually with general input-output pins increases input-output terminals. Also STM32 blue pill model does not have enough general input-output pins to control all step drivers at required conditions such as waking up the driver, setting the voltage and current limits or changing the step size. Therefore, an integrated step motor driver circuit is needed which has communication protocol such as SPI, I2C. Thıs, the control of multiple motor drivers can be achieved with limited general purposed input-output terminals. The dot size dimension within a cell is designed according to the recommended standard referred to as Marburg Medium. The motor and electromagnet type of Braille displayers have a problem with satisfying Marburg medium standards due to their size. Thus the spacing between the cells and the dots is way larger than the standards recommend. However, with the paddle system, the distance between the dots and the cells is kept the same as the Marburg standards stated.

The module was designed to be compact, easy to use, and light-weighted as one of the purposes of this device is handheld usage. For handheld usage, high battery life is needed. However, having a large battery would make the module heavier. Also, the center of weight would shift to the battery side, which may cause comfort problems. The battery used in the prototype is standardized in size and can be replaced easily as required. During the development phase, batteries with higher capacity were unavailable for delivery. The current battery life span with continuous work can last 5 hours. Enlarging the battery would certainly increase the life span of the battery.

The case is designed for 6 Braille cells, which can display up to 6 characters. However, the modules are not easily replaceable, but it can be extended or shortened depending on the mobile phone size. The mechanical pieces can be produced in large scale plastic production rather than 3D printing. The cost of mechanical parts can be lowered in large amounts of output. Although the step motors are small and fast, they are not capable of working under the slightest force exerted on them.

Braille alphabet varies significantly in the languages and alphabets. Not only the abbreviations also concerning special characters and punctuations can affect the pin

layout of each character. The current state of the development of the Braille display, there is a hardcoded Braille chart implemented only for English. The table has to be expanded to other languages as well. The language selection for the user can be made before the device is delivered. A significant improvement would be to store predefined and adjustable Braille tables of the desired languages on it. By doing so may help the user and the distributor to set the device in a state of most prominent advantage. The mobile software application that has been used for communicating with the module was a generic Bluetooth connection application for non-commercial use. A Braille display software must be created to convert Braille formats, depending on the format store messages, texts, or documentations, and set the settings of microprocessors via the application.

Due to the failures of chosen components such as step motors, fragileness of paddles, time limitations, and lack of funding, the step motor Braille module couldn't be completed. Although the designed module has promising features such as offering mobility, power usage, the module is yet to become available to users. There has not been a mobile carriable Braille displayer either as a single product or a product that operates with a mobile phone. Thus this study may offer an essential effect on the Braille displayer industry. To achieve it, commercially available better step motors must be used, which have a similar sizing as used in this thesis. But with better robustness and more straightforward assembly methods, the designed Braille module can be operated without failures or deflections either in electronic and mechanical components.

5. CONCLUSION

Braille displayers are getting more popular and smaller each day with unorthodox methods and operation topologies are presented in the industry. The amount of people who are having dysfunctionalities in the world always provides a market. However, the preference of these people will always determine the usage of these Braille devices. The focus lies on the possibility of manufacturing Braille cells referring to CAD drawings via rapid prototyping technologies, and the micromotor based Braille topology shows excellent promises. Further improvements on the design have to be made in order to increase the life span of the battery and having an operational linear actuator with small spacing and reliability. Software applications either for communication and embedded are implemented using either open-source resources or free available products such as the communication between the Braille displays with mobile phones.

The dynamic Braille designed in this thesis has flaws both in mechanical and electronic concepts. The Braille standards made mechanical paddles and other related parts so small that they cannot be produced consistently. The number of actuators, whether electromagnets or step motors, more extensive or comprehensive microprocessors, must be selected in order to operate efficiently. The concept proves that a mobile Braille display can be manufactured and developed through prototyping techniques as well as controlled with a microprocessor. All the concept and implementation prove that a braille display can be manufactured and developed through prototyping techniques as well as open source software applications in order to decrease the costs significantly while keeping state of the art technologies.

Due to the failures of chosen components such as step motors, the fragility of paddles, time limitations, and lack of funding, the step motor Braille module could not be completed. Although the designed module has promising features such as offering mobility, lower power usage, the module is yet to become available to users. There has

not been a mobile carriable Braille displayer either as a single product or a product that operates with a mobile phone. Thus, this study may offer an essential effect on the Braille displayer industry. In order to achieve it, first, better commercially available step motors will be used. These stepper motors will have similar sizing as used in this thesis but with better robustness and more convenient assembly methods. Second, the mechanical part will be revised, simplified to be able to produce quickly by using force calculations. Thus, the designed Braille module can be operated without failures or deflections either in electronic and mechanical components. Future studies regarded on this topic will be continued to make this Braille module available to user use.

REFERENCES

[1] **Global data on visual impairment**. (2010). Retrieved 9 May 2019, from https://www.who.int/blindness/publications/globaldata/en/

[2] **Bourne, R., Flaxman, S., Braithwaite, T., Cicinelli, M., Das, A., & Jonas, J. et al**. (2017). Magnitude, temporal trends, and projections of the global prevalence of blindness and distance and near vision impairment: a systematic review and meta-analysis. *The Lancet Global Health*, *5*(9), e888-e897. doi: 10.1016/s2214-109x (17)30293-0

[3] **Jiménez, J., Olea, J., Torres, J., Alonso, I., Harder, D., & Fischer, K.** (2009). Biography of Louis Braille and invention of the Braille alphabet. *Survey of ophthalmology*, *54*(1), 142-149.

[4] **European Commission, (**2009) "Guideline on the Readability of the Labelling and Package Leaflet of Medicinal Products for Human Use" . Retrieved 17 May 2019, from https://ec.europa.eu/health/ sites/health/files/files/eudralex/vol-2/c/2009_01_12_readability_ guideline_final_en.pdf

[5**] Roth, G. A., & Fee, E.** (2011). "The invention of Braille.". *American Journal of Public Health*, *101*(3), 454.https://doi.org/10.2105/AJPH.2010.200865

[6**] Braille Codes – Pharma Braille**. (2016). Retrieved 25 April 2019, from https://www.pharmabraille.com/braille-codes/

[7**] Marburg Medium Braille Font Standard – Pharma Braille**. (2017). Retrieved 26 March 2019, from https://www.pharmabraille.com/pharmaceutical-braille/marburg-medium-font-standard/

[8] **D'Andrea, F. M.** (2012)**,** Preferences and practices among students who read Braille and use assistive technology. *Journal of Visual Impairment & Blindness*, *106*(10), 585.

[9] **Phillips, A. Beasley, L.**, (2011), "Braille Profiling Project," RNIB, Retrieved 24 March 2019, from https://www.rnib.org.uk › sites › default › files › braille_profiling

[10] **National Library Service for the Blind and Physically Handicapped,** (2008), Library of Congress. Specification 800: Braille Books and Pamphlets. Retrieved 11 Feb 2019, from www.loc.gov/nls/specs/800_ march5_2008.pdf>,

[11]**Fonts, B., Codes, B., Braille, P., Braille, I., Artwork, P., & Standard, M. et al.** (2015). Introduction to European Braille Guidance – Pharma Braille. Retrieved 14 April 2019, from https://www.pharmabraille.com /european-braille-guidance/introduction-to-european-braille-guidance/

[12] **Nadeem, M., Aziz, N., Sajjad, U., Aziz, F., & Shaikh, H.** (2016). A comparative analysis of Braille generation technologies. In *Advanced Robotics and Mechatronics (ICARM), International Conference on* (pp. 294-299). IEEE.

[13**] Roberts, J., Slattery, O., & Kardos, D.** (2000). Rotating-Wheel Braille Display for Continuous Refreshable Braille. *SID Symposium Digest of Technical Papers*, *31*(1), 1130. doi: 10.1889/1.1832864

[14] **PandaBraille.** (2013). A Refreshable Electro-Tactile Braille Display with No Moving Parts", *RESNA: Rehabilitation Engineering and Assistive Technology Society of North America*.

[15] **Perkins Solutions.** (2015). "Perkins Mini Braille Display**,"** Retrieved 24 April 2017, from http://www.perkinsproducts.org/store/en/notetakers/531-perkins-mini-Brailledisplay.html.

[16] **Velázquez, R., Pissaloux, E. E., Hafez, M., & Szewczyk, J.** (2007). Toward Low-Cost Highly Portable Tactile Displays with Shape Memory Alloys. *Applied Bionics and Biomechanics*, *4*(2), 57–70. doi: 10.1155/2007/543472

[17] **Smithmaitrie, P.** (2009). Analysis and Design of Piezoelectric Braille Display. *Rehabilitation Engineering*. doi: 10.5772/7391

[18] **METEC AG,** (2017) "Modul P20 Modul P20 Data," Retreived 20 April 2019, from https://www.metec-ag.de/downloads/p20.pdf .

[19] **I. Madaeon, Supplyframe.** (2017)."MOLBED Modular Low cost Braille Electronic Display, Available: https://hackaday.io/project/12442-molbed-modular-low-cost-Braille-electronic-display. [Accessed: 21-FEB-2019].

[20] **Vijay Raghav Varada.** (2017). "REFRESHABLE BRAILLE DISPLAY AND BRAILLE KEYBOARD, Retrieved 15 Feb 2019, from http://hackaday.com/2016/04/28/refreshable-Braille-display-and-Braille-keyboard/.

[21] **Mouser Electronic.** (2015)**.** "Bluetooth Low Energy (BLE) 5 Micro Module BC832.",Retrieved 6 March 2019, from, https://www.mouser.com /datasheet/2/915/BlueNor_BC832_datasheets-1360471.pdf

[22] **Sony Energy Devices Corporation Device. Solutions Business Group. Sony Corporation,** (2015)**,** "Lithium Ion Rechargeable Battery Technical Information - Model Number US18650VTC5A," Prog. Batter. Sol. Cells.

[23] **Linear Technology Corporation.** (2016)**. "**LTC4056 Linear Li-Ion Charger with Termination in ThinSOT," no. V, pp. 1–16.

[24] **Vokoun, D., Beleggia, M., Heller, L., & Šittner, P.** (2009). Magnetostatic interactions and forces between cylindrical permanent magnets. *Journal of magnetism and Magnetic Materials*, *321*(22), 3758-3763.

[25] **Vokoun, D., Beleggia, M., Rahman, T., Hou, H. C., & Lai, C. H.** (2008). The two-spin model with dipolar interactions for the exchange-coupled composite media. *Journal of Applied Physics*, *103*(7), 07F520.

[26] **Eason, G., Noble, B., & Sneddon, I. N.** (1955). On certain integrals of Lipschitz-Hankel type involving products of Bessel functions. Phil. Trans. R. Soc. Lond. A, 247(935), 529-551.

[27]**Url -1**
<https://en.wikipedia.org/wiki/Elliptic_integral#Incomplete_elliptic_integral_of_the_first_kind>, date retrieved 30.05.2019

[28] **Camacho, J. M., & Sosa, V.** (2013). An alternative method to calculate the magnetic field of permanent magnets with azimuthal symmetry. *Revista mexicana de física E*, *59*(1), 8-17.

[29] **Wands, R. H., & Krebs, H. J.** (1990). Magnetic Field and Force Calculations for an SSC Detector Solenoid Using a Commercial Finite Element Code. *Advances in Cryogenic Engineering*, 581–588. doi: 10.1007/978-1-4613-0639-9_68

[30] **Runyan, N., & Blazie, D.** (2010). EAP actuators aid the quest for the 'Holy Braille' of tactile displays. In *Electroactive Polymer Actuators and*

Devices (EAPAD) 2010 (Vol. 7642, p. 764207). International Society for Optics and Photonics

[31] **AIYIMA Corporation**.(2018).“Step Motors DC 5V 30ohm Micro 2 Phase 4 Wires Line Stepper” Retrieved 10 March 2019, from https://www.aliexpress.com/store/627093

[32] **ARM Limited**, “Cortex -M0,” Tech. Ref. Man., 2009.

[33] **Texas Instruments Corporation**. (2015). “DRV8834 Step Motor Controller,” Retrieved 6 March 2019, from, http://www.ti.com/lit/ds/symlink/drv8834.pdf

[34] **Xinna, L., Yanzhi, L., & Jinming, L.** (2015). Raille display device design based on STM32. *2015 3rd International Conference on Computer and Computing Science (COMCOMS)*. doi: 10.1109/comcoms.2015.21

[35] **Ulbinger C.**(2017). “*Design and Development of a Refreshable Braille Display*” (Master Thesis), University of Applied Sciences Technikum Wien, Wien, Austria

[36] **FECEGYPT.**(2013). **“**HC Serial Bluetooth Products”Retrieved 19 April 2019, from http://www.fecegypt.com/uploads/dataSheet/1480849570_hc06.pdf

APPENDICES

APPENDIX A: Matlab code for force calculation of 2 magnetic source.
APPENDIX B: The code for step motor based braille displayer.

APPENDIX A

```
function F = CalculateForce(a_,L1_,L2_,R_,M)

  syms t

  a = a_*10^-3;
  L1 = L1_*10^-3;
  L2 = L2_*10^-3;
  R = R_*10^-3;

  tau1 = L1/(2*R);
  tau2 = L2/(2*R);
  sigma = (L1/2 + L2/2 + a)/R;
  Kd = 4*pi*M^2/20;

  sums = [];

  c = -1;
  b = -1;
  count = 1;

  while c <= 1
     while b <= 1

        w = (sigma + c * tau1 + b * tau2)/2;

        k1_2 = 4/(4+w.^2);
        k1 = sqrt(k1_2);

        conts1 = w/(pi*k1);
        const2 = -(2+0.5*(w.^2))*k1*w/(2*pi);
        const3 = 1/2;

        [K,E] = ellipke(k1_2);
        A = conts1*E + const2*K +const3;
        sums(count) = (c*b) * A;

        b = b +1;
        count = count + 1;
     end
     c = c +1;
     b = -1;
  end
  sums = sum(sums);
  F = (2 * pi * Kd * (R.^2) * sums)/10^-6;
End
```

APPENDIX B

```
#include <TeensyStep.h>

//position step ups

#define STEPUNIT 20  //DEGERLERIN HEPSINI DUZELT

#define PP_1 STEPUNIT*5

#define PP_2 STEPUNIT*20

#define PP_3 STEPUNIT*40

#define PP_4 STEPUNIT*60

#define PP_5 STEPUNIT*80

#define PP_6 STEPUNIT*100

#define PP_7 STEPUNIT*120

#define PP_8 STEPUNIT*140

#define StringBufferSize 32

#define cellCount 4

#define blueSerial Serial1

// The look up

static int Braille_a[2]={PP_2, PP_6};

static int Braille_b[2]={PP_3, PP_6};

static int Braille_c[2]={PP_2, PP_5};

static int Braille_d[2]={PP_2, PP_4};

static int Braille_e[2]={PP_2, PP_8};

static int Braille_f[2]={PP_2, PP_5};

static int Braille_g[2]={PP_3, PP_4};

static int Braille_h[2]={PP_3, PP_8};

static int Braille_i[2]={PP_8, PP_5};

static int Braille_j[2]={PP_8, PP_4};

static int Braille_k[2]={PP_1, PP_6};
```

```
static int Braille_l[2]={PP_7, PP_6};

static int Braille_m[2]={PP_1, PP_5};

static int Braille_n[2]={PP_1, PP_4};

static int Braille_o[2]={PP_1, PP_8};

static int Braille_p[2]={PP_7, PP_5};

static int Braille_q[2]={PP_7, PP_8};

static int Braille_r[2]={PP_7, PP_4};

static int Braille_s[2]={PP_4, PP_5};

static int Braille_t[2]={PP_4, PP_4};

static int Braille_u[2]={PP_1, PP_2};

static int Braille_v[2]={PP_7, PP_2};

static int Braille_w[2]={PP_8, PP_7};

static int Braille_y[2]={PP_1, PP_7};

static int Braille_z[2]={PP_1, PP_3};

char BrailleText[StringBufferSize];// a string to hold incoming data

//char position

int16_t TextPosition; //position number

char BrailleTextToShow[cellCount+1]; //AMOUNT OF CELL TO DİSPLAY

char BrailleTextCalc[32]; //loop to calculate char position

uint8_t calcPos; // position number

boolean stringComplete = false

Stepper
M11(3,11),M12(4,11),M21(5,11),M22(6,11),M31(9,12),M32(10,12),M41(23,12),M
42(12,12); //

StepControl controller;

Stepper* cell1[] = {&M11, &M12};

Stepper* cell2[] = {&M21, &M22};

Stepper* cell3[] = {&M31, &M32};
```

```
Stepper* cell4[] = {&M41, &M42};
void setup(){
  Serial.begin(9600);
  //while(!Serial);
  //BT
  Serial1.begin(9600);
  stringComplete = false;
}
void loop() {
  char * inputBuffer;
  SerialReadLine(inputBuffer);
  String input(inputBuffer);
  input.toUpperCase();
  for(int i = 0 ; i<cellCount && input[i] != "" && input[i] != "\n" ; i++)
  {
    switch(i)
    {
     case 0:
       moveMotor(cell1,input[i]);
       controller.move(cell1);
       break;
     case 1:
       moveMotor(cell2,input[i]);
       controller.move(cell2);
       break;

     case 2:
```

```
        moveMotor(cell3,input[i]);
        controller.move(cell3);
        break
      case 3:
        moveMotor(cell4,input[i]);
        controller.move(cell4);
       break;
     }
  }
}
void ClearBrailleTextCalc()
{
  calcPos = 0;
  for(uint8_t i = 0; i < 32; i++)
  {
    BrailleTextCalc[i] = '\0';
  }

void ClearBrailleTextBuffer()
{
  for(uint8_t i = 0; i <= cellCount; i++)
  {
    BrailleTextToShow[i] = '\0';
  }
  for(uint16_t i = 0; i < StringBufferSize; i++)
  BrailleText[i] = '\0'}
  TextPosition = 0
```

```
}
void PrepareBrailleTextFromBuffer()
{
  for(uint8_t i = 0; i < (cellCount); i++)
  {
    BrailleTextToShow[i] = BrailleText[i + TextPosition];
    TextPosition=TextPosition++;
    if(BrailleTextToShow[i] == '\0')
    {
     break;
    }
  }
  BrailleTextToShow[cellCount] = '\0';
}
void SerialReadLine(char * buffer)
{
 uint8_t idx = 0;
 char c;
   while (Serial.available() && (idx < StringBufferSize-1))
   {
    c = Serial.read();
    if ((c == '\n')||(c =='\r')) {
      stringComplete = true;
    }
    else
    {
       buffer[idx++] = c;
```

```
      }
    }   buffer[idx] = 0;
}
void SerialWriteLine(String line)
{
    delay(10);
    Serial.println(line);
    delay(10);
    Serial1.println(line);
}
void moveMotor(Stepper* cell[2], char input)
{
  switch(input)
  {
    case 'A':
      cell[0]->setTargetAbs(Braille_a[0]);
      cell[1]->setTargetAbs(Braille_a[1]);
      break
    case 'B':
      cell[0]->setTargetAbs(Braille_b[0]);
      cell[1]->setTargetAbs(Braille_b[1]);
      break;
    case 'C':
      cell[0]->setTargetAbs(Braille_c[0]);
      cell[1]->setTargetAbs(Braille_c[1]);
      break;
```

```
case 'D':
  cell[0]->setTargetAbs(Braille_d[0]);
  cell[1]->setTargetAbs(Braille_d[1]);
  break;
case 'E':
  cell[0]->setTargetAbs(Braille_e[0]);
  cell[1]->setTargetAbs(Braille_e[1]);
  break;
case 'F':
  cell[0]->setTargetAbs(Braille_f[0]);
  cell[1]->setTargetAbs(Braille_f[1]);
  break;
case 'G':
  cell[0]->setTargetAbs(Braille_g[0]);
  cell[1]->setTargetAbs(Braille_g[1]);
  break;
case 'H':
  cell[0]->setTargetAbs(Braille_h[0]);
  cell[1]->setTargetAbs(Braille_h[1]);
  break;
case 'I':
  cell[0]->setTargetAbs(Braille_h[0]);
  cell[1]->setTargetAbs(Braille_h[1]);
  break;
 case 'J':
  cell[0]->setTargetAbs(Braille_h[0]);
  cell[1]->setTargetAbs(Braille_h[1]);
```

```
  break;
case 'K':
  cell[0]->setTargetAbs(Braille_h[0]);
  cell[1]->setTargetAbs(Braille_h[1]);
  break;
case 'L':
  cell[0]->setTargetAbs(Braille_h[0]);
  cell[1]->setTargetAbs(Braille_h[1]);
  break;
case 'M':
  cell[0]->setTargetAbs(Braille_h[0]);
  cell[1]->setTargetAbs(Braille_h[1]);
  break;
case 'N':
  cell[0]->setTargetAbs(Braille_h[0]);
  cell[1]->setTargetAbs(Braille_h[1]);
  break;
case 'O':
  cell[0]->setTargetAbs(Braille_h[0]);
  cell[1]->setTargetAbs(Braille_h[1]);
  break;
case 'P':
  cell[0]->setTargetAbs(Braille_h[0]);
  cell[1]->setTargetAbs(Braille_h[1]);
  break;
case 'Q':
  cell[0]->setTargetAbs(Braille_h[0]);
```

```
  cell[1]->setTargetAbs(Braille_h[1]);
  break;
case 'R':
  cell[0]->setTargetAbs(Braille_h[0]);
  cell[1]->setTargetAbs(Braille_h[1]);
  break;
case 'S':
  cell[0]->setTargetAbs(Braille_h[0]);
  cell[1]->setTargetAbs(Braille_h[1]);
  break;
case 'T':
  cell[0]->setTargetAbs(Braille_h[0]);
  cell[1]->setTargetAbs(Braille_h[1]);
  break;
 case 'U':
  cell[0]->setTargetAbs(Braille_h[0]);
  cell[1]->setTargetAbs(Braille_h[1]);
  break;
 case 'V':
  cell[0]->setTargetAbs(Braille_h[0]);
  cell[1]->setTargetAbs(Braille_h[1]);
  break;
case 'W':
  cell[0]->setTargetAbs(Braille_h[0]);
  cell[1]->setTargetAbs(Braille_h[1]);
  break;
case 'Y':
```

```
    cell[0]->setTargetAbs(Braille_h[0]);
    cell[1]->setTargetAbs(Braille_h[1]);
    break;
  case 'Z':
    cell[0]->setTargetAbs(Braille_h[0]);
    cell[1]->setTargetAbs(Braille_h[1]);
    break;
}
```

CURRICULUM VITAE

Name Surname **: Remzi Yalın SÖNMEZ**

Place and Date of Birth **: Cambridge 07.10.1992**

E-Mail **: ryalinsonmez@gmail.com**

EDUCATION **:**

- **B.Sc.** **:** 2016, Istanbul Technical University, Electrical and Electronics Faculty, Department of Electrical Engineering